



1-1-2019

NMR Characterization And Chemical Enhanced Oil Recovery Using Surfactants In Unconventional Reservoirs

Mohamed Mohamed Awad Mohamed

Follow this and additional works at: <https://commons.und.edu/theses>

Recommended Citation

Mohamed, Mohamed Mohamed Awad, "NMR Characterization And Chemical Enhanced Oil Recovery Using Surfactants In Unconventional Reservoirs" (2019). *Theses and Dissertations*. 2475.
<https://commons.und.edu/theses/2475>

This Thesis is brought to you for free and open access by the Theses, Dissertations, and Senior Projects at UND Scholarly Commons. It has been accepted for inclusion in Theses and Dissertations by an authorized administrator of UND Scholarly Commons. For more information, please contact zeineb.yousif@library.und.edu.

**NMR CHARACTERIZATION AND CHEMICAL ENHANCED OIL
RECOVERY USING SURFACTANTS IN UNCONVENTIONAL
RESERVOIRS**

by

Mohamed Mohamed Awad Mohamed
Bachelor of Science, Zagazig University, Egypt, 2011

A Thesis
Submitted to the Graduate Faculty
of the
University of North Dakota
In partial fulfillment of the requirements

for the degree of

Master of Science
Petroleum Engineering

Grand Forks, North Dakota, USA

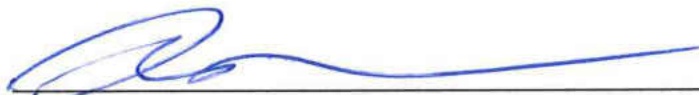
May
2019

Copyright
by
Mohamed Mohamed Awad Mohamed
2019

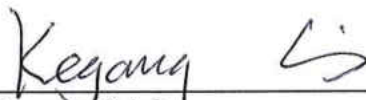
This thesis, submitted by Mohamed Mohamed Awad Mohamed in partial fulfillment of the requirements for the Degree of Master of Science in Petroleum Engineering from the University of North Dakota, has been read by the Faculty Advisory Committee under whom the work has been done and is hereby approved.



Hui Pu

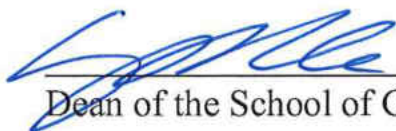


Mehdi Ostadhassan



Kegang Ling

This thesis is being submitted by the appointed advisory committee as having met all of the requirements of the School of Graduate Studies at the University of North Dakota and is hereby approved.



Dean of the School of Graduate Studies

5/3/19

Date

PERMISSION

Title	NMR Characterization and Chemical Enhanced Oil Recovery Using Surfactants in Unconventional Reservoirs
Department	Petroleum Engineering
Degree	Master of Science

In presenting this thesis in partial fulfillment of the requirements for a graduate degree from the University of North Dakota, I agree that the library of this University shall make it freely available for inspection. I further agree that permission for extensive copying for scholarly purposes may be granted by the professor who supervised my thesis work or, in his absence, by the Chairperson of the department or the dean of the School of Graduate Studies. It is understood that any copying or publication or other use of this thesis or part of it for financial gain shall not be allowed without my written permission. It is also understood that due recognition shall be given to me and to the University of North Dakota in any scholarly use which may be made of any material in my thesis. It is also understood that any publication of the work done in this thesis even if not for financial gain shall not be allowed without my written permission.

Mohamed Mohamed Awad Mohamed

May 01, 2019

Table of Contents

LIST OF FIGURES	vii
LIST OF TABLES	ix
LIST OF EQUATIONS	x
ACKNOWLEDGMENTS	xi
ABSTRACT.....	xii
CHAPTER 1: INTRODUCTION.....	1
1.1 Goal of the Study.....	2
1.2 Outline of the Thesis	2
1.3 Enhanced Oil Recovery (EOR)	2
1.4 Wettability.....	3
1.5 Interfacial Tension (IFT) and Capillary Pressure.....	6
1.6 Nuclear Magnetic Resonance (NMR)	7
1.7 The Geology of the Bakken and Three Forks Formations	9
CHAPTER 2: MATERIAL AND METHODOLOGY	12
2.1 Wells and Reservoir Properties	12
2.2 Rock Core Plugs Preparation	14
2.3 Core Cleaning.....	17
2.4 Core Samples Saturation	18
2.5 X-ray Diffraction (XRD) and Scanning Electronic Microscope (SEM).....	20
2.6 Nuclear Magnetic Resonance (NMR)	20
2.7 Phase Behavior	21
2.8 Interfacial Tension (IFT).....	22
2.9 Spontaneous Imbibition.....	25

CHAPTER 3: RESULTS AND DISCUSSION	26
3.1 Porosity Results	26
3.2 XRD and SEM Results.....	28
3.3 Nuclear Magnetic Resonance (NMR)Results	30
3.3.1 NMR Results using 2.3 MHz Larmor Frequency – 30°C	31
3.3.2 NMR Results using 2.3 & 22 MHz Larmor Frequencies at 30°C	36
3.3.3 NMR Results using 2.3 MHz at 25° and 100°C	45
3.4 Phase Behavior Results	47
3.5 IFT Measurements.....	57
3.6 Spontaneous Imbibition.....	59
CHAPTER 4: CONCLUSIONS	64
REFERENCES.....	66

LIST OF FIGURES

Figure 1-North Dakota Formations in the Devonian age [4]	1
Figure 2-Wettability of Rock/Oil/Water System	4
Figure 3-Bakken Formations and Three Forks [3].....	10
Figure 4- Three Parameters Diagram for Microemulsion System Containing no alcohol at 78°F [71]	13
Figure 5-Bakken Core Picture [3].....	14
Figure 6- core plug sampling system	15
Figure 7- Core Plugs Samples Used in NMR	16
Figure 8- Core Plugs Samples 1.5” Diameter Pictures	17
Figure 9- Soxhlet Extraction Method Apparatus [75].....	18
Figure 10- Core Saturation Setup.....	19
Figure 11- Surfactant detection Using Laser Beam Scattering	23
Figure 12- Grace M6500 Spinning Drop Tensiometer	24
Figure 13- Solutions Used for IFT Measurements after Equilibrium	24
Figure 14- Sample Preparation for SEM Test.....	28
Figure 15- XRD Results for Upper Bakken, Middle Bakken and Lower Bakken.....	29
Figure 16- SEM Images for Upper Bakken	29
Figure 17- SEM Images for Middle Bakken.....	30
Figure 18- SEM Images for Lower Bakken.....	30
Figure 19- T ₁ -T ₂ 2D Map for Upper Bakken 2.3 MHz (Depth 10596 ft)	31
Figure 20- T ₁ -T ₂ 2D Map for Upper Bakken 2.3 MHz (Depth 10607 ft)	32
Figure 21- T ₁ -T ₂ 2D Map for Middle Bakken 2.3 MHz (Depth 10620 ft).....	33
Figure 22- T ₁ -T ₂ 2D Map for Middle Bakken 2.3 MHz (Depth 10631 ft).....	33
Figure 23- T ₁ -T ₂ 2D Map for Middle Bakken 2.3 MHz (Depth 10650 ft).....	34
Figure 24- T ₁ -T ₂ 2D Map for Three Forks 2.3 MHz (Depth 10687 ft).....	34
Figure 25- T ₂ and T ₁ Distribution Summary - 2.3 MHz	35
Figure 26- Comparison of LSM and NMR Porosity Change Results.....	35
Figure 27- T ₁ -T ₂ 2D Map - Octane Saturated Upper Bakken 2.3 & 22 MHz (Depth 10596 ft)	36
Figure 28- T ₁ -T ₂ 2D Map – Octane Saturated Upper Bakken 2.3 & 22 MHz (Depth 10607 ft)	37
Figure 29- T ₁ -T ₂ 2D Map – Brine Saturated Upper Bakken 2.3 & 22 MHz (Depth 10596 ft).....	37
Figure 30- T ₁ -T ₂ 2D Map – Brine Saturated Upper Bakken 2.3 & 22 MHz (Depth 10607 ft).....	38
Figure 31- T ₁ -T ₂ 2D Map – Octane Saturated Middle Bakken 2.3 & 22 MHz (Depth 10620 ft).....	38
Figure 32- T ₁ -T ₂ 2D Map – Octane Saturated Middle Bakken 2.3 & 22 MHz (Depth 10631 ft).....	39
Figure 33- T ₁ -T ₂ 2D Map – Octane Saturated Middle Bakken 2.3 & 22 MHz (Depth 10650 ft).....	39
Figure 34- T ₁ -T ₂ 2D Map – Octane Saturated Three Forks 2.3 & 22 MHz (Depth 10687 ft)	40
Figure 35- T ₁ -T ₂ 2D Map – Brine Saturated Middle Bakken 2.3 & 22 MHz (Depth 10620 ft)	40
Figure 36- T ₁ -T ₂ 2D Map – Brine Saturated Middle Bakken 2.3 & 22 MHz (Depth 10631 ft)	41
Figure 37- T ₁ -T ₂ 2D Map – Brine Saturated Middle Bakken 2.3 & 22 MHz (Depth 10650 ft)	41
Figure 38- T ₁ -T ₂ 2D Map – Brine Saturated Three Forks 2.3 & 22 MHz (Depth 106 ft).....	42
Figure 39- T ₂ & T ₁ Octane Saturated -T ₂ & T ₁ /T ₂ Distribution	43

Figure 40- T ₂ & T ₁ Brine Saturated -T ₂ & T ₁ /T ₂ Distribution	44
Figure 41- T ₂ & T ₁ Octane Saturated -T ₂ & T ₁ /T ₂ Distribution	44
Figure 42- T ₂ & T ₁ Brine Saturated -T ₂ & T ₁ /T ₂ Distribution	45
Figure 43- Octane Saturated -T ₂ Distribution 2.3 MHz (0.2ms) at 25° and 100°C	46
Figure 44- Brine Saturated -T ₂ Distribution 2.3 MHz (0.2ms) at 25° and 100°C.....	47
Figure 45- Surfactant Solution in Bakken Formation Brine – 4% Concentration	48
Figure 46- Aqueous Solution 4% in Formation Brine at 25°C and after Equilibration at 105°C.....	48
Figure 47- Phase Behavior Test at 25°C (after mixing) and after Equilibration at 105°C	49
Figure 48- Blend Scan: 2% over all [XOF 315C&Dow Fax 2A1] WOR ~1 n-Octane/Bakken Brine (309K ppm) ~105°C.....	50
Figure 49- Blend Scan: 2% over all [XOF 316C&Dow Fax 2A1] WOR ~1 n-Octane/Bakken Brine (309K ppm) ~105°C.....	50
Figure 50- Blend Scan: 2% over all [XOF 112C&XOF 316C] WOR ~1 n-Octane/Bakken Brine (309K ppm) ~105°C.....	51
Figure 51- Blend Scan: 2% over all [Avel S150&XOF 315C] WOR ~1 n-Octane/Bakken Brine (309K ppm) ~105°C.....	52
Figure 52- Blend Scan: 2% over all [L 38&Dowfax 2A1] WOR ~1 n-Octane/Bakken Brine (309K ppm) ~105°C	52
Figure 53- Blend Scan: 2% over all [L 38&Dowfax 8390] WOR ~1 n-Octane/Bakken Brine (309K ppm) ~105°C	53
Figure 54- Blend Scan: 2% over all [Dowfax 8390&EN 0332] WOR ~1 n-Octane/Bakken Brine (309K ppm) ~105°C.....	54
Figure 55- Blend Scan: 2% over all [Dowfax 2A1&EN 0332] WOR ~1 n-Octane Bakken Brine (309K ppm) ~105°C:.....	54
Figure 56- Blend Scan: 2% over all [EN 0332& Avel S150] WOR ~1 n-Octane/Bakken Brine (309K ppm) ~105°C.....	55
Figure 57- Solubilization Parameters for ENORDET 0332/Avel S150 CGN Blend Scan	55
Figure 58- Blend Scan: 2% over all [Lauryl Betaine&EN 0332] WOR ~1 n-Octane/Bakken Brine (309K ppm) ~105°C.....	56
Figure 59- Solubilization Parameters for LB/ENORDET 0332 Blend Scan	56
Figure 60- IFT Extrapolation for Octane and the Surfactant Blend.....	58
Figure 61- IFT Extrapolation for Crude Oil and the Surfactant Blend	59
Figure 62- The Injection Composition (0.8% LB+0.2% ENORDET 0332 + 0.02% White Oil)	59
Figure 63- Spontaneous Imbibition Cells used in the Test	60
Figure 64- Crude Oil Solubilization with the surfactant Blend	61
Figure 65- Oil Recovery at 105°C	61
Figure 66- Picture of the Impurities after the End of the Test at Room Temperature and Under the Microscope.....	62
Figure 67- Recovery Efficiency – Octane Saturated Core Samples	62
Figure 68- Recovery Efficiency – Crude Oil Saturated Core Samples.....	63

LIST OF TABLES

Table 1- Formation Brine Composition	13
Table 2- Bakken Crude Oil and Used Crude Oil Properties [54], [72]	14
Table 3- Core Samples Used in NMR Characterization Properties	20
Table 4- Surfactants Composition and Activity	23
Table 5- Porosity Measurements for the core samples used in the NMR Characterization Tests	27
Table 6- Porosity Measurements for the core samples used in the EOR Experiments	27
Table 7- IFT Calculation results with using Octane and Crude Oil	58

LIST OF EQUATIONS

Equation 1- IFT Calculation	22
Equation 2- LSM Porosity Calculation	26
Equation 3- Angular Velocity Calculation Equation	57
Equation 4- Calculation Equation	57

ACKNOWLEDGMENTS

I wish to express my sincere appreciation to the members of my advisory committee Dr. Hui Pu, Dr. Kegang Ling and Dr. Mehdi Ostadhassan for their guidance and support during my time in the master's program at the University of North Dakota. I will always remain grateful and express my deepest thanks to Dr. George Hirasaki, Dr. Maura Puerto and Dr. Philip Singer who have inspired and motivated me to keep exploring the unknown scientific problems during my time at Rice University. Without the help of all of them I would not be able to complete my research and thesis. There is no way to thank them enough on the opportunity, knowledge, supervision, support and guidance they offered me during my research work and for their insightful comments and suggestions during my research work and thesis defense. I would like to thank my colleagues for their insightful discussions and suggestions.

I would like to express my warm thanks for Fulbright represented in US State Department, Fulbright Commission in Egypt and Amideast for giving me this opportunity and funding my MS degree. I am extremely thankful and grateful for Dianne Price and Shannon Conheady for their support, supervision and guidance through my Fulbright journey.

I would like to thank North Dakota Geological Survey Wilson M. Laird Core and Sample Library for providing me with the core samples used in this study. I also would like to thank Core Labs for helping in measuring NMR using 22 MHz Larmor frequency which helped in the enhancing the research work.

Finally, I would like to thank my mother, my wife, my daughters and sisters for their unconditional love. Without their support this could not have been possible.

To my mom Huda, my wife Alaa,
my cute daughters Rodina and Kenzy
and my sisters Aya and Dana,
The world's best Family!

ABSTRACT

The main goal in this research is characterization of the Bakken and Three Forks formations using NMR and conduct phase behavior tests to find a formulation suitable for spontaneous imbibition test for Middle Bakken core samples under the Bakken reservoir temperature and brine salinity.

NMR measurements were performed for as-received twin core samples from the Upper Bakken, Middle Bakken and Three Forks formation and after saturation with Bakken formation brine and octane. The measurements were conducted using 2.3 MHz and 22 MHz Larmor frequencies. The measurements also conducted at 25° and 100°C using 2.3 MHz Larmor frequency only. EOR potential of surfactants on oil production from middle Bakken core samples was evaluated. Surfactants were selected from phase behavior test results of 13 thermally stable surfactants and 24 blend scan tests. Interfacial Tension (IFT) was measured and spontaneous imbibition test was conducted using octane and light crude oil.

This research presents the use of NMR to characterize the Bakken and Three Forks formations as well as frequency and temperature dependence effect. The selected surfactant blend was able to increase the oil recovery in both octane and light crude oil saturated core samples with ~ 11% more than brine only.

CHAPTER 1 : INTRODUCTION

Unconventional reservoirs are any reservoir that requires utilizing special extraction and recovery operations outside the conventional recovery operations. The Bakken formation was named after Henry Bakken, a farmer in Tioga, North Dakota, who owned the land where the formation was initially discovered [1]. J.W. Nordquist was the geologist who first described the Bakken formation in 1953 [2]. The Bakken formation was deposited from the Late Devonian to Early Mississippian age (Figure 1). There is three membranes in the Bakken formation, the Upper Bakken and Lower Bakken are organic shale, separated by dolomitic siltstone and sandstone called Middle Bakken [3]. The new Bakken wells have high decline rate from the initial production rate, sometimes as high as 85% per year, this high decline rate is because of the complex nature of the Bakken formation, and the formation porosity ranges from 4 to 8% with low permeability as $\sim 0.01-0.001$ md.

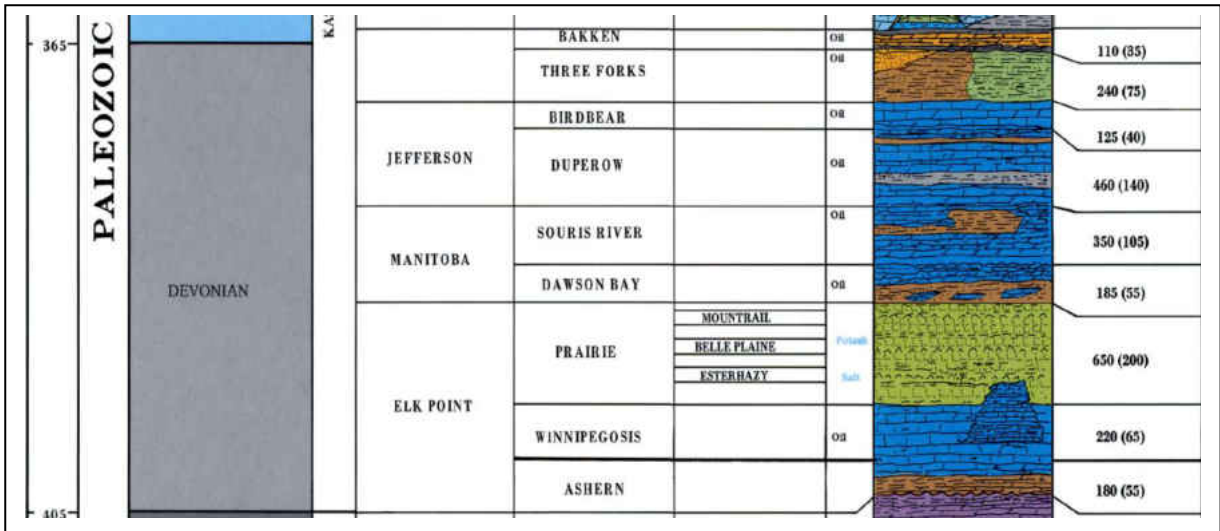


Figure 1-North Dakota Formations in the Devonian age [4]

Surfactants are chemicals which can be used to alter the wettability of the rocks and/or lower the interfacial tension (IFT) between oil and water. Surfactants alter the wettability from oil wet to water wet or intermediate wet. Surfactants are used to enhance the oil production. There are four types of surfactants: anionic, nonionic, cationic, Amphoteric, and there is new type of surfactants called

switchable surfactants which can reversibly fully convert between active and inactive forms [5].

1.1 Goal of the Study:

The goal of this study is to use NMR for Bakken characterization and screen surfactants which are thermally stable under Bakken reservoir temperature, and tolerant to Bakken reservoir salinity. Then, identify a blend of these surfactants which can lower the IFT and/or alter the wettability to water wet or intermediate wet. The experiments of this study have been done on two wells located in Blue Buttes field, McKenzie County, ND. The reservoir temperature is 105°C (221°F), and the salinity is 309,612 ppm with ~ 15,000 ppm divalent ions. The surfactants used in this study is anionic surfactants, single surfactants and blends with different blend. A few surfactants blends have been selected based on thermal stability, salinity tolerance, and phase behavior. We were interested in one surfactant blend ratio that was able to lower the interfacial tension measurements (IFT), and we used his blend for a spontaneous imbibition test. Spontaneous imbibition test was conducted with and without surfactants to evaluate and study the effect of the surfactants blend on the oil recovery.

1.2 Outline of the Thesis:

This chapter contains the introduction, objective of the study, the definitions of various concepts used in this work, and literature review on each section and description of the Bakken Formation and Three Forks geology. Chapter 2 includes the experimental materials, equipment and methodology of work. Chapter 3 presents and discusses the results of the experiments performed in this study. Chapter 4 states the conclusions from this study and future work recommendations. All the references used in the thesis are listed at the end.

1.3 Enhanced Oil Recovery (EOR):

Enhanced oil recovery or tertiary recovery is the process used after the primary recovery “reservoir pressure combined with artificial lift” and secondary

recovery “injecting water into the reservoir to increase the reservoir pressure to maintain the oil production rate”. Enhanced oil recovery is the process of changing the chemical and/or the physical properties of the reservoir rocks to increase the oil recovery.

There are three main types of EOR processes:

- Thermal recovery: mainly used for heavy oil reservoirs, by injecting steam to lower the viscosity of the heavy oil.
- Gas EOR: by injecting gases such as CO₂, natural gas, nitrogen, and/or other gases that can dissolve in the oil and lower oil viscosity and improve the flow rate.
- Chemical EOR: by injecting chemical compounds such as surfactants to lower the IFT and/or alter the wettability of the reservoir rocks from oil wet to mixed wet or water wet. Polymers also used to increase the effectiveness of the water flooding.

Chemical EOR contributes roughly 11% of 3.7 Million barrels per day global EOR production [6]. There are many challenges related to chemical EOR, for example water and oil separation challenges due to stabilized emulsions formation, oily water flocculation problems, deposition of mineral scale caused by alkalis, the increase in corrosion and scale, asphaltene deposition, and high adsorption rates of surfactants [6]. Ultrahigh imbibition rates must be achieved to have successful and economical surfactant recovery process, in addition to maintain ultralow critical micelle concentration (CMC) and low adsorption to minimize the deployment of surfactant [7].

1.4 Wettability:

Fluid flow, distribution of fluids in the reservoir, capillary pressure, and relative permeability of the reservoir rocks are some of the major factors affecting the oil recovery. Wettability has major effect on all the previous parameters. The definition of wettability is “the tendency of one fluid to adhere to or spread on the solid surface in the presence of other immiscible fluids” [8]. In the ultralow permeability reservoirs, the surfactant imbibition rate is more important than the ultimate recovery factor [7].

Wettability is a preference that the rock has for one fluid of the two or more present immiscible fluids. Rocks can be classified according to wettability as follows: water wet, mixed wet, intermediate wet, and oil wet. There are two ways to quantify wettability: contact angle, and wettability index. Contact angle is the angle between the edge of a drop of the less dense fluid and the rock surface in the presence of the high dense fluid (Figure 2) [9]. Wettability index can be calculated by subtracting the displacement by oil ratio from the displacement by water ratio [10]. There are two methods to measure the wettability index, Amott wettability index is the amounts of oil and water imbibed by a sample spontaneously and by force (either centrifuge or core flooding), the second method is U.S. Bureau of Mines (USBM) which is work required to imbibe oil and water [11].

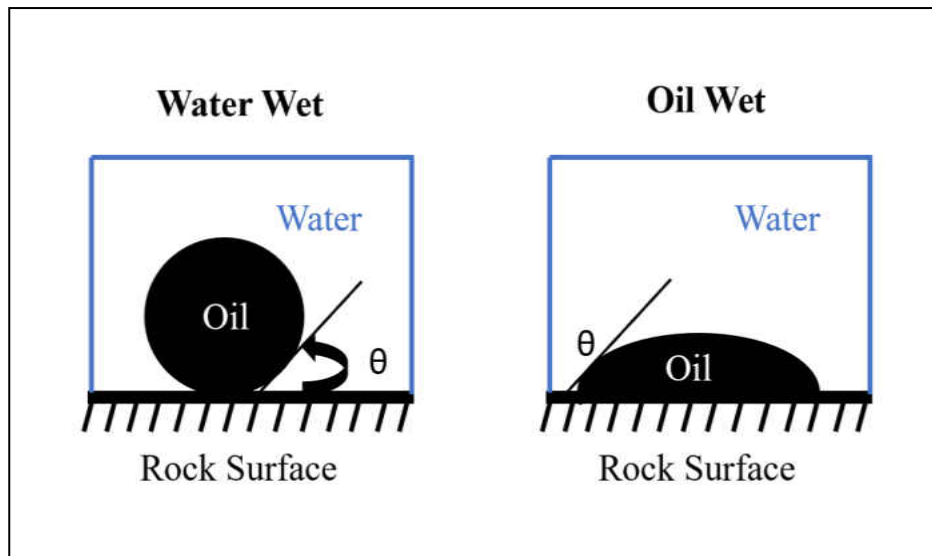


Figure 2-Wettability of Rock/Oil/Water System

In a rock/oil/water system the rock is water wet when the contact angle is between the oil droplet and the rock surface is small and no hysteresis, as a result the water tendency to fill the small pores and to contact most of the rock surface is higher than oil. The rock is mixed wet when there is small receding contact angle which will increase to advanced contact angle before the contact line of water and oil moves, and there is hysteresis. The rock is oil wet when both receding and advanced contact angle is almost 180° and initially thick oil film is present or no water film exist on the rock surface, as a result the oil tendency to fill the small pores and to contact most of the rock surface is higher than water. The rock is

intermediate wet when both receding and advanced contact angle are nearly 90° [12].

Historically, there was a belief that all petroleum reservoirs are water wet, and this assumption is based on two major reasons: almost all the clean sedimentary rocks are strong water wet, and sandstone reservoirs were deposited in aqueous environments where oil migrated to later [13]. In 1934, Nutting realized that some producing reservoirs were strongly oil-wet [14]. Based on the laboratory tests, it is believed now that most known reservoirs are intermediate or mixed wet to oil wet [15]. Some crude oils can change the rock wettability from water wet to oil-wet by depositing a thick organic layer or by the adsorption of polar compounds, some of these compounds are sufficiently water soluble to pass through the aqueous phase of the rock, on the mineral surfaces [8], [16]–[22].

Capillary forces, gravity forces, and viscous forces are the driving forces for imbibing and draining of wetting and nonwetting phases from the matrix blocks of fractured reservoirs [23]. Water can imbibe by capillary forces into bypassed zones and reduce bypassing in water wet rock surfaces, but in case of oil wet media, capillary forces will discourage water invasion to bypassed zones and increase bypassing [24]. Wettability alteration will change the capillary pressure from negative to positive which will mobilize more oil with countercurrent imbibition [25]. Bakken cores are originally oil wet to intermediate wet [26], [27]. Wettability alteration using surfactants depends on the rock mineral composition [26]. Anionic surfactants is more suitable for siliceous formations, cationic and non-ionic surfactants perform better in case of carbonate rocks [26]. Higher oil recovery in spontaneous imbibition tests using anionic surfactants was observed comparing to water alone [26].

Number of studies have been done on wettability as well as wettability in the Bakken. Low concentrations of mixtures of cationic and non-ionic surfactants can recover 70-80 % of OOIP by spontaneous imbibition from carbonate cores, as well as secondary water flood for carbonate cores with wettability alteration surfactants can increase the oil recovery in the lab scale by 11% in the first 5 pore volume (PV) [24]. Dimethyl amine oxide, ethoxylated alcohol, internal α -olefin sulfonate, and anionic linear α -olefin sulfonate altered the wettability of the Bakken cores towards water wet and yielded 6.8-10.2% OOIP more oil recovery than brine alone in spontaneous imbibition tests [25]. Surfactant system with oil

1 recovery factors in spontaneous imbibition test range from ~30-40% with initial rates ~10cm/day in ~1μD permeability Bakken cores has been designed in previous researches [28], but in this research the researches neglected the effect of solution gas drive which is important factor in the oil recovery efficiency. The Bakken crude oil is light oil with API gravity ~ 42 as well as in the saturation process the core oil saturation was 30-35% because the researcher just pressurized the cores without mentioning using any vacuum and as result the cores which resulted of low saturations values due to the large amounts of air present not removed. The presence of air during the saturation process as well as the light crude oil increase the effect of the solution gas drive, also there was no mention of using back pressure in the spontaneous imbibition tests.

Surfactants efficiency in enhancing the oil recovery can be maximized by identifying an optimal brine salinity, and divalent cation content as well as the optimal concentration of surfactant used [27]. Oil recovered by spontaneous imbibition using formation brine is minimal [29]. Anionic surfactants and sodium carbonate can be used to alter wettability of sandstone and/or carbonate formations and gravity drainage will drive spontaneous oil displacement [30].

Several researchers have studied the large-scale pilot projects in the Bakken formation. Since 2008, there is more than seven injection pilots in the Bakken but none of them were successful [31]. In all the performed pilots was found that injectivity is not a problem even with the very low permeability which may be because of the effect of the length of the horizontal wells and/or the multi-stage hydraulic fractures in the wells [31].

1.5 Interfacial Tension (IFT) and Capillary Pressure:

Interfacial tension is the energy per unit area associated with creating an interface between two fluids or it is the forces at the interface between two immiscible liquids in dynes/cm, and it will be called surface tension when single liquid surface is present [32].

Capillary pressure is the pressure difference across the interface of two immiscible phases occupying the same pore the capillary pressure caused by the IFT between

the two immiscible phases. To initiate the flow capillary pressure must be higher than IFT. IFT is an important factor in chemical EOR [32].

Capillary pressure resulted from the oil/water IFT which contributes effectively in the rate of oil production without water production [33]. IFT can be calculated using correlations or measured by experiments. Direct measurements are more reliable and trusted results [32]. Composition of oil and formation water affect the IFT values, also reservoir temperature has high impact on the IFT measurements.

By assuming constant permeability, oil production rate increases with increasing capillary pressure [33]. The curve of the capillary pressure for the forced imbibition is very steep and it is also proved that there is difference between the first and the second drainage capillary pressure due to the trapping mechanism [29].

1.6 Nuclear Magnetic Resonance (NMR):

Scientists at Stanford and Harvard Universities were the first to observe the nuclear magnetic resonance in 1946 [34]–[36]. NMR is a powerful tool used in chemistry for identification of chemical states in matter which known as NMR spectroscopy.

NMR applications are in many fields such as petroleum industry, biomedicine, and food. The NMR applications started in exploration in 1950's. The first scientists to use NMR were scientists at Exxon, Mobil, Shell, Chevron, and Texaco [37]. However most of the early use of NMR in petroleum industry was for composition determination for petroleum and petroleum fractions, Chevron scientists-maintained study program focusing on NMR application in petrophysical studies of fluids and rocks. Chevron also developed logging tool for formation evaluation in consultation with Varian Associates [38]. Early research in Chevron, Schlumberger, Texaco, Mobil, Varian, and Borg-Warner led to commercialize well logging services development by Pan Geo Atlas Corporation and Schlumberger in 1960's, and illustrated important application of NMR [39]–[46]. Until 1994, the commercial NMR tools were operated by the earth magnetic field, nowadays NMR logging tools carry its own magnets and operate at higher Larmor frequencies.

Many studies have been done on the Bakken formation, some of these studies to improve the NMR applications in unconventional reservoirs and the rest for evaluating the Bakken formation. Content and distribution of the paramagnetic minerals is an important factor for surface relaxivity determination, which prove that assuming constant surface relaxivity for a rock type, formation or well is not accurate [47]. NMR measurements proved the presence of the brine in smaller pores as well as formation of brine film on grains regardless of aging time in addition to the strong rock-fluid interaction because of core fluids redistribution with time [48].

Xie and Gan confirmed the possibility of using 20MHz NMR to measure the organic matter in mudstone [49]. Other studies used low-field NMR for identification of the bitumen, bound water signals, and the oil in organic porosity as well as oil separation from the free fluids [50]. Using NMR to monitor the brine and oil imbibition in wettability study results in quantifying the amount of imbibed fluids comparing to the gravimetric measurements, study the TOC effect on the amount of oil imbibed, and relaxation times indicated the shale wettability [51].

Xie and Gan used NMR 2D maps at 20°-90°C to quantify the water and organics comparing to Dean-Stark Analysis and Rock Evaluation Pyrolysis [49]. This study was conducted on as received Bakken cores as well as Permian shale samples. They were able to use 20MHz NMR to measure the water as well as organics in mudstone and the results agreement with Dean-Stark analysis was excellent, and satisfying results comparing to Rock Evaluation Pyrolysis. Kausik et al, used core data and wireline logs to study the potential targets for horizontal drilling and hydraulic fracturing in the Middle Bakken and Three Forks using 400 MHz NMR equipment where they did not find temperature dependence in the bulk state, kerogen and bulk water comparing to temperature dependence of bitumen and heavy viscous oils relaxation times, clear frequency dependence for T_1 of bulk bitumen with a small reduction when confined to the organic kerogen pores, no frequency dependence in T_1 of light oil in the bulk state due to motional averaging but shows a clear frequency dependence when confined to the kerogen pores [52].

Simpson et al, used NMR to confirm cleaning of core plugs using Dean-Stark method and to identify new T_2 cut off parameters as well as correcting the salinity

measurements to achieve more accurate results from NMR logs [53]. The results of this research showed that incomplete cleaning of the rock pores using Dean-Stark method, the salinity of Bakken/Three Forks formation water must be accounted because of the large difference in hydrogen index compared to water or low salinity brine, T_2 cut off ranges from 1.0ms to 0.7ms for the Bakken free fluid while T_2 cut off ≤ 0.4 ms for clay bound water which indicated much lower T_2 cut for free fluid than conventional interpretation T_2 cut, and the small pores are water wet, while the larger pores are oil wet and clays also appear to be oil wet.

1.7 The Geology of the Bakken and Three Forks Formations:

Bakken reservoir is considered one of the world largest unconventional resources, according to the U.S. Geological Survey in 2013 with approximately 7.4 billion barrels estimated recoverable oil [54]. The Bakken formation lies on the subsurface of the Williston Basin with depth range ~11,000 ft at the center of the basin and ~3000 ft along the northern limit [55]. North Dakota and Montana where the Bakken formation is in the U.S., but third of the Bakken is in Saskatchewan and Manitoba in Canada [56]. The structural features are the main factors in controlling the general hydrocarbon distribution in the Williston Basin and the oil production from the Bakken formation [57].

The Bakken system consists of the Lodgepole, Upper Bakken, Middle Bakken, Lower Bakken, and Three Forks (Figure 3). The Bakken formation overlies the Three Forks and overlain with the Lodgepole limestone. The average thickness of the Bakken formation in the U.S. side is ~80 ft, and the maximum thickness is ~145 ft which is located near western Mountrail county, North Dakota [58]. The Upper Bakken and Lower Bakken are organic-rich, the hydrocarbon source rocks, fissile, laminated to massive, hard, brittle, naturally fractured, siliceous, pyritic, and slightly calcareous, and the total organic carbon (TOC) content range is from 12-36 wt% with average 11 wt% [59]–[61]. The Middle Bakken lithology is highly variable which include interbedded siltstone, sandstone, siliceous limestone, limestone, and sandy dolomite while calcareous, dolomitic, or argillaceous siltstone is the dominant lithology in the Middle Bakken [55], [58]. The Middle Bakken consists of five distinct lithofacies[62].

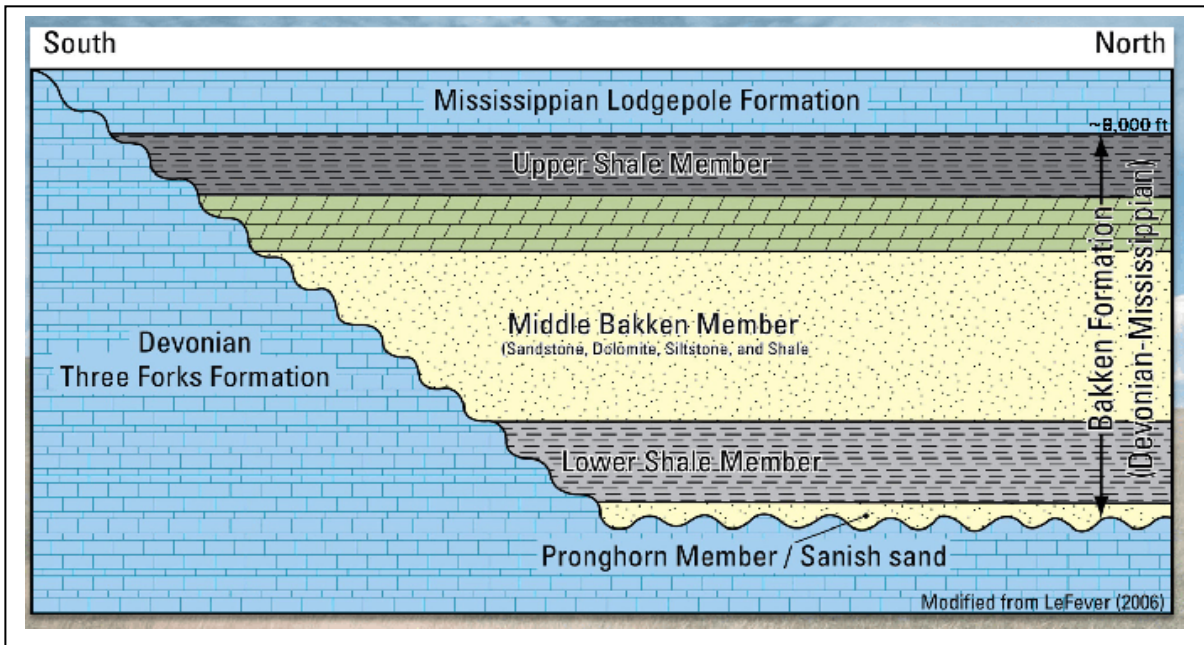


Figure 3-Bakken Formations and Three Forks [3]

The organic matter in the Upper and Lower Bakken is mainly type II (marine algal) oil prone kerogen which was deposited in a stratified marine during the periods of sea level rise under anoxic conditions [63]. Different lithologies of the Middle Bakken have different mineralogy, generally consists of 30-60% quartz and feldspar, 30-80% carbonate, and the rest will be minor matrix clay minerals such as illite, smectite, kaolinite, and chlorite as well as pyrite and siderite [64]. The upper layer of the Three Forks is located under the Lower Bakken which is well sorted, very fine grained, 10 ft thickness layer of sanish sand [65]. Laminations of illite-rich clay with dolomitized limestone is the main composition of the Three Forks. The TOC of Middle Bakken and Three Forks formations ranges from 0.1 to 0.3 wt% [60].

The first hydrocarbon generation occurred at 9,000 ft depth (shale development), 10,000 ft is the average depth of the Middle Bakken[54]. Middle Bakken and Three Forks have porosity range of ~5-6% and 0.001-0.01 mD permeability or less[54], [65]. Oil API gravity average for the Bakken is ~42°API[66]. The gas oil ratio range (GOR) is 507 – 1,712 SCF/bbl, and 1,617 – 3,403 psi is the bubble point pressure range [67]. The pressure gradient of the Bakken formation is up to 0.73 psi/ft in the central part of the basin [68].

The temperature range of the Middle Bakken formation is 80°-120°C [63]. The brine salinities range based on chemical analysis of formation water in the Bakken, pre-Mississippian rocks, and Williston Basin as well as statistical data from over 200 wells is 150,000 to 300,000 mg/L (15% to 30%) of total dissolved salts (TDS) [27], [69].

CHAPTER 2 : MATERIAL AND METHODOLOGY:

The experiments performed is divided into two main parts: the first part is characterization of the Bakken formations using X-ray Diffraction (XRD), Scanning Electron Microscope (SEM), and Nuclear Magnetic Resonance (NMR). The second part is focusing on screening thermally stable surfactants under the reservoir temperature, and tolerant to the reservoir salinities to get suitable surfactant blend which can lower the IFT to enhance the oil production.

2.1 Wells and Reservoir Properties:

Two wells in Blue Buttes Field have been chosen for this study, wells A & B. It was taken in consideration that the chosen the wells were close to each other in distance. All the information on the two wells drilling, cores, and production are available at North Dakota Industrial Council website. Both are active producing, horizontal wells, and no water or gas injected to both wells. The two wells started production in 2007. Cumulative oil production till February 2019 for well A is 26806 BBL, cumulative water production is 47199 BBL, and cumulative gas production is 81625 MCF, while for well B, cumulative oil production is 32437 BBL, cumulative water production is 50180 BBL, and cumulative gas production is 46403 MCF.

The two wells lithology was almost the same, according to the visual inspection for the cores and core plugs as well as the mud logging report of the cuttings from the well files. The Upper Bakken and Lower Bakken samples are black, dark gray, firm to brittle, and show scattered yellow gold fluorescence with instant milky rapid streaming cut. The Upper Bakken is approximately 21ft thick and Lower Bakken is 28ft thick. The Middle Bakken is mostly sandstone, light brown to brown, tan, clear, and even yellow fluorescence with thin streaming good cloudy to milk yellow cut. The Middle Bakken is approximately 54 ft thick. Three Forks is sandstone, light tan or beige color with grace of light gray, and a cream green to gray green shale is present. Three Forks is approximately is 62ft thick[70].

Formation brine composition and reservoir temperature were obtained from the well files on North Dakota Industrial Council website. The reservoir temperature is $\sim 105^{\circ}\text{C}$ (221°F) [70]. All the EOR experiments have been conducted under the reservoir temperature. Formation brine was prepared with the same salinity and composition as the formation brine composition in the two wells from the analysis

reports in the well files, except sodium bicarbonate and sodium sulfate they were replaced with sodium chloride with the same ionic strength to prevent precipitation. No precipitation was observed in the collected formation brine samples from the wells because all the salts are in equilibrium with the reservoir rock. The prepared formation brine composition in Table 1.

Table 1- Formation Brine Composition

Salt	ppm	Remarks
NaCl	259,298	
CaCl ₂	37,434	
MgCl ₂	5,603	
KCl	7,246	
BaCl ₂	31	
TDS	309,612	

Based on conducting phase behavior tests for number of n-alkanes and comparing surfactants blends based on solubilization parameters at optimal salinity Puerto and Reed concluded that initial surfactant evaluation can be conducted using pure n-alkanes and NaCl brine as shown in the three phase diagram Figure 4 [71].

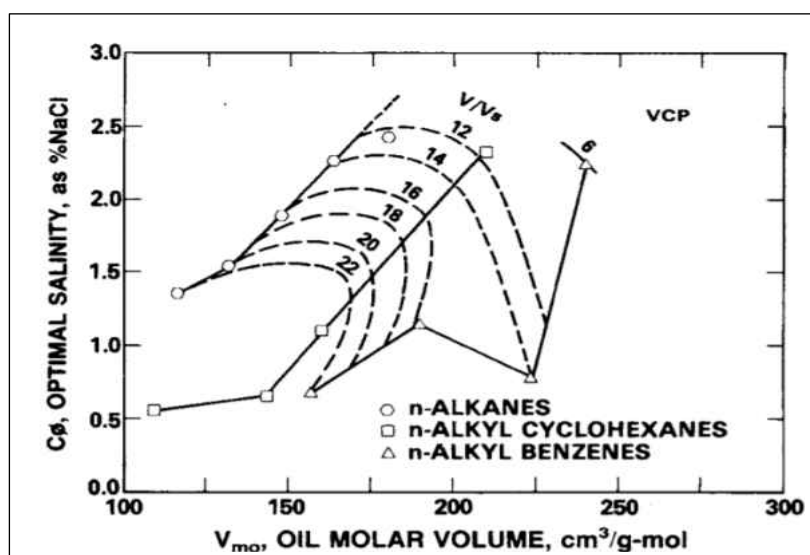


Figure 4- Three Parameters Diagram for Microemulsion System Containing no alcohol at 78°F [71]

In this study n-octane was used as a model oil to conduct the phase behavior test for different surfactants, then both n-octane and light crude oil with properties close to the Bakken crude oil was used to measure the IFT and perform spontaneous imbibition tests so we can evaluate using n-octane as model oil for light crude oils in EOR experiments. The properties of the Bakken crude oil and the used crude oil in Table 2.

Table 2-Bakken Crude Oil and Used Crude Oil Properties [54], [72]

Properties	Bakken Oil	Light Crude Oil
API Gravity	42	38
Specific Gravity	0.816	0.836
Asphaltenes %	0.060	0.5
Water %	0.100	0.1
TAN	<0.1	0.17

2.2 Rock Core Plugs Preparation:

All the cores collected from the Williston Basin wells are stored at the North Dakota Geological Survey's Core Library. All the core plugs used in this study was drilled from non-preserved cores stored at the core library (Figure 5).



Figure 5-Bakken Core Picture [3]

In this study, the core samples were cored with two different diameters, 2.54cm (1”) for the NMR measurements and 3.81cm (1.5”) for the EOR experiments, and

some of the cuttings were used for the XRD and SEM tests. The coring was conducted using core plug sampling system (using wet coring bit) located in the Geology and Geological Engineering Department at the University of North Dakota (Figure 6).



Figure 6- core plug sampling system

For the NMR measurements, 12 core plugs were prepared with 2.54cm (1") diameter, All the cores are twin cores. All the twin cores one is ~ 4.8cm (1.89") length and the second one ~3.1cm (1.22") length. Both edges of all core samples used in any of the experiments were removed using electrical saw to eliminate the effect of the inverted drilling mud used in the coring process. There are two broken cores, but they fit as a core plug as shown Figure 7. Four core samples are from the Upper Bakken, 6 core samples from Middle Bakken, and 4 core samples from Three Forks formation.

The core samples used in the EOR experiments are 3.81 cm (1.5") in diameter and from 3.81 to 7.62cm (1.5 to 3") in length. Total number of 3.81cm (1.5") diameter

core samples is 9 core samples, one Upper Bakken, one Lower Bakken, and 7 Middle Bakken cores (Figure 8). Three core samples from the Middle Bakken formation were used in spontaneous imbibition test. Two Middle Bakken cores were saturated with n-octane and used in spontaneous imbibition test and the third Middle Bakken core sample was divided into two twin cores, saturated with crude oil, aged and used in spontaneous imbibition test. All the core samples used in spontaneous imbibition were cleaned with Soxhlet extractor using 3:1 toluene to methanol

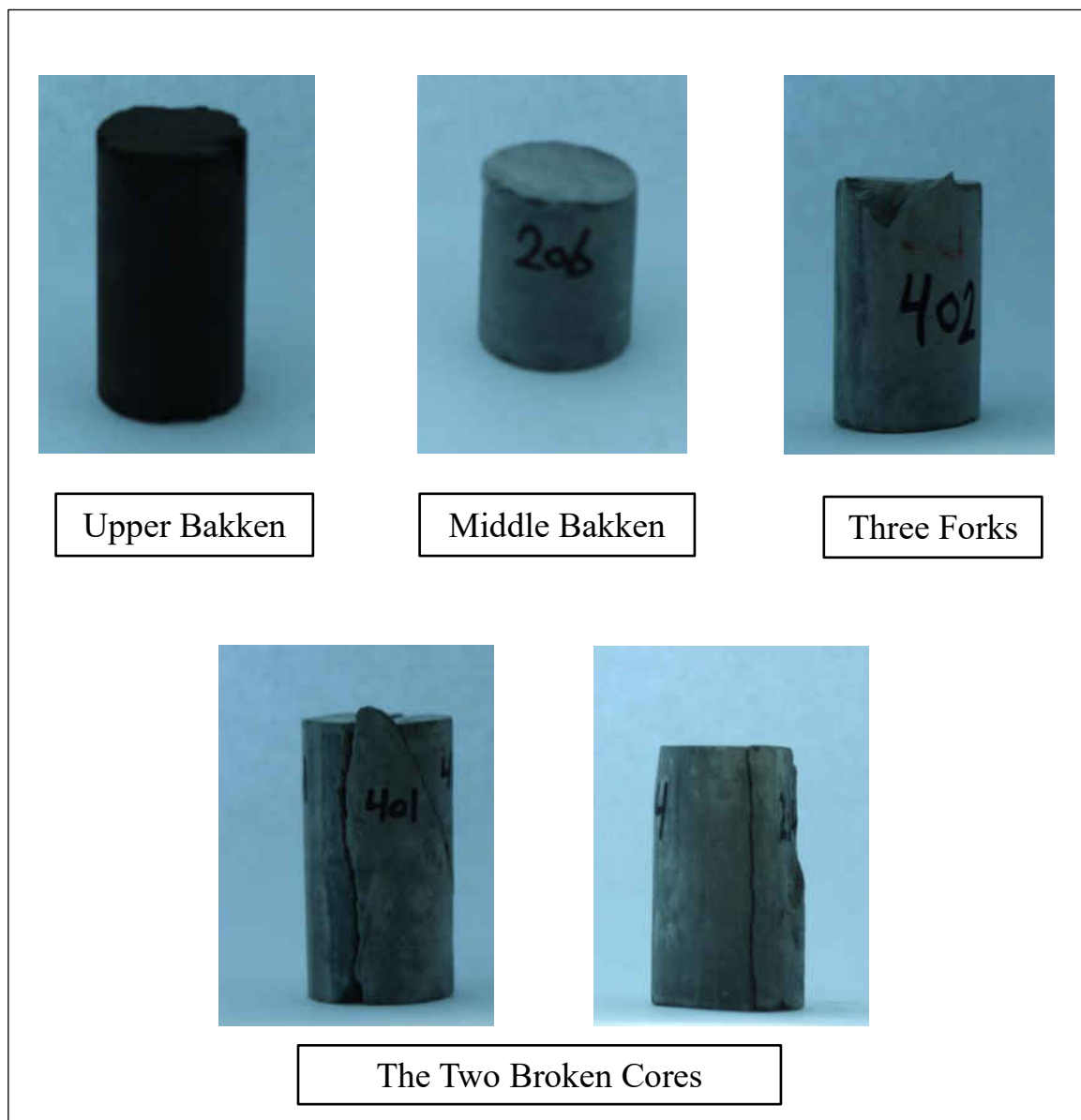


Figure 7- Core Plugs Samples Used in NMR

Porosity was measured for all the 3.81cm (1.5”) diameter core samples using Liquid Saturation Method (LSM) and NMR, and permeability was calculated using Coats with Cut off Model. All the procedures will be discussed later in this chapter.

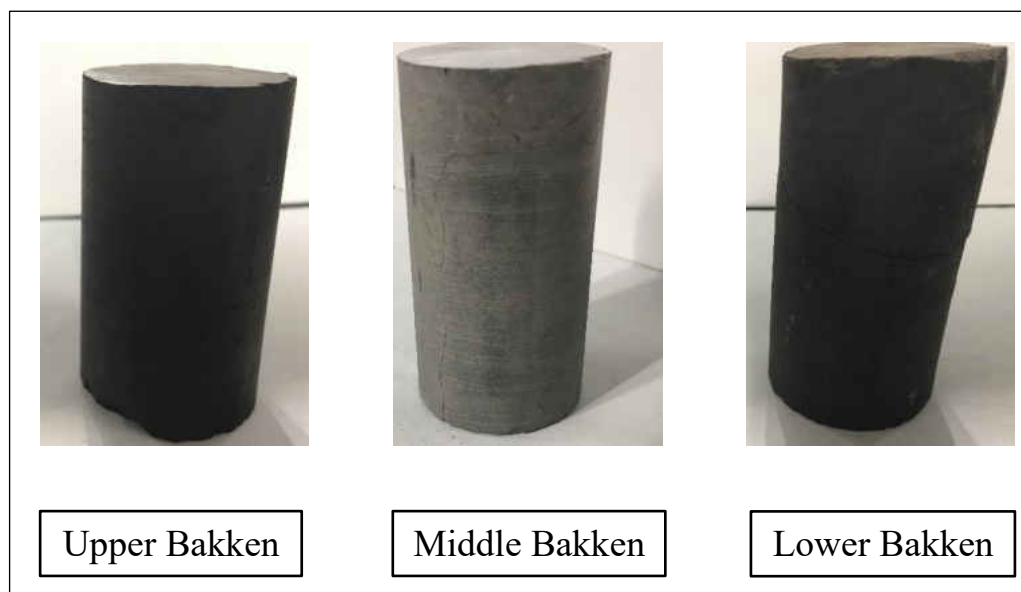


Figure 8- Core Plugs Samples 1.5” Diameter Pictures

2.3 Core Cleaning:

All of the 3.81cm (1.5”) diameter core samples were cleaned using Soxhlet Extraction apparatus. The solvent used was 3:1 toluene to methanol. Toluene was used to dissolve the hydrocarbon components and methanol was used to dissolve the salts [73]. Franz von Soxhlet invented the Soxhlet Extractor in 1879 for extracting lipids from solid material, however now Soxhlet Extractor applications in many fields such petroleum analysis, food analysis, and environmental analysis [74].

The Soxhlet Extractor consists of a flask which contains the cleaning solvent in the bottom and the core sample to be cleaned in filter paper, the flask is in a heater, and a condenser is installed at the flask opening to condense all the evaporated solvent back to flask. The sample should be in a thimble, a thick filter paper. Schematic diagram for the Soxhlet Extractor is shown in Figure 9.

The Soxhlet Extraction Method theory is a continuous solid-liquid extraction. The extraction solvent is heated to reflux, the vapor of the extraction solvent will engulf the core, then the condenser will condense all the evaporated solvent and the condensed solvent drops will drip back to the chamber containing the solid, the solid is surrounded with the thimble, the extraction solvent will soak the core, and the hydrocarbons will dissolve in the toluene while methanol will dissolve the salts and the water will evaporate as the toluene boiling point is 110°C (230°F) [73]. The cleaning process lasted for approximately 7 days, and the cleaning process stopped when the color of the solvent stays clear with no change in the color.

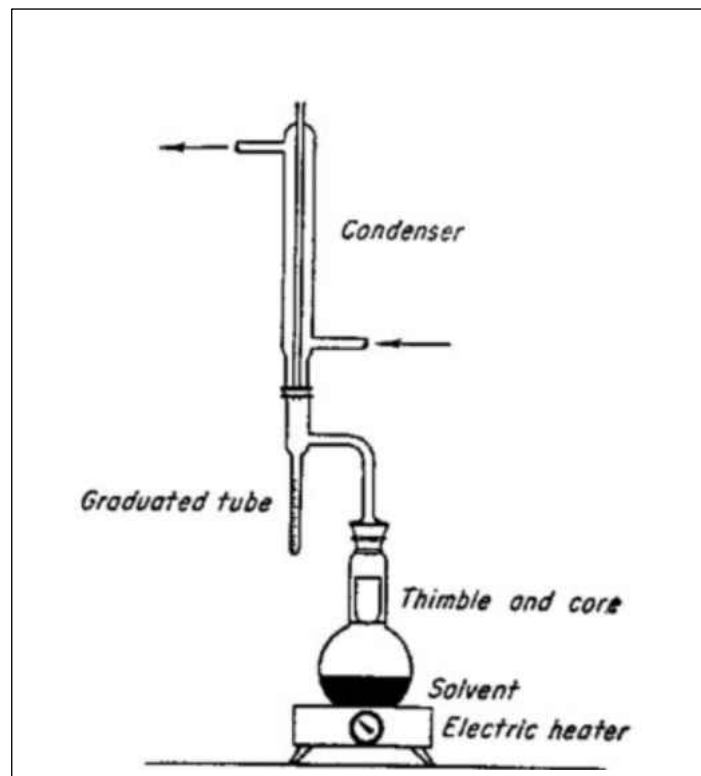


Figure 9- Soxhlet Extraction Method Apparatus [75]

2.4 Core Samples Saturation:

All core samples in this study were saturated using the same method. The saturation setup consists of vacuum pump, two vacuum gauges, saturation cell,

pressure gauge, hand pump for saturation fluid, and saturation fluid tank (Figure 10).

The core samples were vacuumed for 1-1.5 hours (-29.5 in Hg), then saturated with CO₂ for 4 hours, were vacuumed again for 1-1.5 hours (-29.5 in Hg) followed with saturation with CO₂ for 4 hours, then were vacuumed again (-29.5 in Hg) for 1-1.5 hour, and finally introduce the saturation fluid which either formation brine, octane, or crude oil, and pressurize the cell using the hand pump with the saturation fluid to 2,000 psi. During the saturation process, the pressure was monitored continuously to increase the pressure again to 2,000 psi when it decreases.

Saturating the core samples with CO₂ after the vacuum is to replace any air inside the pores with CO₂, because CO₂ is more soluble in both brine and oil to achieve the highest applicable saturation [73]. The saturation process lasted for approximately 4 days, one day for vacuuming and CO₂ saturations and 3 days where the fluid is under 2,000 psi pressure. The core samples will be saturated when no pressure change will be noticed for one day.



Figure 10- Core Saturation Setup

2.5 X-ray Diffraction (XRD) and Scanning Electronic Microscope (SEM):

Rigaku SmartLab XRD analyzer located in the Institute of Energy Studies – College of Engineering at University of North Dakota was used to determine the composition of the Upper Bakken, Middle Bakken, and Lower Bakken formations for the wells in the study. The equipment utilizes cross-beam optics (CBO) which enables changing the incident X-rays by substituting selection slits, and the equipment can be operated in both Bragg-Brentano or parallel beam focusing methods. The equipment is also equipped with both a scintillation counter detector and a D/tex detector for fast data acquisition.

FEI Quanta 650 FEG SEM located in the Institute of Energy Studies – College of Engineering at University of North Dakota was used to take SEM images for the Upper Bakken, Middle Bakken, and Lower Bakken to study the surface of the formations. All the samples used in the XRD and SEM were rock chips from the cores at the same depths.

2.6 Nuclear Magnetic Resonance (NMR):

Oxford Geospec2 Core NMR was used to measure the T_2 and T_1/T_2 ratio for 12 core samples 2.54cm (1”) diameter. As mentioned earlier in the core samples description, the cores are twin cores. All the 2.54cm (1”) diameter core samples used in the NMR characterization was from the well B. The properties of the cores are all listed in Table 3.

Table 3- Core Samples Used in NMR Characterization Properties

Formation	Core Depth (ft)	Diameter (cm)	Sample Mass (g)	Length (cm)	Bulk Volume (cm ³)	Bulk Density (g/cm ³)	Remarks
Upper Bakken (UB)	10596	2.56	58.2740	4.7723	24.57	2.37	
Upper Bakken (UB)	10596	2.56	37.3627	3.0690	15.74	2.37	
Upper Bakken (UB)	10607	2.56	51.6351	4.5480	23.45	2.20	
Upper Bakken (UB)	10607	2.56	34.8792	3.1533	16.19	2.15	
Middle Bakken (MB)	10620	2.57	60.3595	4.6693	24.17	2.50	
Middle Bakken (MB)	10620	2.58	42.7755	3.3700	17.55	2.44	
Middle Bakken (MB)	10631	2.57	61.6073	4.6770	24.23	2.54	
Middle Bakken (MB)	10631		45.2302		17.79	2.54	(Broken)
Middle Bakken (MB)	10650	2.57	64.5841	4.7373	24.60	2.63	
Middle Bakken (MB)	10650	2.58	42.2231	3.1333	16.40	2.57	
Three Forks (TF)	10687	2.57	42.2230	3.2740	16.99	2.49	
Three Forks (TF)	10687		61.7735		24.85	2.49	(Broken)

As it is in the table there is two twin as-received core samples (no cleaning performed, not preserved) from each depth, the first one was saturated with octane and the second was saturated with formation brine. Then T_2 and T_1/T_2 ratio were measured at ambient temperature 30°C (86°F) using 2.3MHz frequency. The measurements were done using Carr, Purcell, Meiboom and Gill (CPMG) pulse sequence. Data acquisition time was 2.5s. T_2 and T_1/T_2 ratio were also measured using 22MHz frequency using NMR equipment located at Core labs (Houston) to study the effect of frequency change in the NMR response. T_2 was measured using 2.3MHz frequency at 25° (77°) and 105°C (221°F) to study the effect of temperature on NMR response for the Bakken cores. All the previous measurements except the 22 MHz measurements were conducted at Rice University.

At University of North Dakota labs, NMR was also used to measure the porosity of the 3.81 cm (1.5") diameter after saturating the core samples with brine solution with 10,000 ppm salinity, and the permeability was calculated using Coats with cut off Model.

2.7 Phase Behavior:

In the phase behavior study, n-octane was used as a model oil. Thirteen thermally stable surfactants were used in this study. Surfactants composition and activity are shown in Table 4. All the phase behavior samples were prepared in sealed pipettes, and the pipettes were immersed in silicon oil in closed tubes to prevent any leakage to contaminate the heating bath, this method called encased pipette method and was developed by Maura Puerto [76].

All the surfactants were prepared 4% concentration in formation brine. 2ml sample of aqueous solution of each surfactant was sealed in pipette and a second sample 2% overall surfactant, n-octane and formation brine, at WOR ~1 was prepared then all the samples were equilibrated at 105° (221°F) in a heating bath. After that 24 blends from the 13 surfactants were done based on the response of each surfactant in the two previously prepared samples. The surfactants which

were present in the oleic phase was blended with the surfactants present in the aqueous phase and the solubilization parameters were calculated for each blend.

The presence of the surfactants in the oleic or aqueous phase was detected by using laser beam scattering as shown in Figure 11. When the surfactant is present in the phase the laser beam will be scattered, and on the other hand there will be no laser beam scattering if there is no surfactant present. Also, if the laser scattering intensity is lower in one phase than the other that indicates more surfactants is present in this phase than the other phase.

2.8 Interfacial Tension (IFT):

After the phase behavior study, one surfactant blend was chosen. IFT measurements were conducted using Spinning Drop method at reservoir temperature 105 (221°F) using Grace M6500 Spinning Drop Tensiometer in Rice University lab (Figure 12). IFT measurements were conducted using n-octane and light crude oil. IFT measurements were conducted with 1% surfactants solution in formation brine after equilibrium at 105°C (221°F) with n-octane or light crude oil (depends on which oil will be used in the IFT measurement) (Figure 13). In the spinning drop method, a drop of oil (lower density phase) was situated in the 1% surfactant solution in formation brine (higher density phase) and rotated with high speed (range from 4,000 to 8,000 rpm), then using the diameter of the drop and the rotation speed the IFT can be calculated using Equation 1.

$$\sigma = IFT = \frac{1}{4} \Delta\rho\omega^2 R^3$$

Equation 1- IFT Calculation

Table 4- Surfactants Composition and Activity

Surfactant Name	Composition	Activity (%)	Remarks
Mackam Lab	Lauryl Betaine C ₁₂ Betaine	36	pH= 8.4
The Lubrizol Corporation	Oleyl Betaine C ₁₈	30	
Avanel S 150 CGN	C ₁₂ -C ₁₅ EO Sulfonate	35	
Avanel S74	C ₈ -EO ₃ Sulfonate	33.5-36.5	
Avanel S70	Alkylethersulfonate (C12)	35	
Enordet 0242	C ₂₀ -C ₂₄ IOS	20-24	
Enordet 0332	C ₁₅ -C ₁₈ IOS	30	
L38	Ethoxylated Carboxylated Surfactant	100	
Dowfax 8390	Alkyldiphenyloxide Disulfonate	35	
Dowfax 2A1	1,1'-oxo bis-tetrapropylene deriv. sulfonate	45.2	
XOF 112C	C12-14 alcohol , Propoxylated, low degree of Ethoxylation, Carboxylated	25	
XOF 315C	mono (2,4-dinonylphenol) ether, Propoxylated, moderate degree of Ethoxylation, Carboxylated	25	
XOF 316C	mono (2,4-dinonylphenol) ether, Propoxylated, high degree of Ethoxylation, Carboxylated	25	

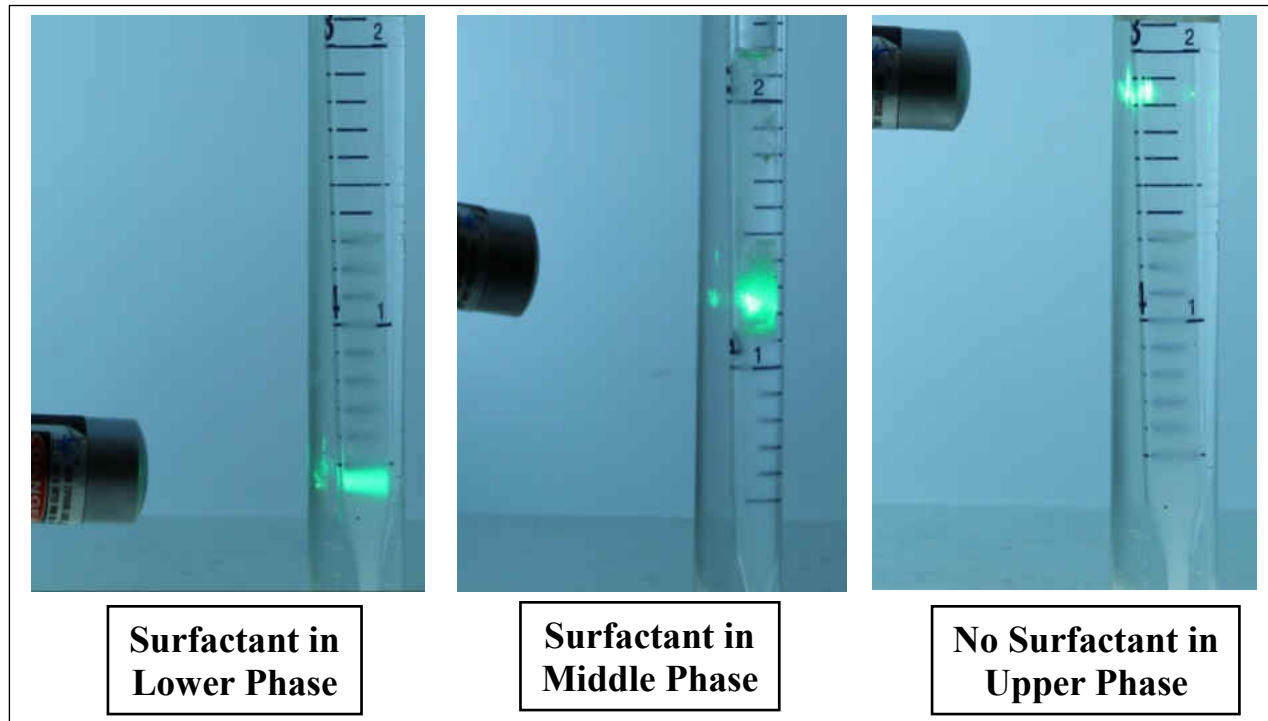


Figure 11- Surfactant detection Using Laser Beam Scattering

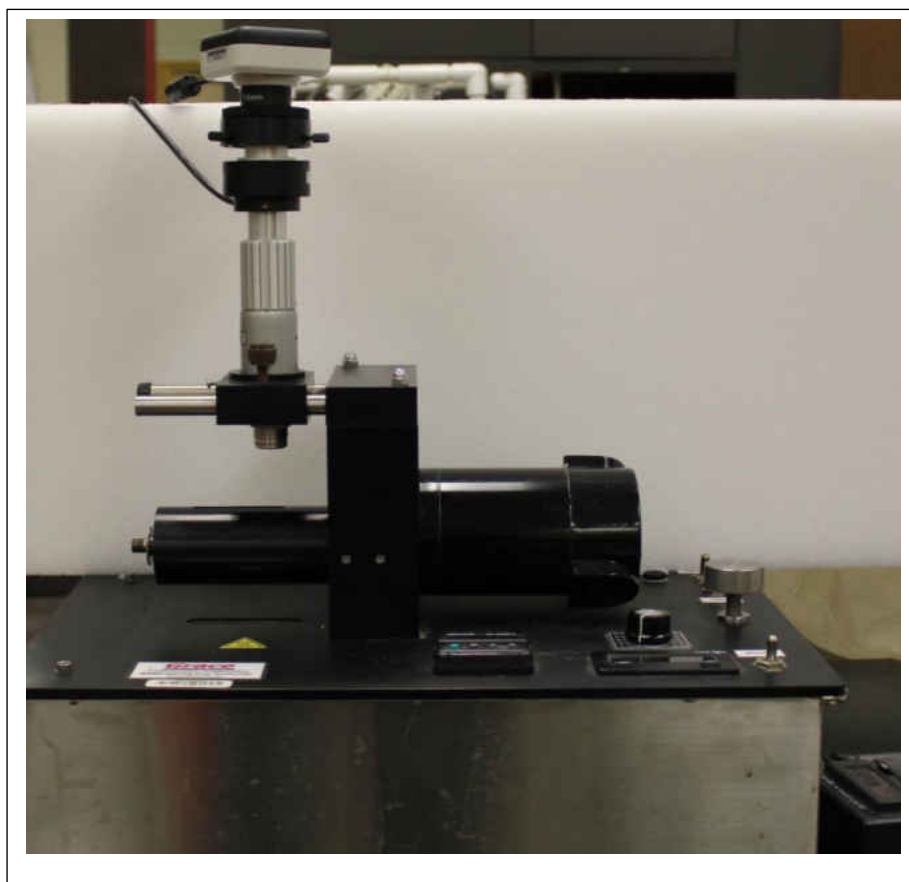


Figure 12- Grace M6500 Spinning Drop Tensiometer

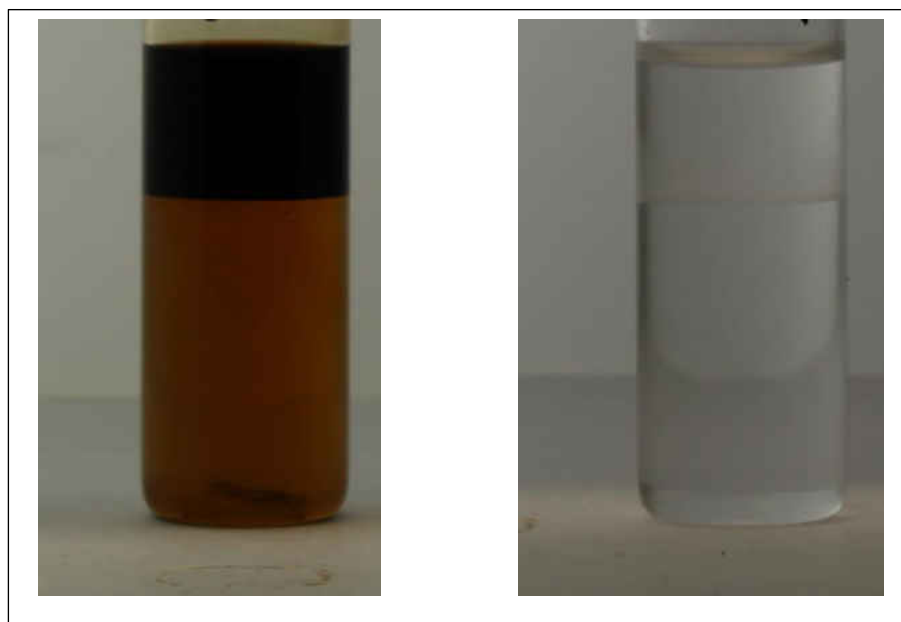


Figure 13- Solutions Used for IFT Measurements after Equilibrium

2.9 Spontaneous Imbibition:

High temperature Amott cells was used to conduct imbibition test under reservoir temperature 105° (221°F). Pressure relief valve was installed on the top of the Amott cell to hold the pressure up to 15 psi to eliminate totally or partially the effect of solution gas drive. All the core plugs used in this test were Middle Bakken samples with diameter of 3.81cm (1.5”). Two core samples were saturated with n-octane, one was used for blank imbibition test using only formation brine and the second in presence of 1% surfactant. Two twin cores were saturated with light crude oil and aged in crude oil at reservoir temperature for 20 days. After aging, one of the core samples was used for blank imbibition test with formation brine and the second was in the presence of 1% surfactant solution. Oil recovery efficiency was calculated.

CHAPTER 3 : RESULTS AND DISCUSSION

3.1 Porosity Results:

Porosity results were obtained using Liquid Saturation Method (LSM) and NMR measurements. The results obtained from LSM and NMR were compared. LSM is used to calculate the porosity of the core samples by weighting. Dimensions of the samples were measured to calculate the bulk volume (V_B). Weights of the core samples before and after saturation were measured (wt_i & wt_{sat}). Density (ρ) of the saturation fluid was measured, then Equation 2 was used to calculate the porosity (Φ).

$$\Phi = \frac{(wt_{sat} - wt_i) / \rho}{V_B}$$

Equation 2- LSM Porosity Calculation

The core samples tested in NMR characterization measurements were 12 twin cores with 1" diameter. Six cores were octane saturated and the other 6 cores were brine saturated. Table 5 summarizes the porosity results for the cores used in NMR characterization and Table 6 shows the porosity results for the core samples with 1.5" diameter used in spontaneous imbibition test and also used to measure the porosity and permeability for different formations. Measurements of the as-received porosity for the 1.5" diameter core samples were not performed and that causes the difference in porosity values between the NMR and LSM porosity. The as-received porosity has been taken in consideration with the NMR characterization measurements.

The porosity range is ~2-7% in all the depths. Permeability was calculated for the 1.5" diameter core samples using Coates with Cut off Model. The permeability range is 0.3-1.8 μd except the Upper Bakken core sample was 11.93 μd and one Middle Bakken sample was 7.61 μd .

Table 5- Porosity Measurements for the core samples used in the NMR Characterization Tests

Description	Depth (ft)	Saturation Fluid	Porosity Change LSM (%)	Porosity Change NMR (pu)	As received Porosity (pu)	Total NMR Porosity (pu)
Upper Bakken-Well 16443	10596	Octane	4.72	5.1	3.1	8.2
Upper Bakken-Well 16443	10607	Octane	5.35	6.3	3.4	9.7
Middle Bakken-Well 16443	10620	Octane	5.85	6.2	2.5	8.7
Middle Bakken-Well 16443	10631	Octane	4.35	4.8	2.5	7.3
Middle Bakken-Well 16443	10650	Octane	2.05	2.1	1.5	3.6
Three Forks-Well 16443	10687	Octane	4.82	5.9	2.9	8.8
Upper Bakken-Well 16443	10596	Bakken Brine	1.56	0.9	3.3	4.2
Upper Bakken-Well 16443	10607	Bakken Brine	2.05	1.9	3.2	5.1
Middle Bakken-Well 16443	10620	Bakken Brine	6.44	6.2	2.5	8.7
Middle Bakken-Well 16443(Broken)	10631	Bakken Brine	5.18	5.1	2.6	7.7
Middle Bakken-Well 16443	10650	Bakken Brine	2.37	2.4	1.5	3.9
Three Forks-Well 16443 (Broken)	10687	Bakken Brine	5.68	6.4	3.0	9.4

Table 6- Porosity Measurements for the core samples used in the EOR Experiments

Description	Depth	Saturation Fluid	LSM Porosity (%)	NMR Porosity (pu)	NMR Permeability (μ d)
Upper Bakken-Well 16652	10639.5	Oil	8.18	10.99	11.93
Middle Bakken-Well 16652	10654.7	Oil	4.70	5.43	1.10
Middle Bakken-Well 16652	10666.5	Oil	5.44	7.11	1.29
Middle Bakken-Well 16652	10676.5	Oil	6.78	8.42	0.48
Lower Bakken-Well 16652	10708	Oil	5.83	7.86	1.12
Middle Bakken-Well 16443	10612	Oil	7.02	8.60	7.61
Middle Bakken-Well 16443	10628	Oil	2.83	4.20	0.34
Middle Bakken-Well 16443	10638	Oil	7.31	8.78	1.75
Middle Bakken-Well 16443	10651	Oil	7.04	8.67	0.60

3.2 XRD and SEM Results:

Three rock samples, from the Upper Bakken, Middle Bakken and Lower Bakken formations were measured with XRD to study the mineralogy of the formations and another three samples were used for SEM analysis to study the surface of the three formations. Sample preparation has high impact on the SEM images. The samples were preserved in epoxy to facilitate the handling as shown in Figure 14. All the samples surface has been polished using abrasive papers starting with 80#, 240# and 600# then 800# and 1200# to make the surface smooth. The smoother the surface is, the better quality the SEM image will be.



Figure 14- Sample Preparation for SEM Test

Quartz is the main mineral in the three formations from these two wells. Upper Bakken has ~47% quartz, ~33% clay minerals and ~15% plagioclase. Plagioclase will form clay minerals. Middle Bakken has ~43% quartz, ~23.6% carbonate minerals, and ~17% clay minerals. Lower Bakken has the highest quartz with

~65.5%, ~4% carbonate minerals, and ~19% clay minerals. Figures 15 shows comparison of the XRD results for the rock samples from the Upper Bakken, Middle Bakken and Lower Bakken formations. The SEM analysis for rocks from the Upper Bakken, Middle Bakken and Lower Bakken formations are shown in Figures 16, 17 and 18.

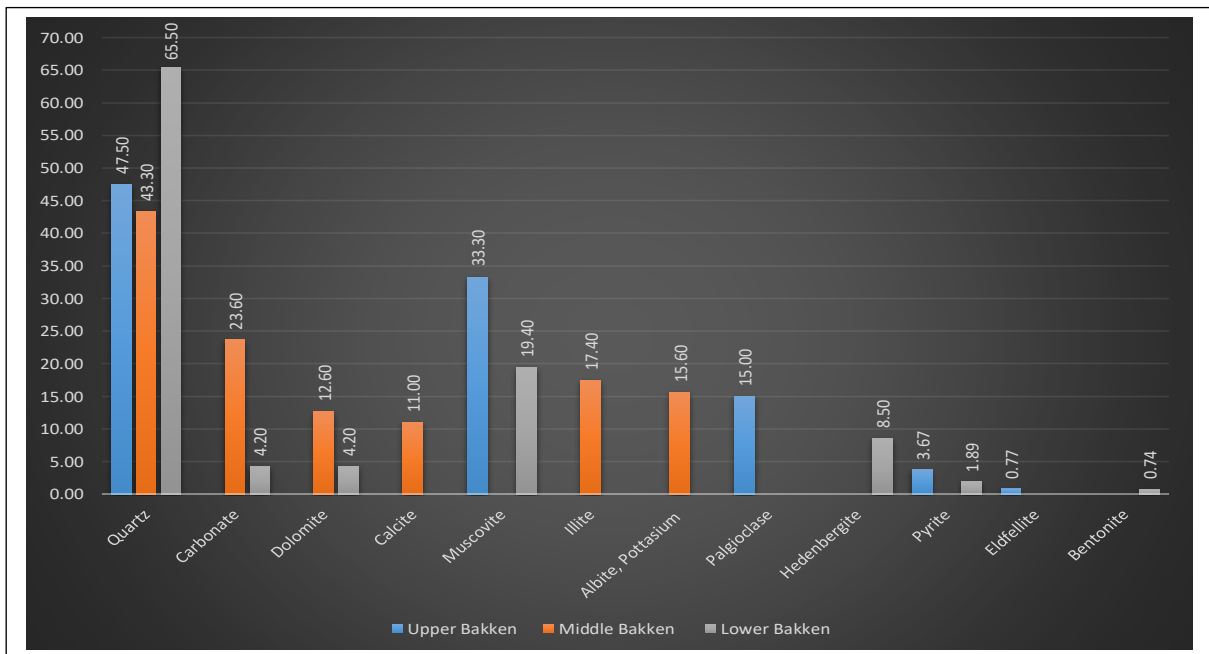


Figure 15- XRD Results for Upper Bakken, Middle Bakken and Lower Bakken

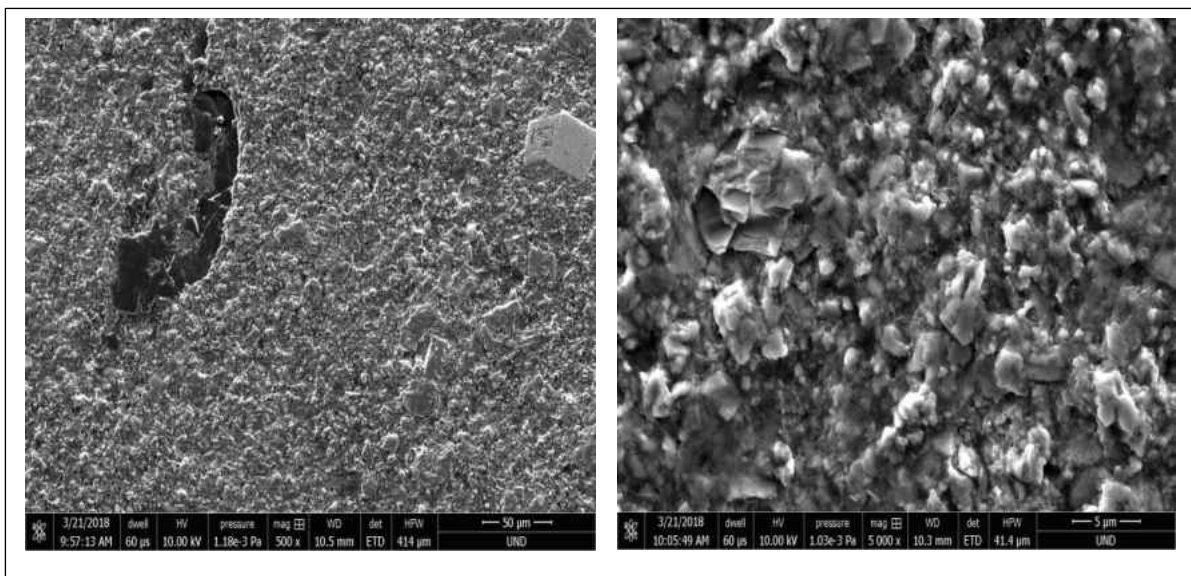


Figure 16- SEM Images for Upper Bakken

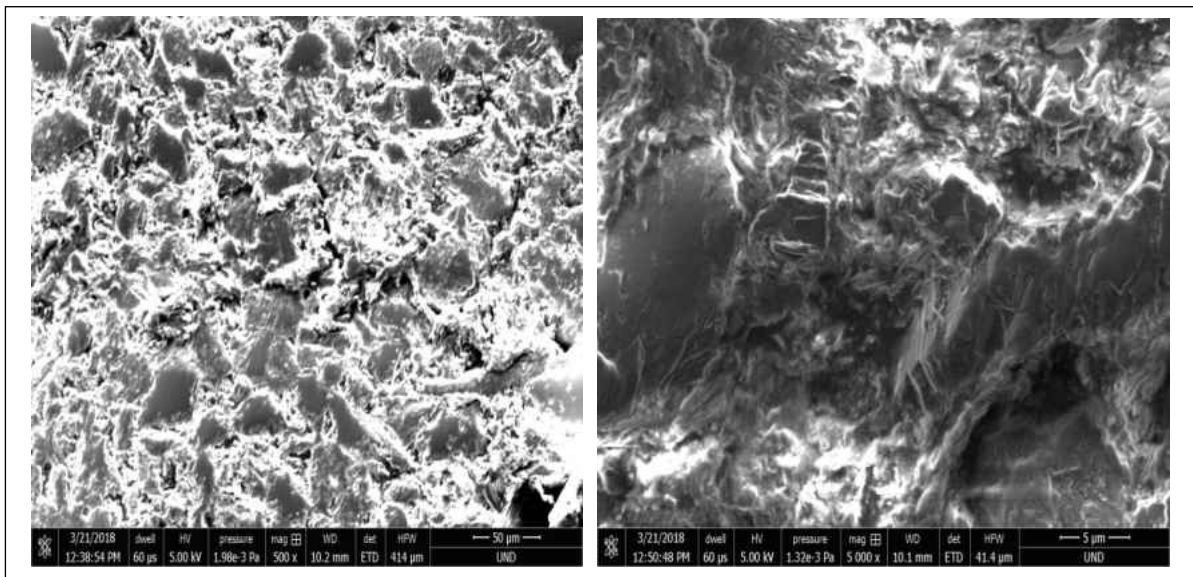


Figure 17- SEM Images for Middle Bakken

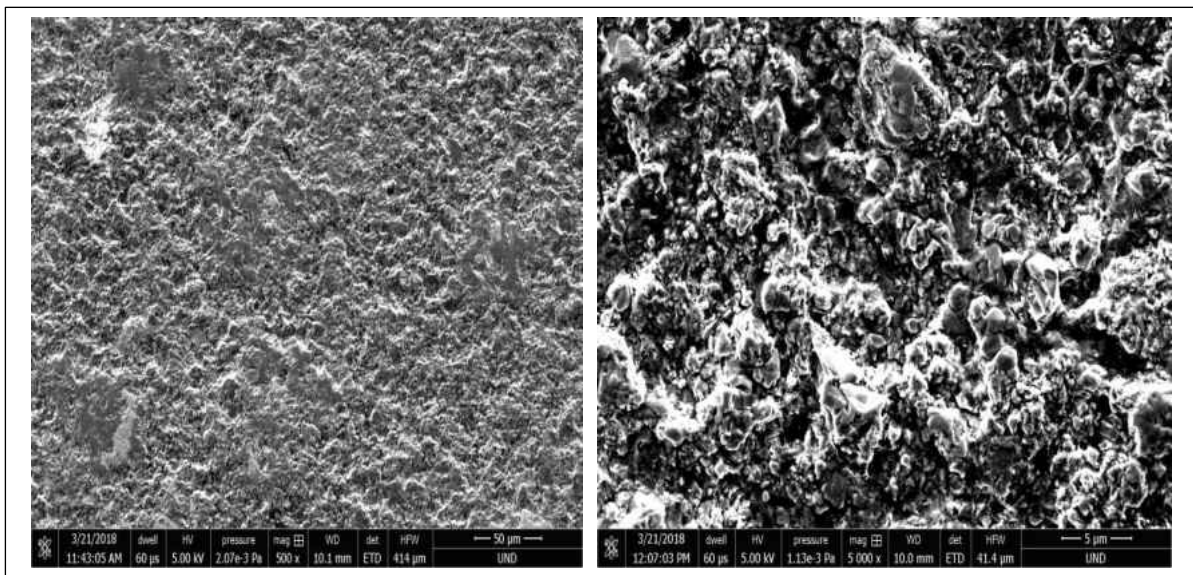


Figure 18- SEM Images for Lower Bakken

3.3 Nuclear Magnetic Resonance (NMR) Results:

NMR results are divided into 3 main sections: results using 2.3 MHz Larmor frequency at 30°C; NMR results using different Larmor frequencies 2.3 MHz and 22 MHz at 30°C; and NMR results using 2.3 MHz Larmor frequency at two different temperatures 25° and 100°C. As mentioned in Chapter 2, Twelve twin core samples with 1” diameter were used in the NMR characterization. T_2 and T_1

were measured for the as-received core samples. Six core samples were saturated with octane and the other 6 samples were saturated with formation brine. The hydrogen index (HI) for the formation brine was measure and used in all the NMR porosity calculations, the HI for the formation brine is 0.913 and the density is 1.135 g/cm³.

3.3.1 NMR Results using 2.3 MHz Larmor Frequency – 30°C:

T₂ and T₁ were measured for the saturated core samples using 2.3 MHz Larmor frequency and echo spacing 0.2 ms at 30°C. In the Upper Bakken cores the octane saturation was higher than the brine saturation in the twin cores because very little amount of brine entered the pores of the Upper Bakken samples, while the same saturation process and pressure was used with all the cores, the octane saturation was consistent with the Liquid Saturation Method results. Surface relaxivity for octane is larger than brine. the two previous observations give indication that the Upper Bakken is preferentially oil wet. For octane-saturated cores, there is noticeable change in T₁-T₂ map, either small change or totally merged with the octane peak. For the brine-saturated samples, there is no noticeable change, which indicates presence of hydrocarbons in the as-received samples. Figures 19 and 20 show the T₁-T₂ 2D maps for the Upper Bakken octane, brine-saturated and as-received core samples.

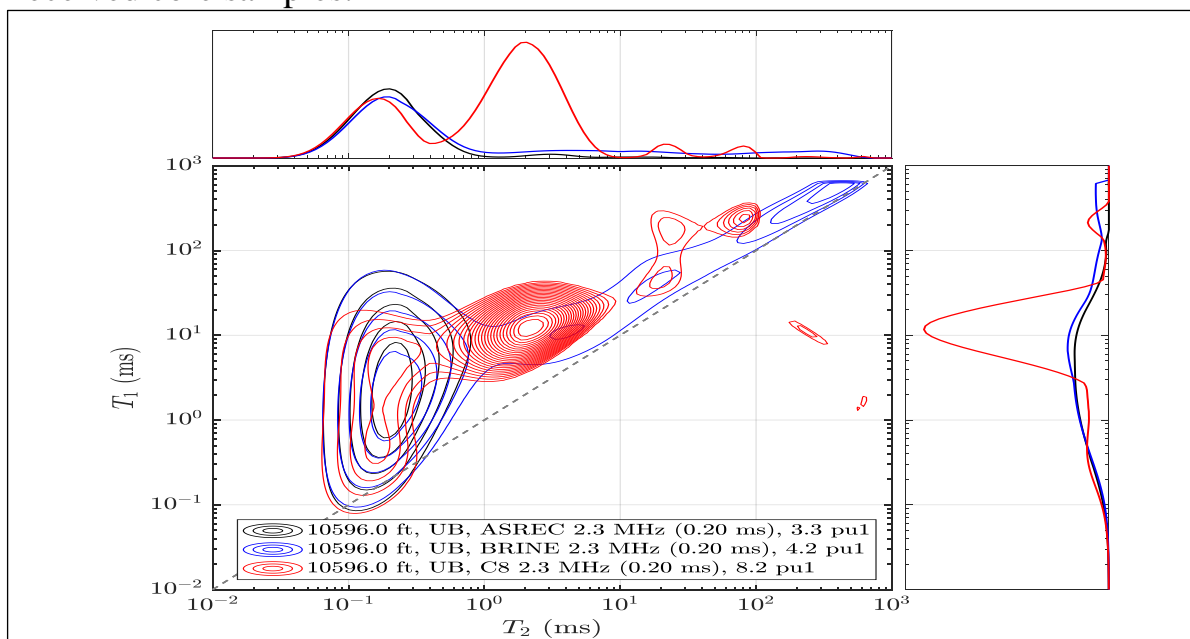


Figure 19- T₁-T₂ 2D Map for Upper Bakken 2.3 MHz (Depth 10596 ft)

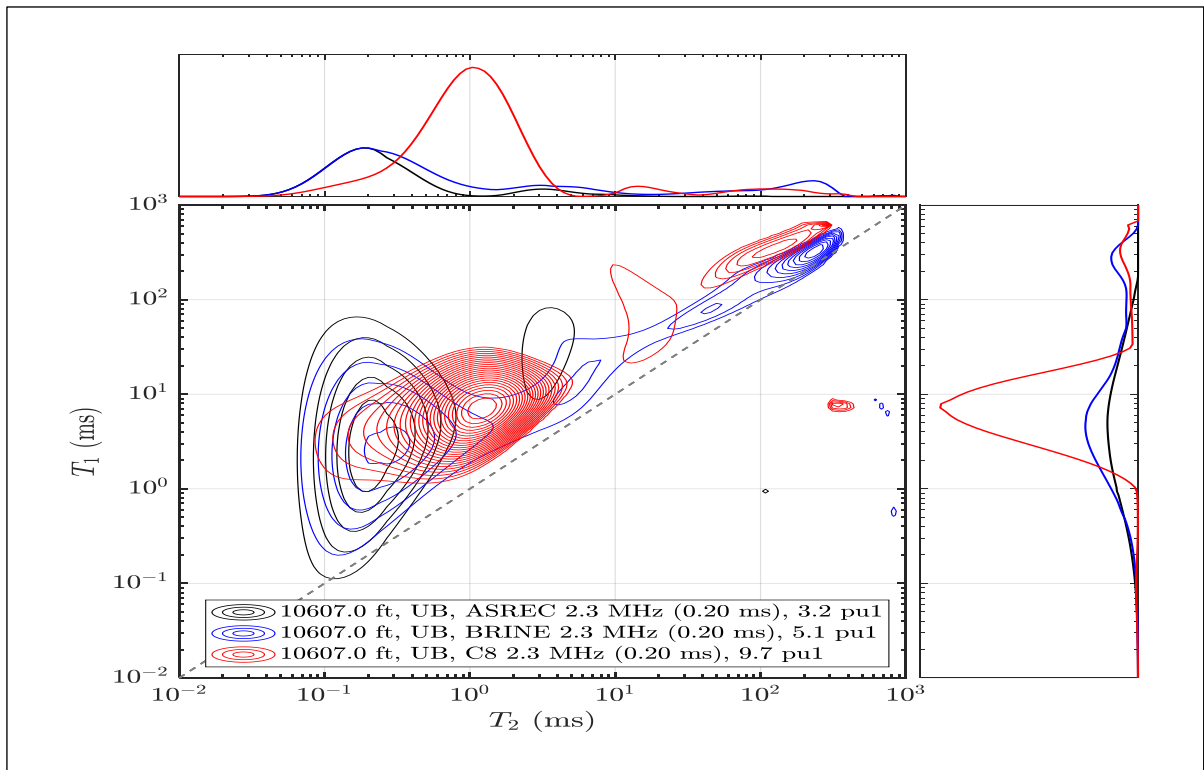


Figure 20- T_1 - T_2 2D Map for Upper Bakken 2.3 MHz (Depth 10607 ft)

For the Middle Bakken and Three Forks core samples, octane and brine saturation in the twin cores was approximately the same and consistent with the Liquid Saturation Method results. Surface relaxivity for brine is larger than for octane. The two previous observations give indication that the Middle Bakken and Three Forks are preferentially water wet or intermediate wet. There are two peaks in the as-received measurements. In the shallower depths, one of the peaks will merge with the octane peak in the octane saturation and the second will merge with the brine saturation but with the deeper samples both peaks will merge with the brine peak which indicates increase of water presence and decrease of hydrocarbons in the as-received samples with the depth increase. Figures 21 to 24 show the T_1 - T_2 2D maps for the Middle Bakken and Three Forks octane, brine saturated and as-received peaks.

Figure 25 shows the summary of the T_2 and T_1 distribution for the octane, brine saturated and as-received core samples measured using 2.3 MHz Larmor frequency at 30°C. Figure 26 shows comparison between the porosity results using Liquid Saturation Method and NMR measurements.

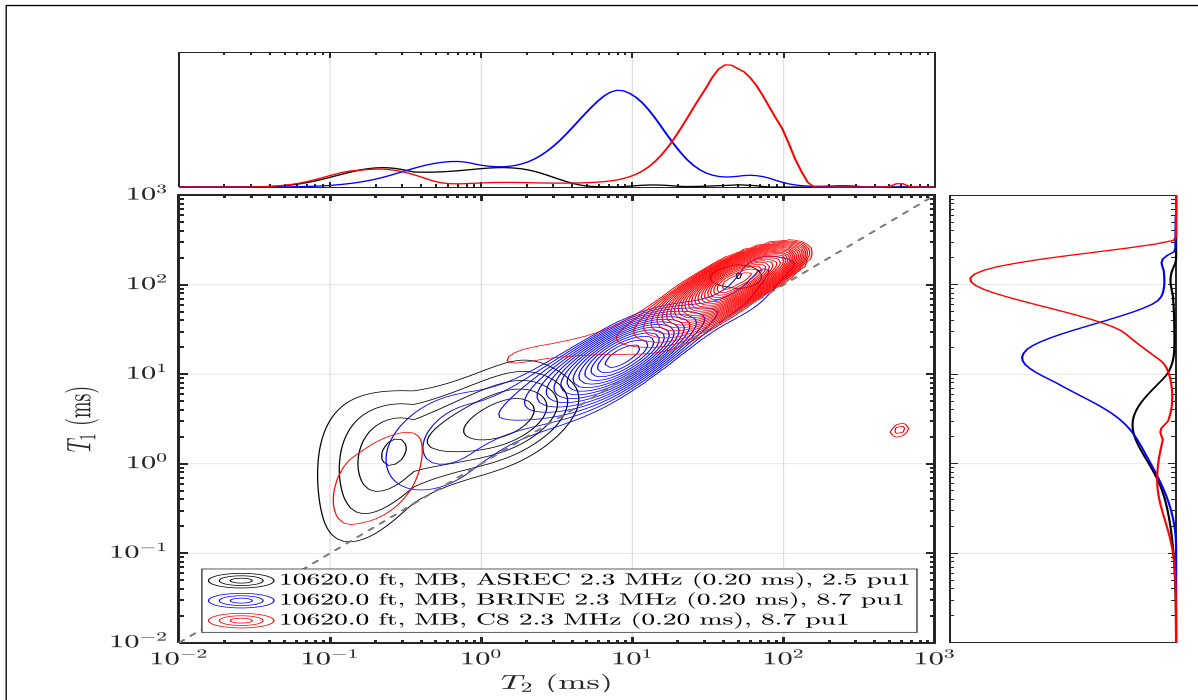


Figure 21- T_1 - T_2 2D Map for Middle Bakken 2.3 MHz (Depth 10620 ft)

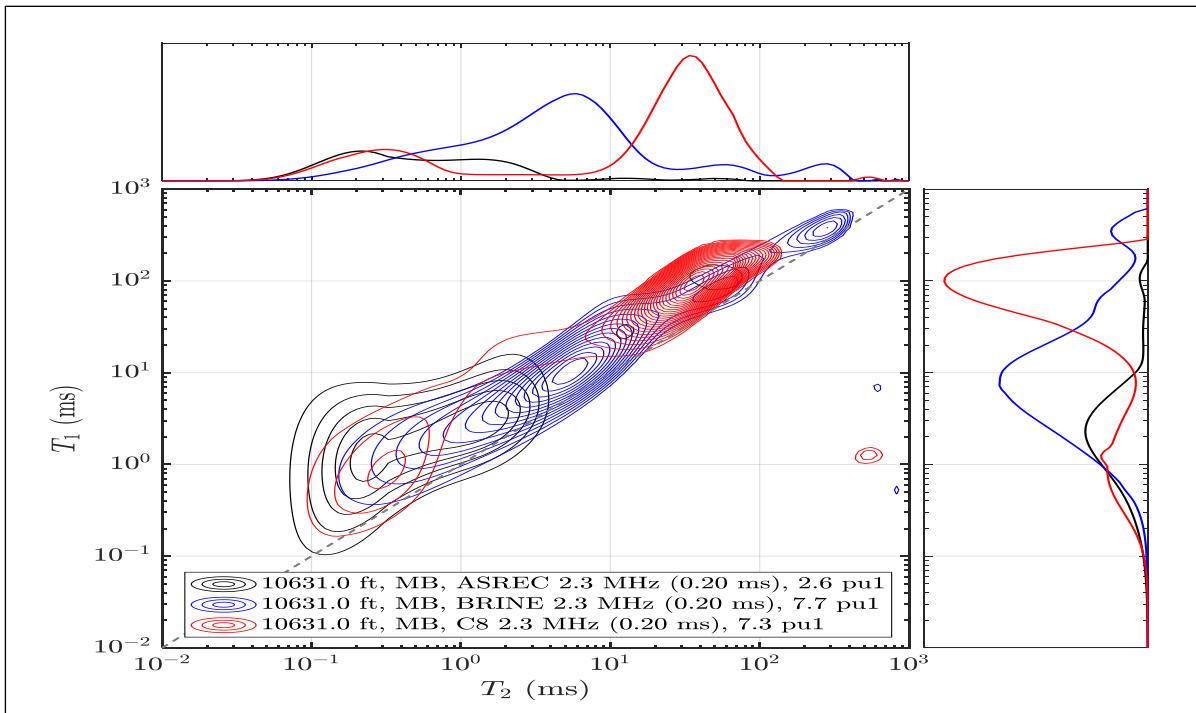


Figure 22- T_1 - T_2 2D Map for Middle Bakken 2.3 MHz (Depth 10631 ft)

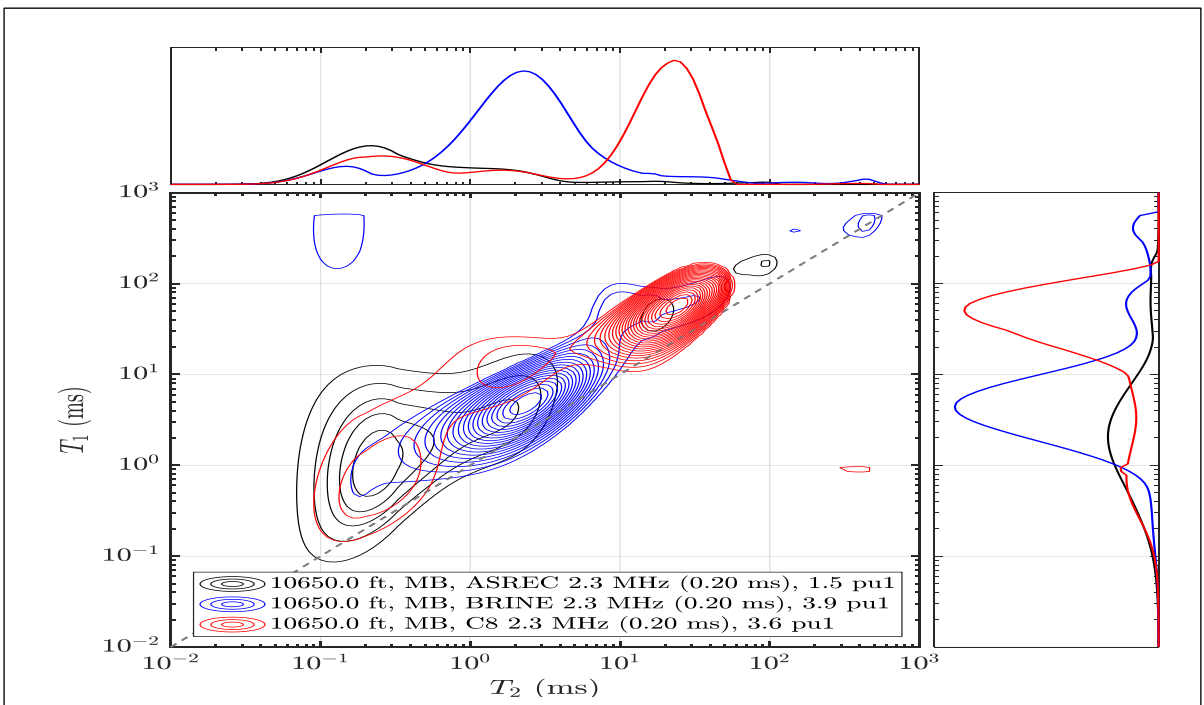


Figure 23- T₁-T₂ 2D Map for Middle Bakken 2.3 MHz (Depth 10650 ft)

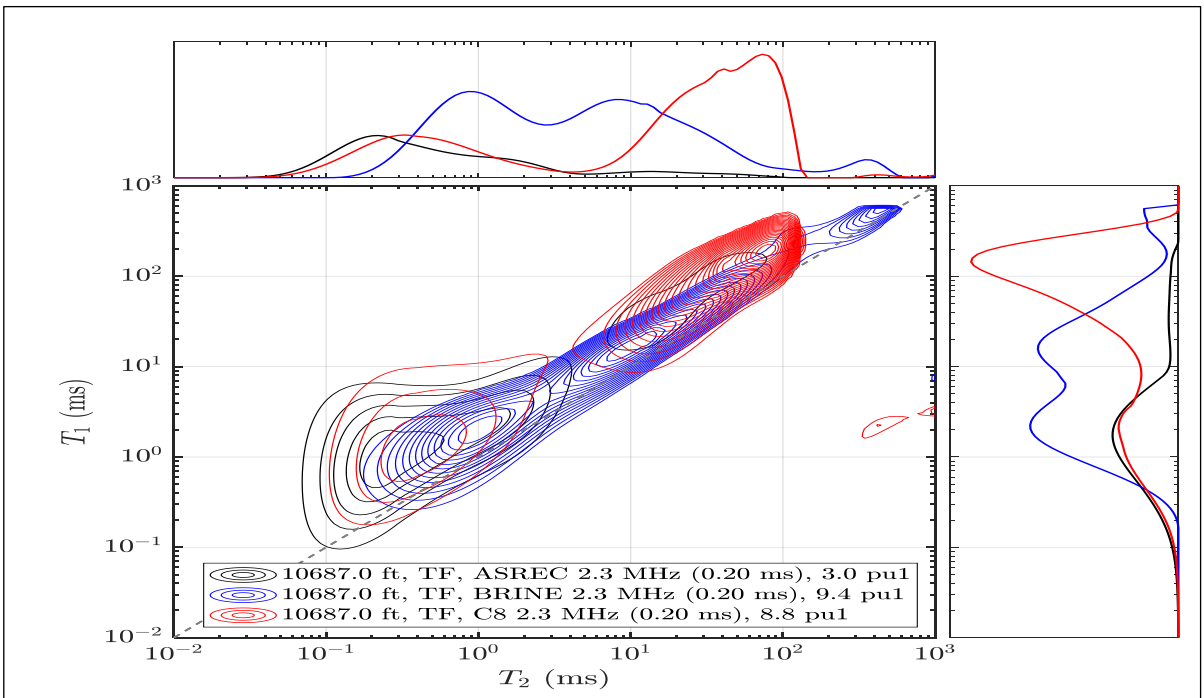


Figure 24- T₁-T₂ 2D Map for Three Forks 2.3 MHz (Depth 10687 ft)

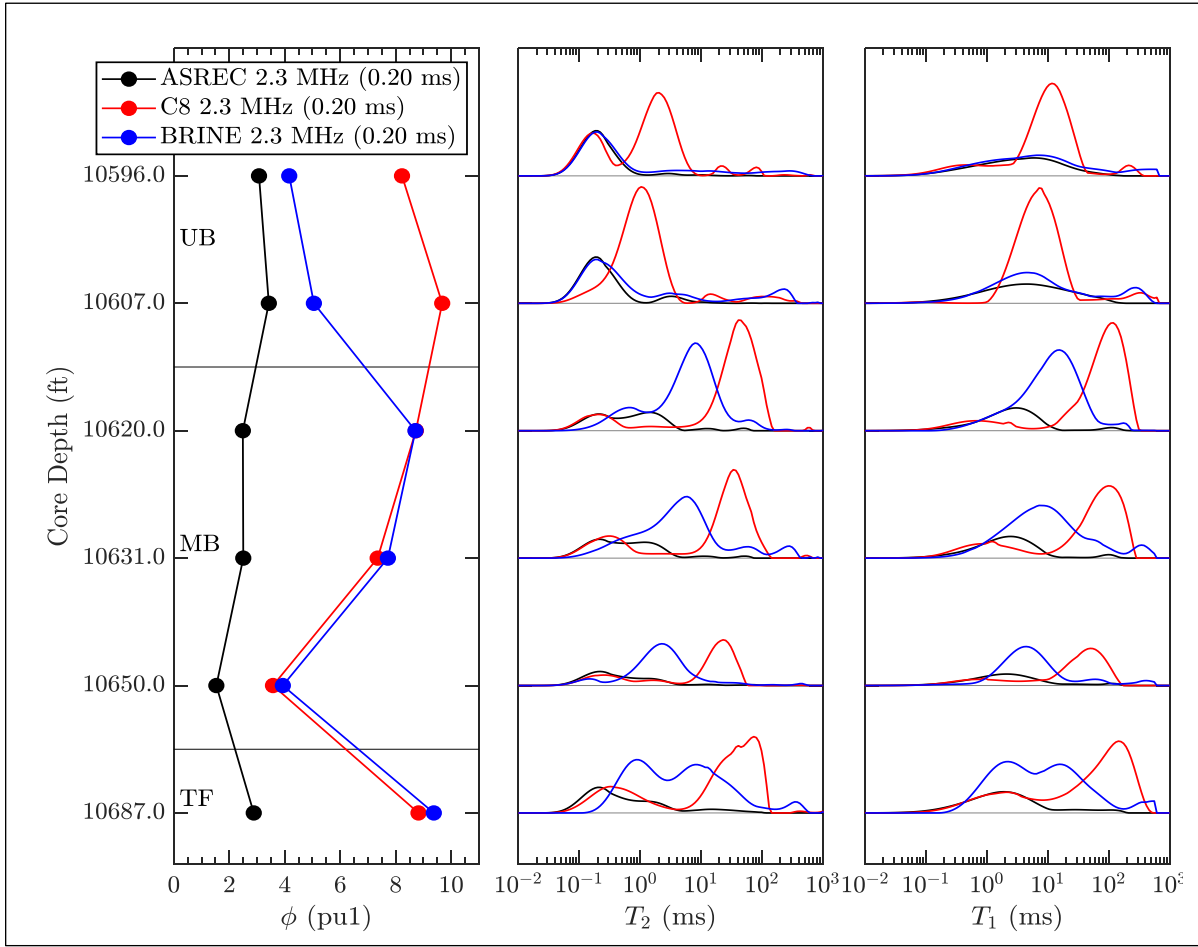


Figure 25- T_2 and T_1 Distribution Summary - 2.3 MHz

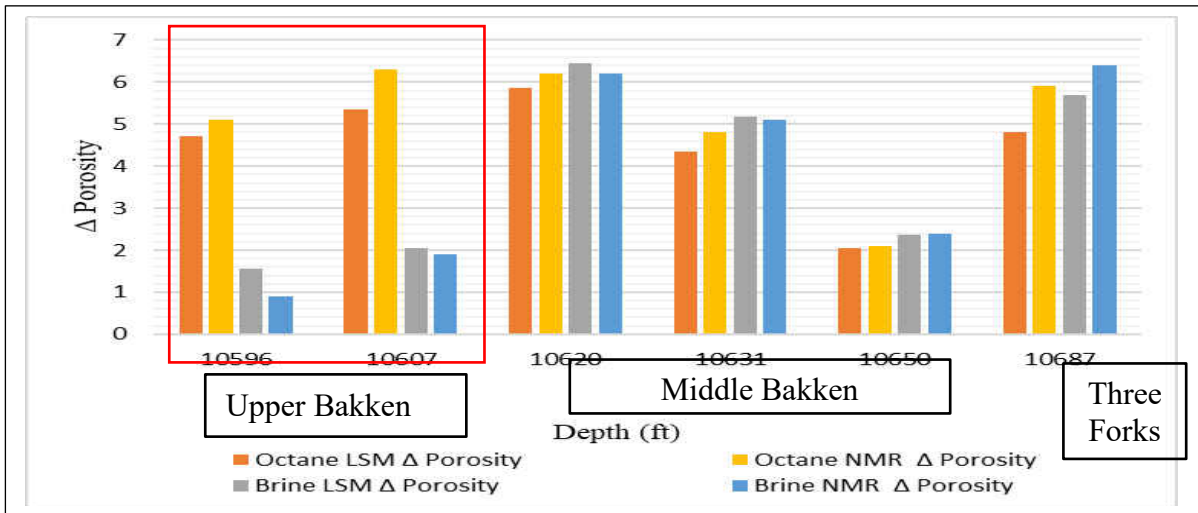


Figure 26- Comparison of LSM and NMR Porosity Change Results

3.3.2 NMR Results using 2.3 & 22 MHz Larmor Frequencies at 30°C:

NMR measurements using 22 MHz Larmor frequency were conducted at the Core Labs. All the data were compared with the 2.3 MHz, the measurements using 22 MHz were measured using two echo spacing of 0.06 and 0.2 ms. All the measurements were conducted on the same samples with the same saturation, the core samples weight was recorded before and after each measurement to confirm that there is no significant loss in the saturating fluid. More fast relaxing peaks can be measured using high frequency with shorter echo spacing. Using high frequency can result in internal gradient making T_2 shorter.

In the octane saturated Upper Bakken core samples, T_1 increased with factor of 6, additional 5 pu at short T_2 was observed with increasing the frequency and no internal gradient observed at 22 MHz. Figure 27 and 28 show the T_1 - T_2 2D maps for the octane saturated Upper Bakken core samples.

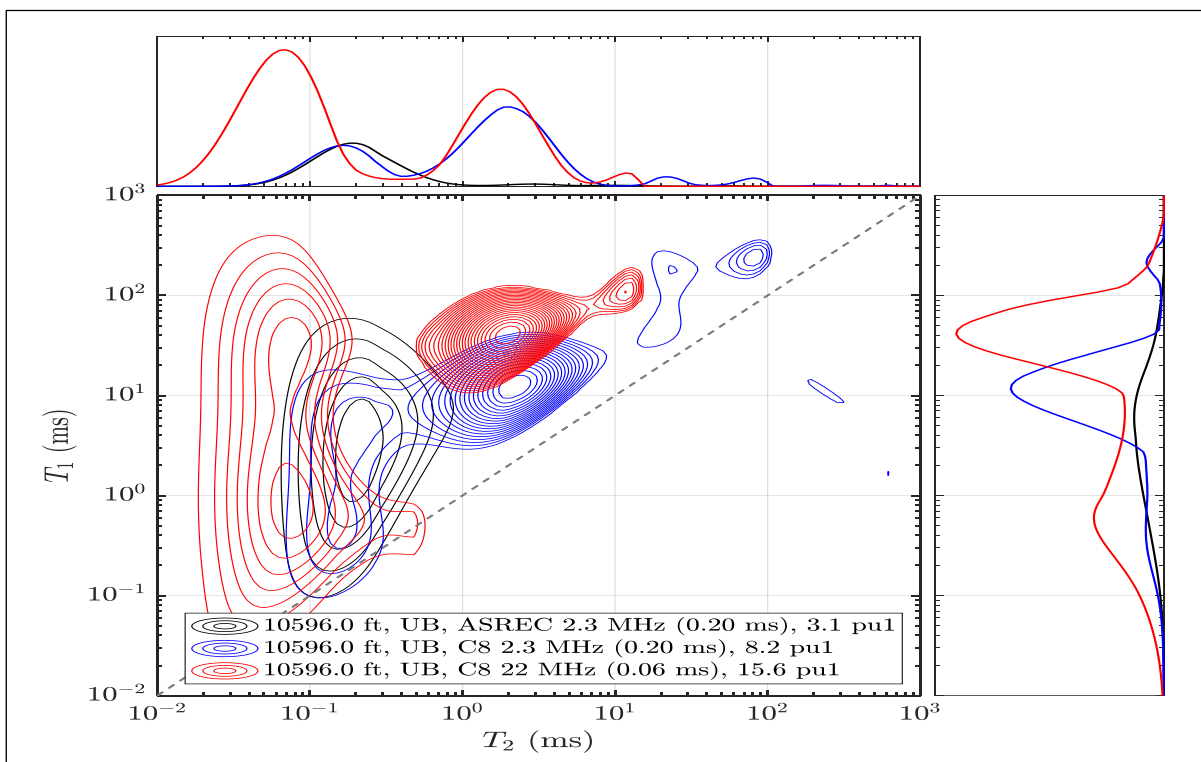


Figure 27- T_1 - T_2 2D Map - Octane Saturated Upper Bakken 2.3 & 22 MHz (Depth 10596 ft) On the other hand, in the brine saturated Upper Bakken core samples, Large T_1/T_2 ratio was observed, additional 7 pu at short T_2 with increasing the frequency. From the previous observations, the additional porosity observed has larger volume of saturating fluid than the actual volume calculated using the Liquid

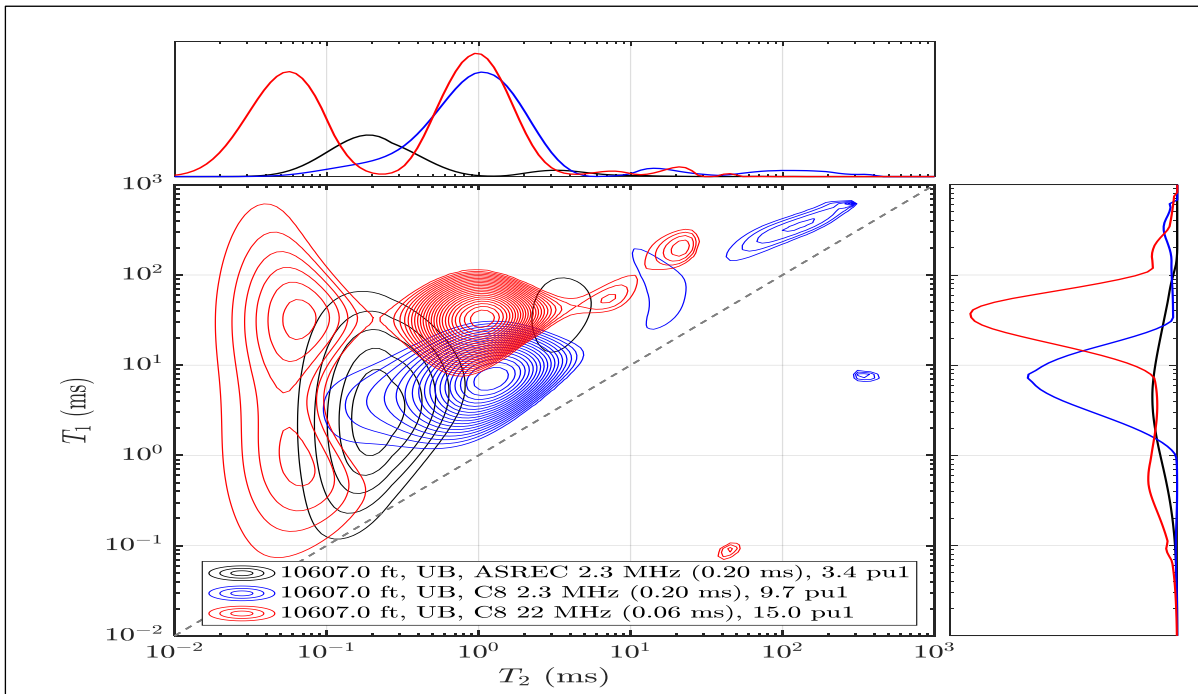


Figure 28- T₁-T₂ 2D Map – Octane Saturated Upper Bakken 2.3 & 22 MHz (Depth 10607 ft) Saturation Method (by weighting) which may be due to the presence of bitumen in the Upper Bakken core samples and this hypothesis can be strengthened by the large T₁/T₂ ratio observed. Figures 29 and 30 show the T₁-T₂ 2D maps for the brine saturated Upper Bakken core samples.

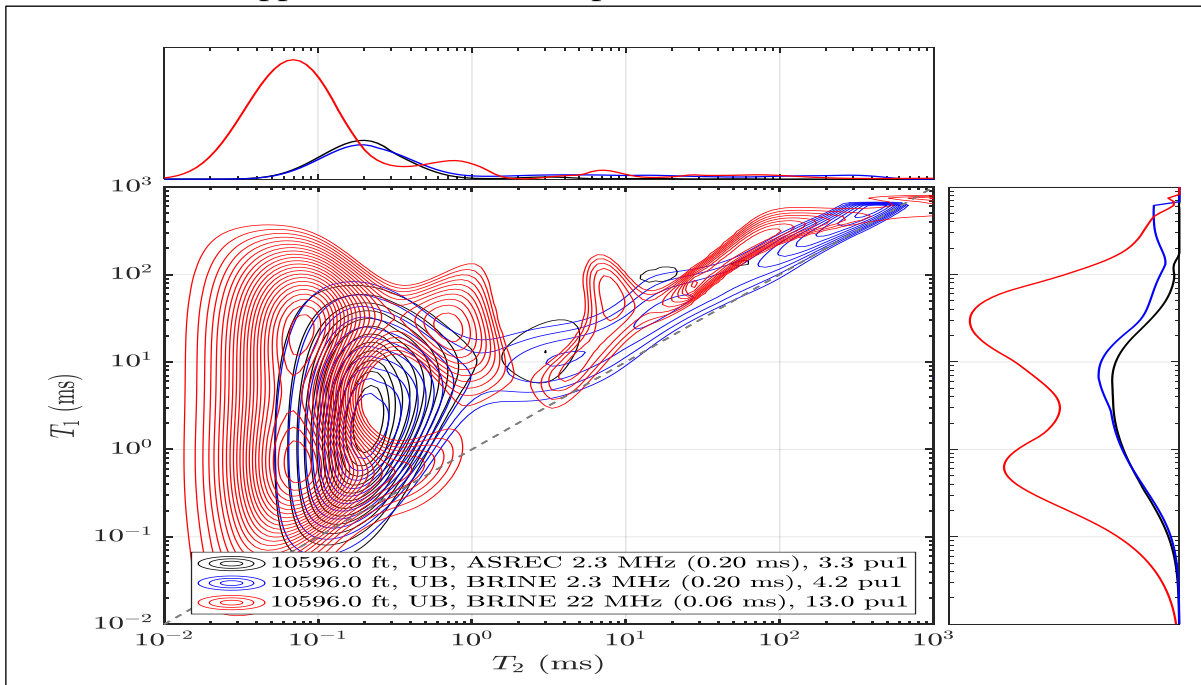


Figure 29- T₁-T₂ 2D Map – Brine Saturated Upper Bakken 2.3 & 22 MHz (Depth 10596 ft)

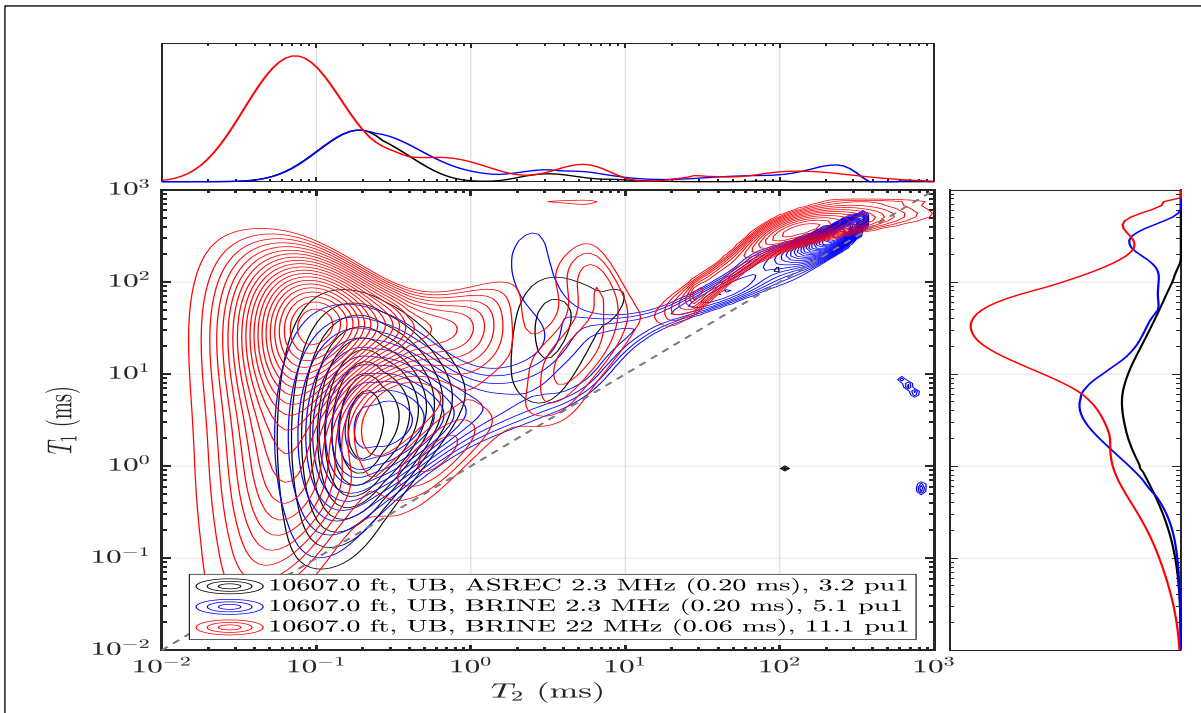


Figure 30- T_1 - T_2 2D Map – Brine Saturated Upper Bakken 2.3 & 22 MHz (Depth 10607 ft)
 In the octane-saturated Middle Bakken and Three Forks core samples, there is additional 2 pu at short T_2 , strong internal gradient was observed which made T_2 shorter, and showed little frequency dependence. Figures 31 to 34 show the T_1 - T_2 2D maps for the octane saturated Middle Bakken and Three Forks core samples.

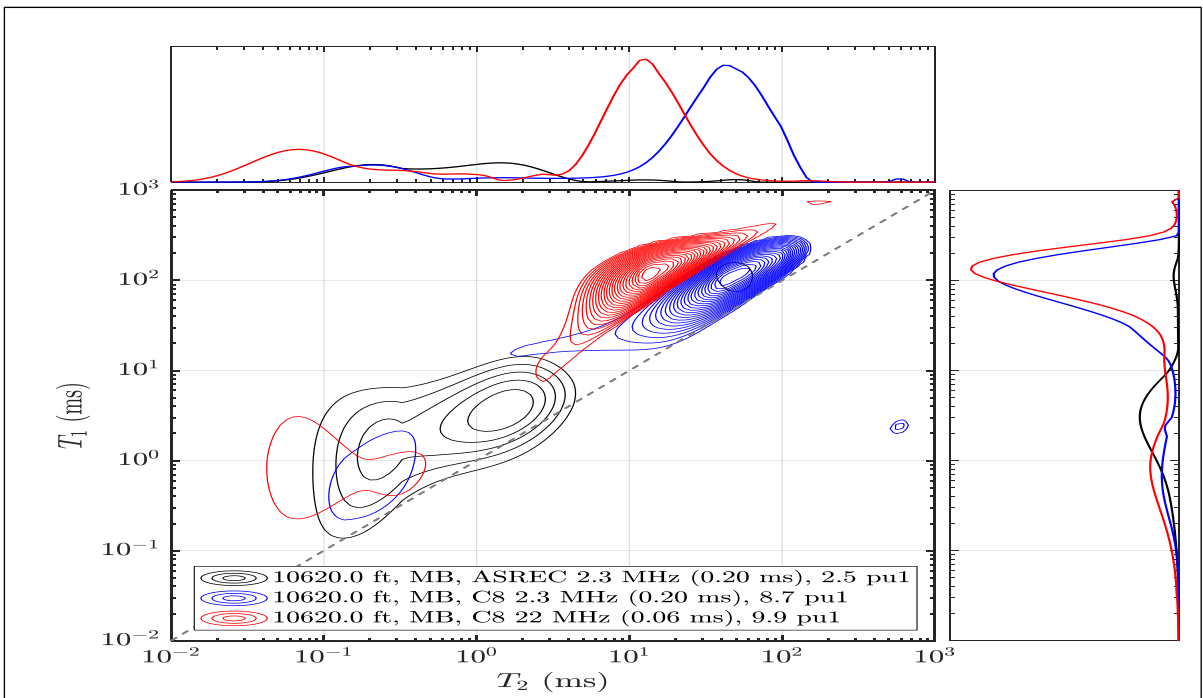


Figure 31- T_1 - T_2 2D Map – Octane Saturated Middle Bakken 2.3 & 22 MHz (Depth 10620 ft)

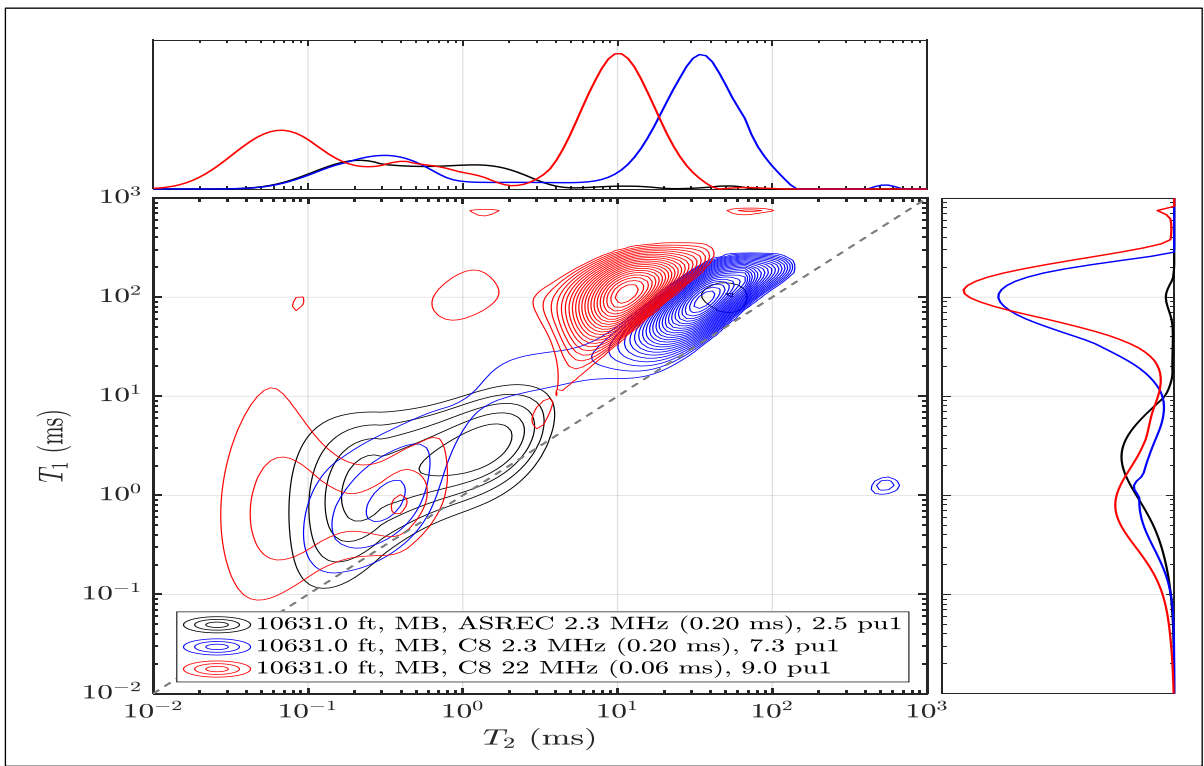


Figure 32- T₁-T₂ 2D Map – Octane Saturated Middle Bakken 2.3 & 22 MHz (Depth 10631 ft)

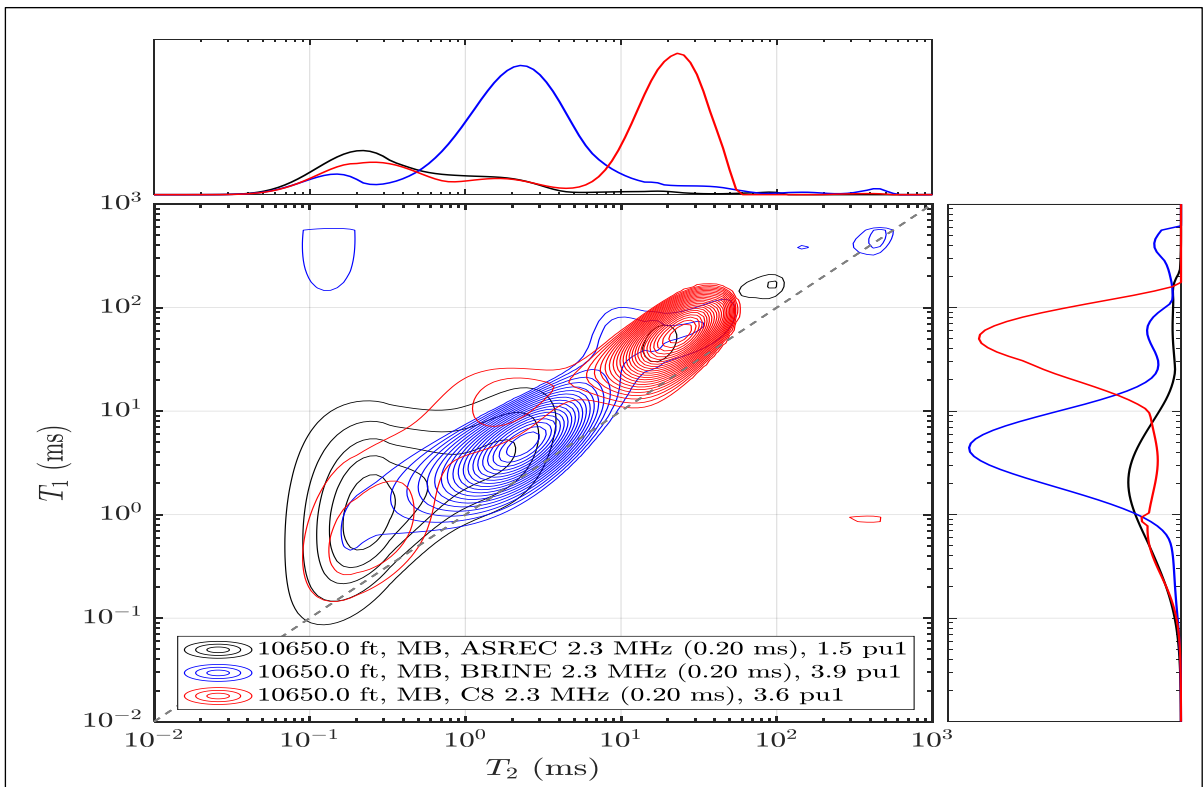


Figure 33- T₁-T₂ 2D Map – Octane Saturated Middle Bakken 2.3 & 22 MHz (Depth 10650 ft)

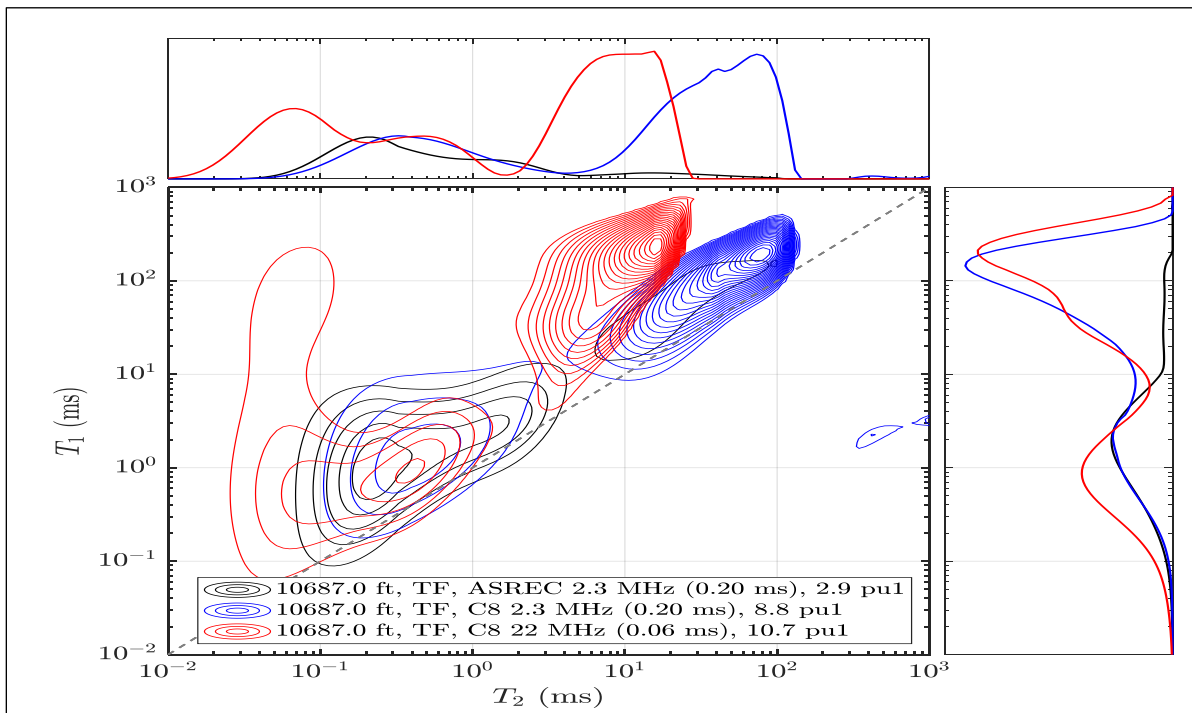


Figure 34- T_1 - T_2 2D Map – Octane Saturated Three Forks 2.3 & 22 MHz (Depth 10687 ft)

In the brine-saturated samples, the same observations were detected except that the samples showed mild internal gradient comparing to the octane saturated samples. Figures 35 to 38 show the T_1 - T_2 2D maps for the brine saturated Middle Bakken and Three Forks core samples.

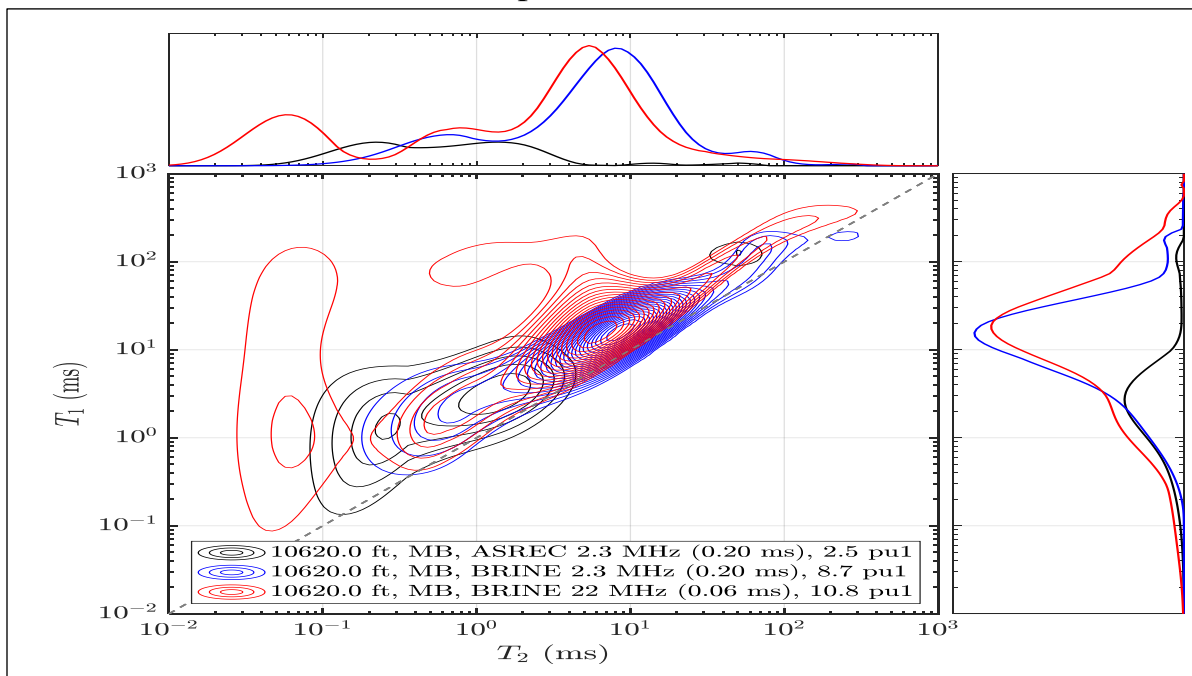


Figure 35- T_1 - T_2 2D Map – Brine Saturated Middle Bakken 2.3 & 22 MHz (Depth 10620 ft)

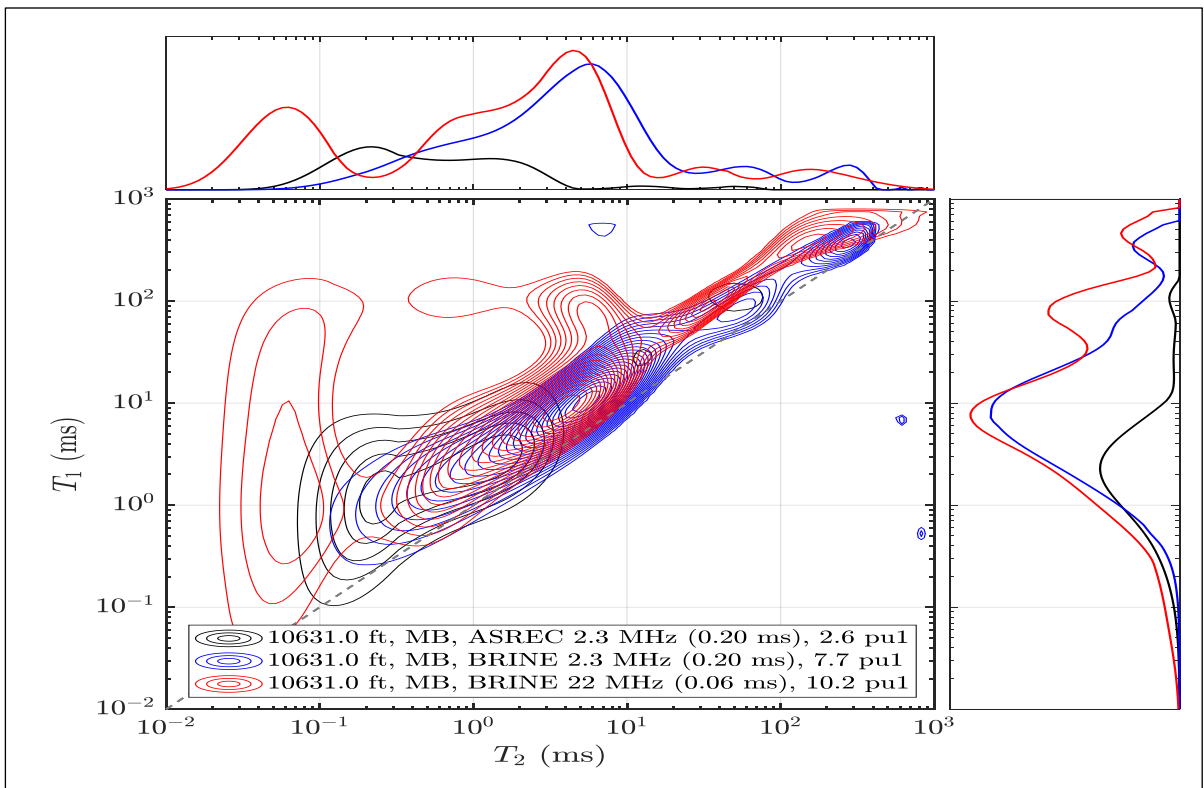


Figure 36- T_1 - T_2 2D Map – Brine Saturated Middle Bakken 2.3 & 22 MHz (Depth 10631 ft)

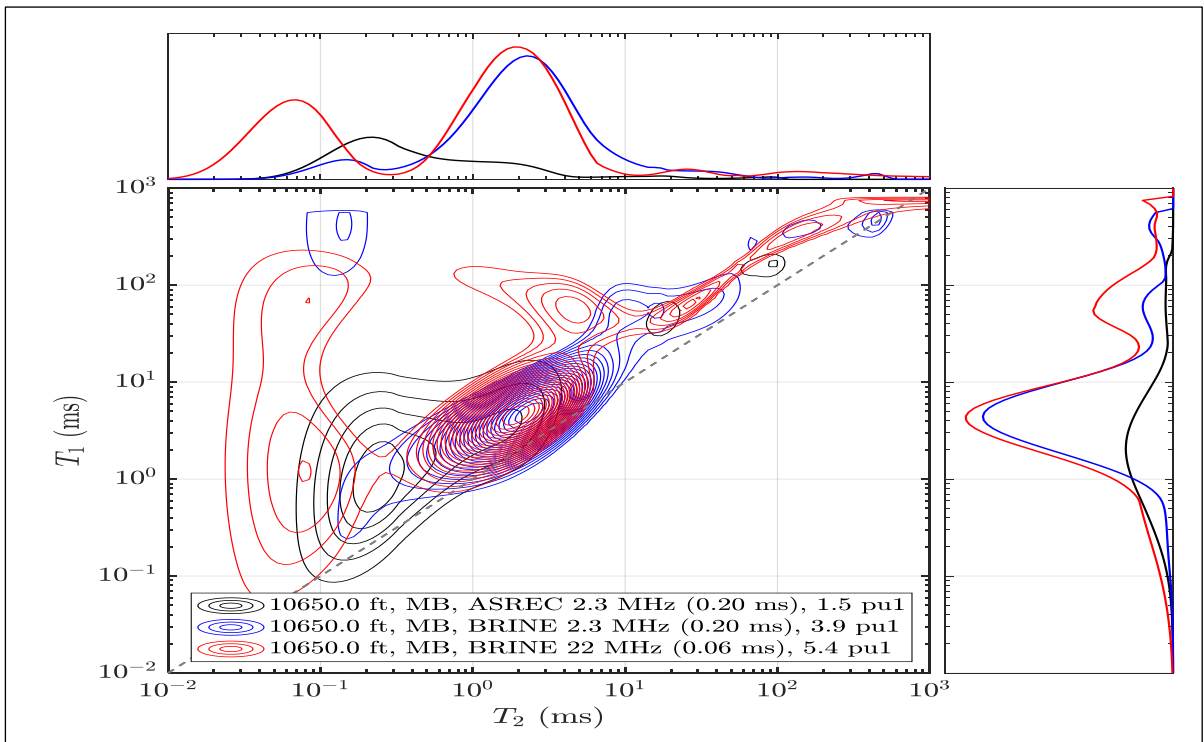


Figure 37- T_1 - T_2 2D Map – Brine Saturated Middle Bakken 2.3 & 22 MHz (Depth 10650 ft)

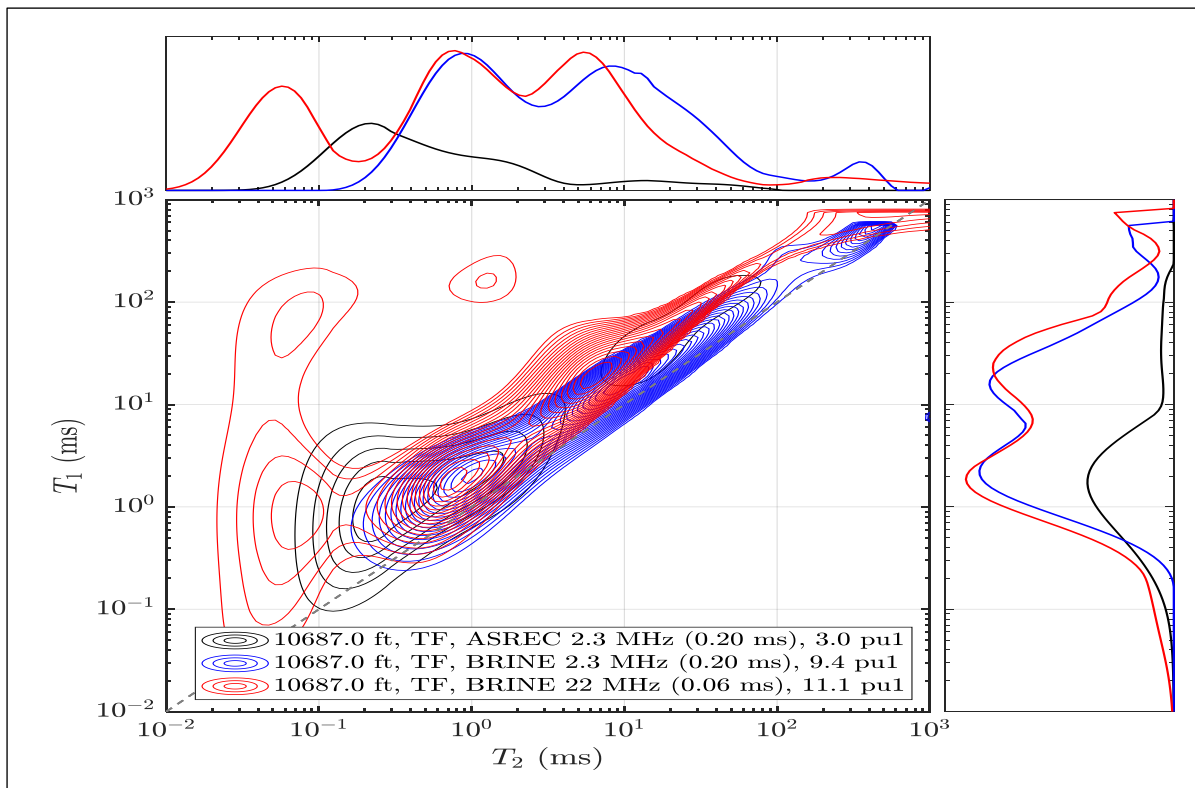


Figure 38- T₁-T₂ 2D Map – Brine Saturated Three Forks 2.3 & 22 MHz (Depth 106 ft)

Figure 39 shows the summary of the T₂ and T₁ distribution using 2.3 MHz (0.2 ms echo spacing) and 22 MHz (0.06 ms echo spacing) for the octane saturated core samples.

Figure 40 shows the summary of the T₂ and T₁ distribution using 2.3 MHz (0.2 ms echo spacing) and 22 MHz (0.06 ms echo spacing) for the brine saturated core samples.

To study the effect of high frequency on the NMR response, measurements have been conducted using 22 MHz using echo spacing 0.2 ms (equal to the low frequency echo spacing) and T₂ and T₁/T₂ ratio distribution for 2.3 and 22 MHz was plotted in the same graph. For the octane saturated core samples, no difference in T₂ peaks was observed in the Upper Bakken cores, except increase in the T₁/T₂ ratio with increasing the frequency which strengthen the hypothesis that the increase of porosity in case of using shorter echo spacing is due to the presence of bitumen as the bitumen usually has high T₁/T₂ ratio. In the octane-

saturated Middle Bakken and Three Forks core samples, strong internal gradient was observed. Figure 41 shows the T_2 and T_1/T_2 ratio measurements for octane saturated core samples using 2.3 and 22 MHz with echo spacing 0.2 ms for both frequencies.

For the brine saturated core samples, no big difference is observed except mild internal gradient. Figure 42 shows the T_2 and T_1/T_2 ratio measurements for the brine saturated core samples using 2.3 and 22 MHz with echo spacing 0.2 ms for both frequencies. By comparing the results from the 2.3 and 22 MHz using the same echo spacing and different echo spacing, it is proved that there is no big difference in the relaxation measurements except the ability to measure the fast-relaxing peaks and the internal gradient.

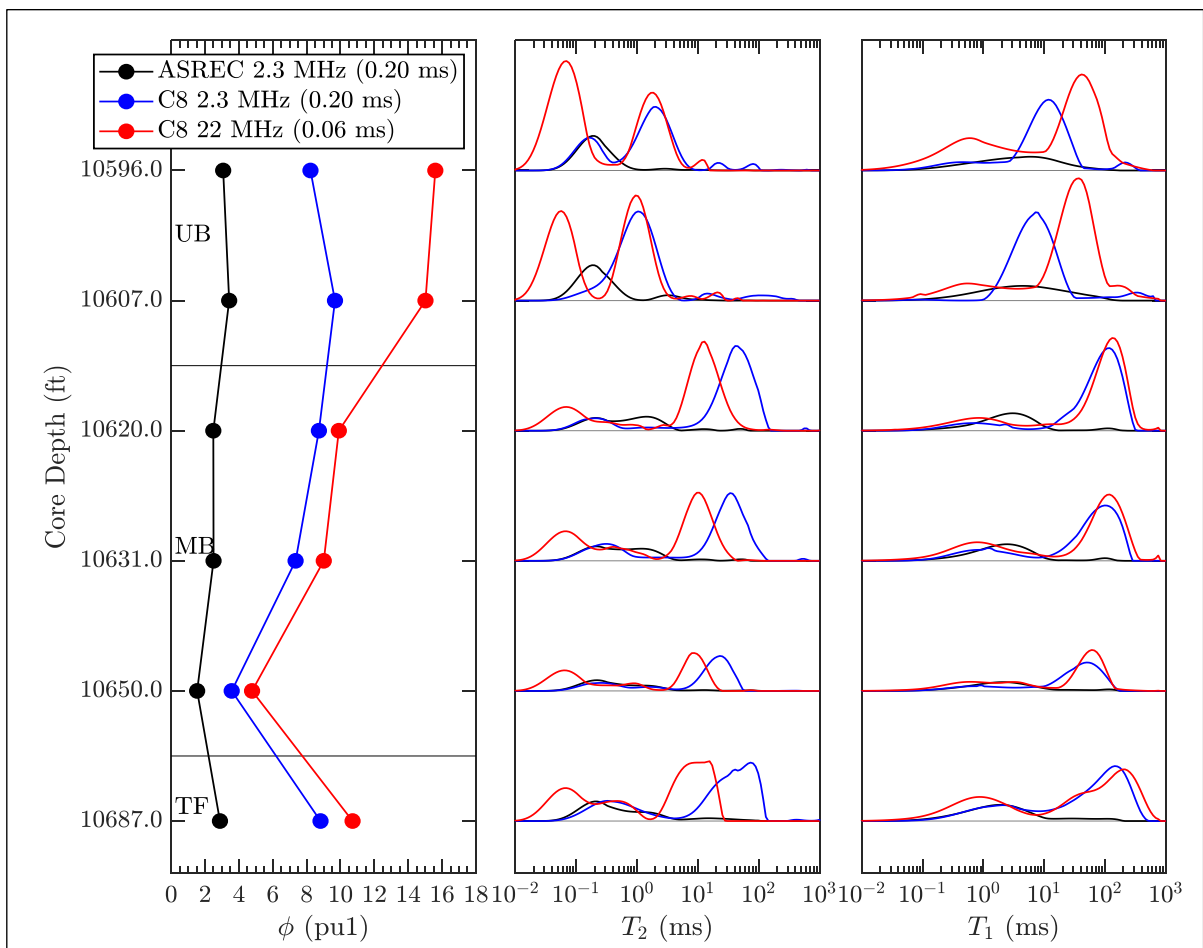


Figure 39- T_2 & T_1 Octane Saturated - T_2 & T_1/T_2 Distribution
2.3 MHz (0.2ms) & 22MHz (0.06ms)

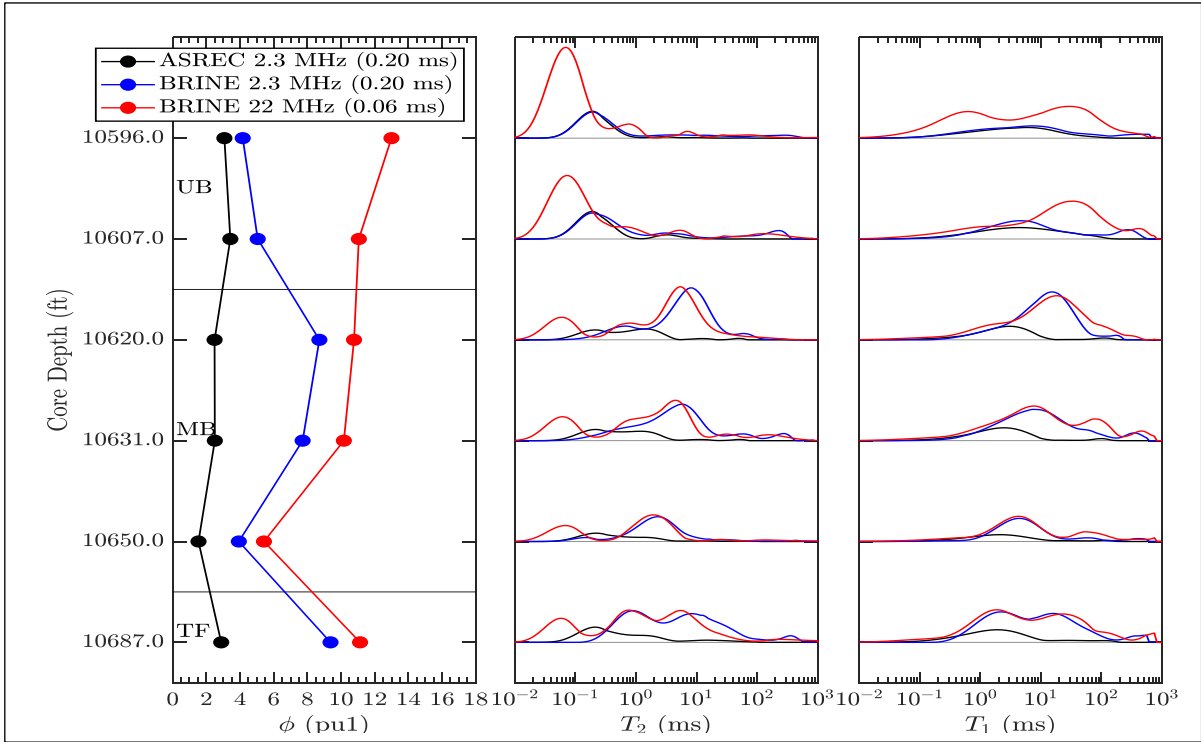


Figure 40- T_2 & T_1 Brine Saturated - T_2 & T_1/T_2 Distribution
2.3 MHz (0.2ms) & 22MHz (0.06ms)

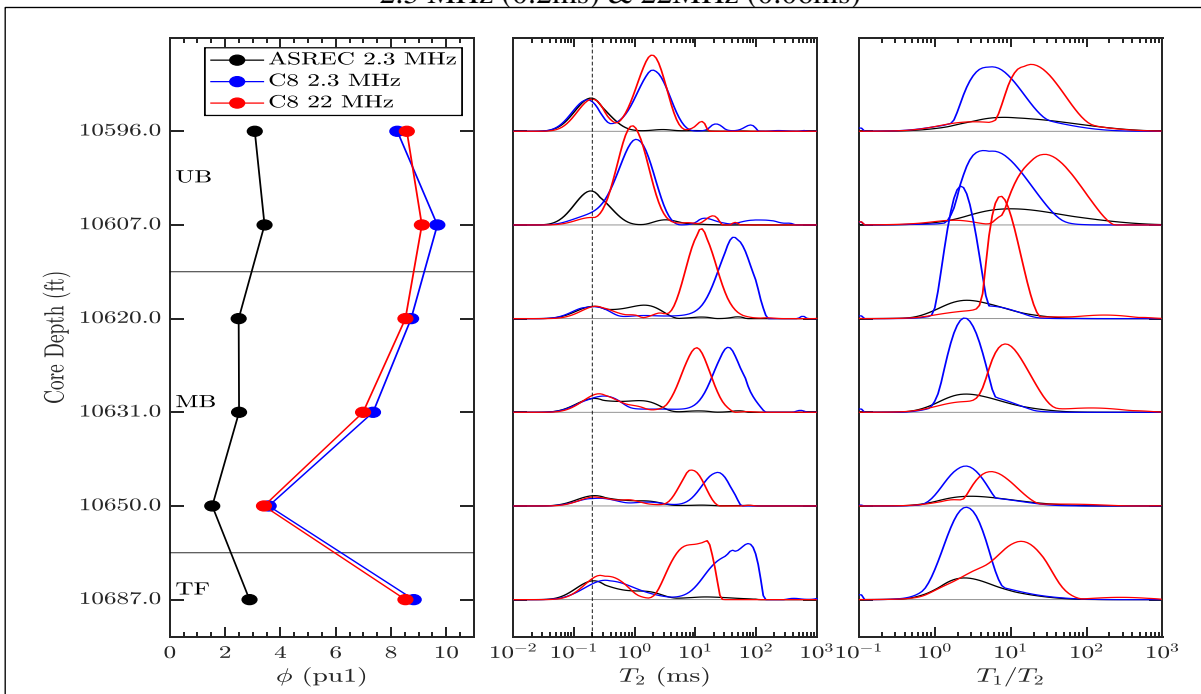


Figure 41- T_2 & T_1 Octane Saturated - T_2 & T_1/T_2 Distribution
2.3 MHz (0.2ms) & 22MHz (0.2ms)

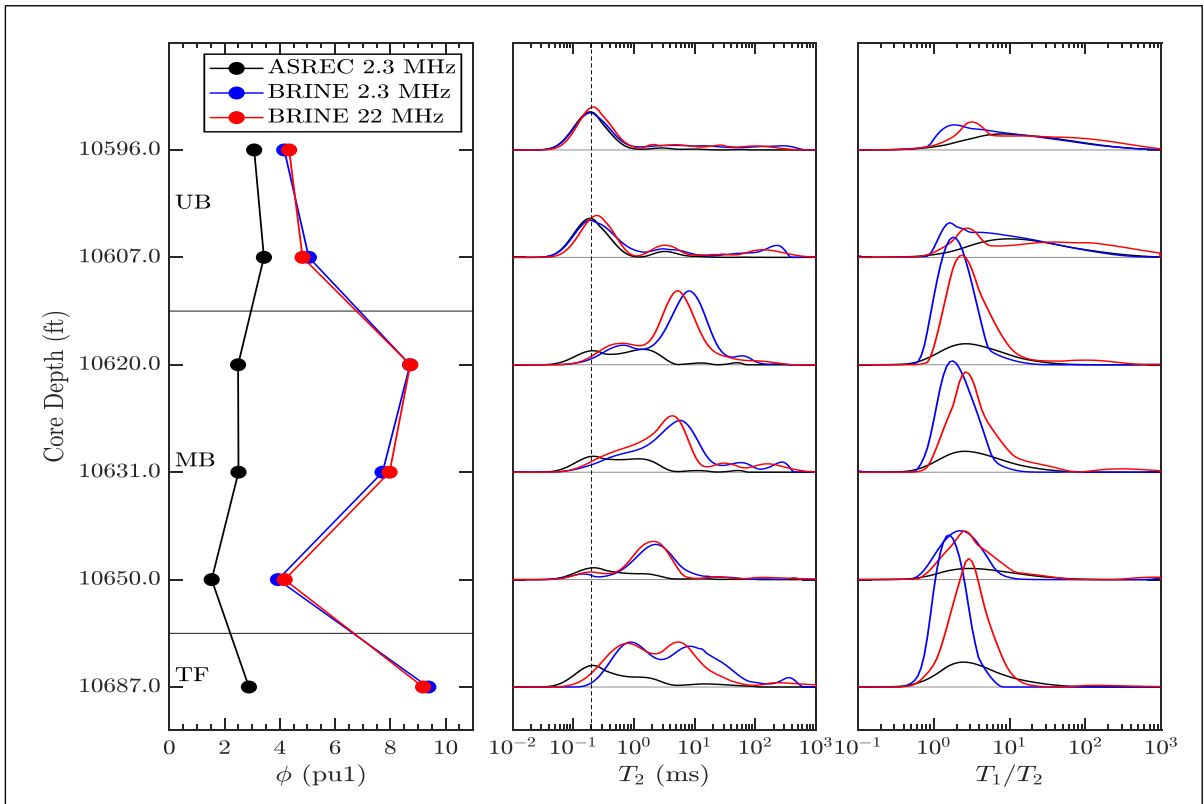


Figure 42- T_2 & T_1 Brine Saturated - T_2 & T_1/T_2 Distribution
2.3 MHz (0.2ms) & 22MHz (0.2ms)

3.3.3 NMR Results using 2.3 MHz at 25° and 100°C:

T_2 relaxation measurements using 2.3 MHz Larmor frequency with 0.2 ms echo spacing were conducted at 25° and 100°C to study the temperature effect. Temperature dependence is expected with the H-H dipole-dipole relaxation mechanism while no temperature dependence is expected with the Paramagnetic relaxation mechanism.

Surface relaxivity decreased by a factor of 3 with the increase of temperature in the Upper Bakken core sampled in both octane and brine-saturation which indicates the H-H dipole-dipole relaxation mechanism. Surface relaxivity decreased by a factor of 2 with temperature increase in the octane saturated Middle Bakken core samples indicating H-H dipole-dipole relaxation mechanism, while the surface relaxivity was roughly constant in the brine saturated Middle Bakken core samples indicating Paramagnetic relaxation mechanism. In both

octane and brine saturated Three Forks core samples, there is no change in the surface relaxivity with the increase of temperature indicating Paramagnetic relaxation mechanism.

Figure 43 shows the NMR results of the octane-saturated core samples measured with 2.3 MHz at 25° and 100°C. Figure 44 shows the brine saturated core samples measured with 2.3 MHz at 25° and 100°C.

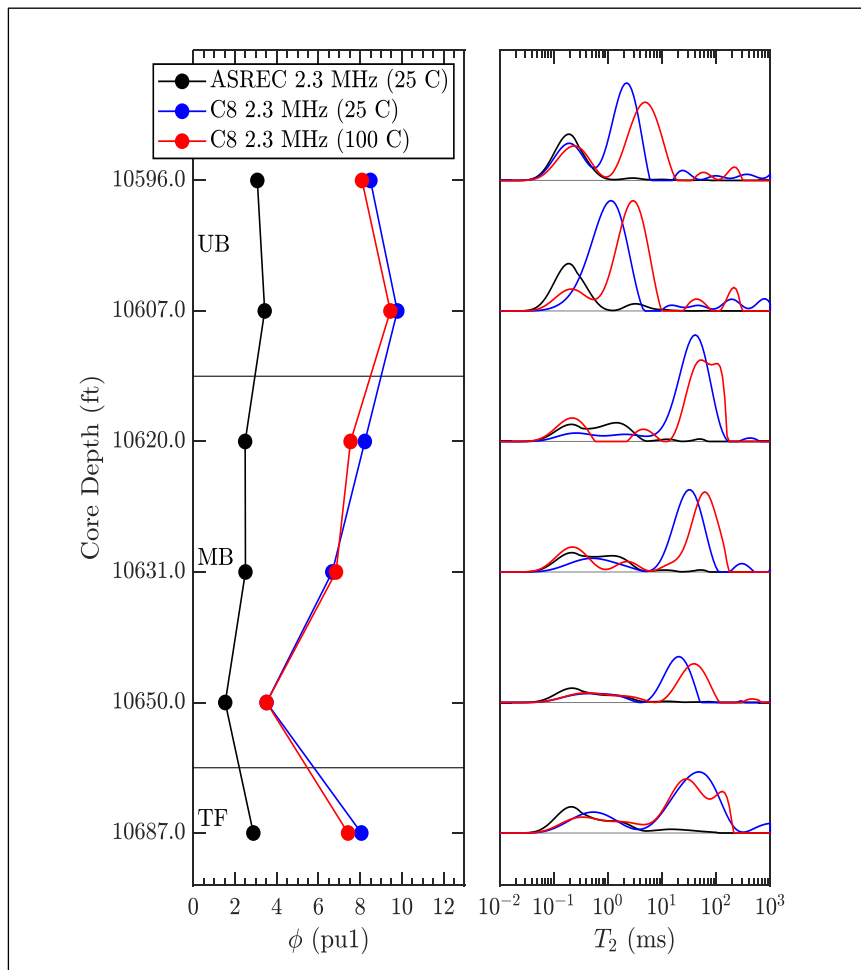


Figure 43- Octane Saturated - T_2 Distribution 2.3 MHz (0.2ms) at 25° and 100°C

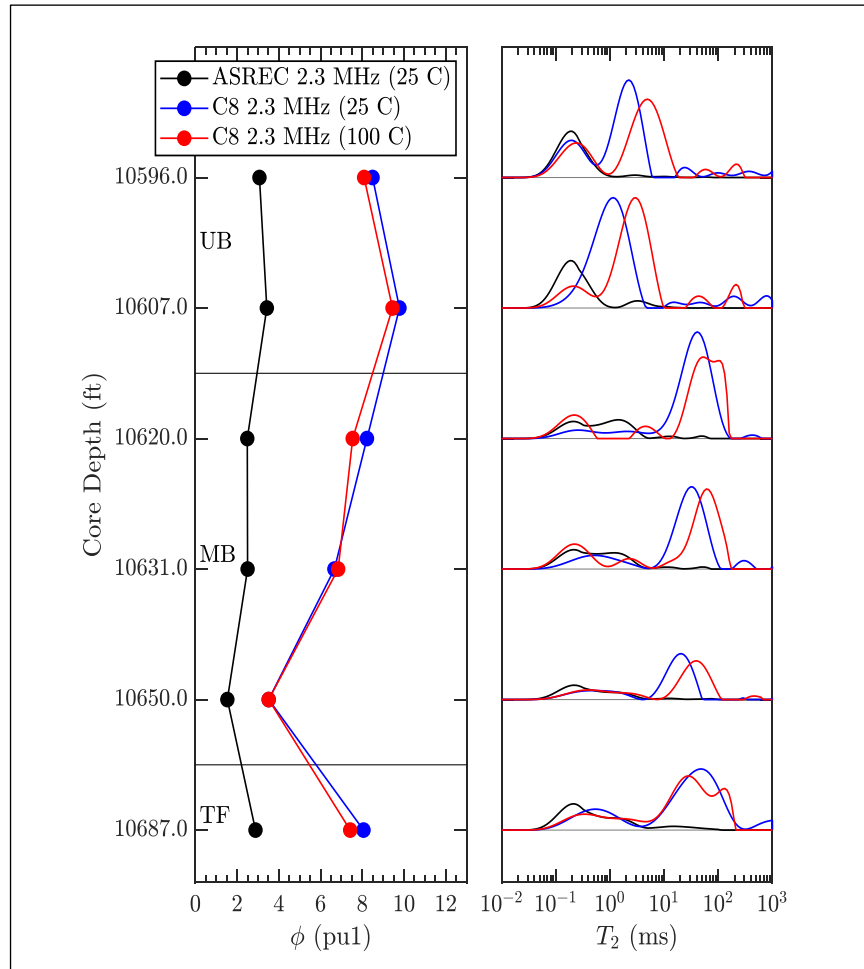


Figure 44- Brine Saturated $-T_2$ Distribution 2.3 MHz (0.2ms) at 25° and 100°C

3.4 Phase Behavior Results:

A 4% concentration solution from each surfactant was prepared in Bakken formation brine as shown in Figure 45. From the aqueous solutions observations, all the 13 surfactants are thermally stable and tolerant to salts in the high salinity formation brine. Figure 46 shows example of aqueous solution of three different surfactants at 25°C and equilibrated aqueous solution for the three surfactants at 105°C. From the phase behavior test for single surfactants, ENORDET 0242, ENORDET 0332 and XOF 315C were more hydrophobic and present in the oleic phase, while Lauryl Betaine, L38, Dowfax 8390 and Dowfax 2A1 were more hydrophilic and present in the water phase. XOF 316C formed middle phase while significant amount of the surfactant in the oleic phase. Avanel S150CGN formed

middle phase with microemulsion has hardly no water in it. Oleyl Betaine, Avanel S74, Avanel S70, and XOF 112C were present in both the oleic and water phase. Figure 47 shows example of phase behavior for 3 surfactants at 25°C and equilibrated phase behavior for the 3 surfactants at 105°C.

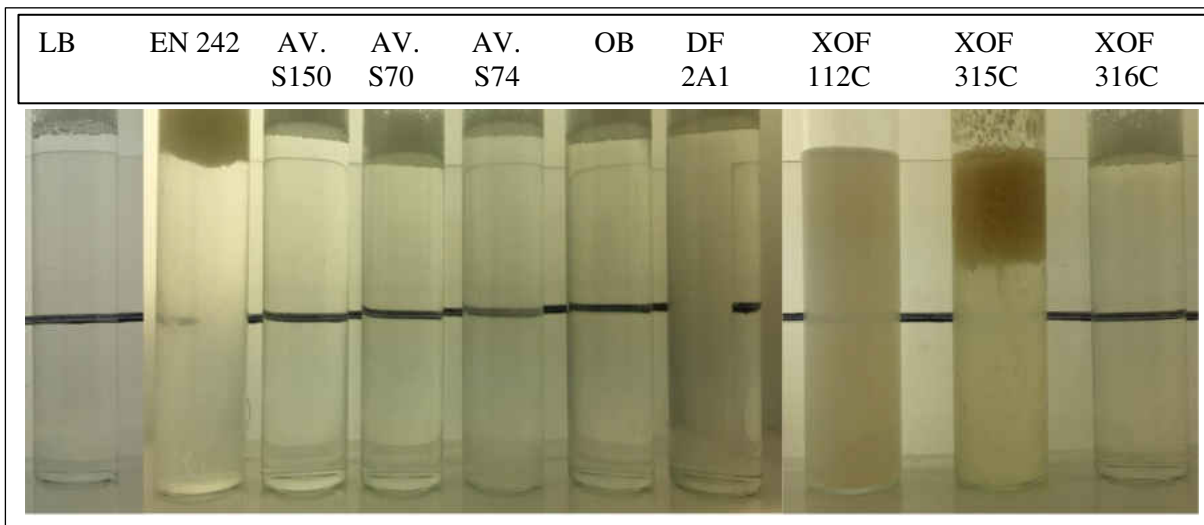


Figure 45- Surfactant Solution in Bakken Formation Brine – 4% Concentration

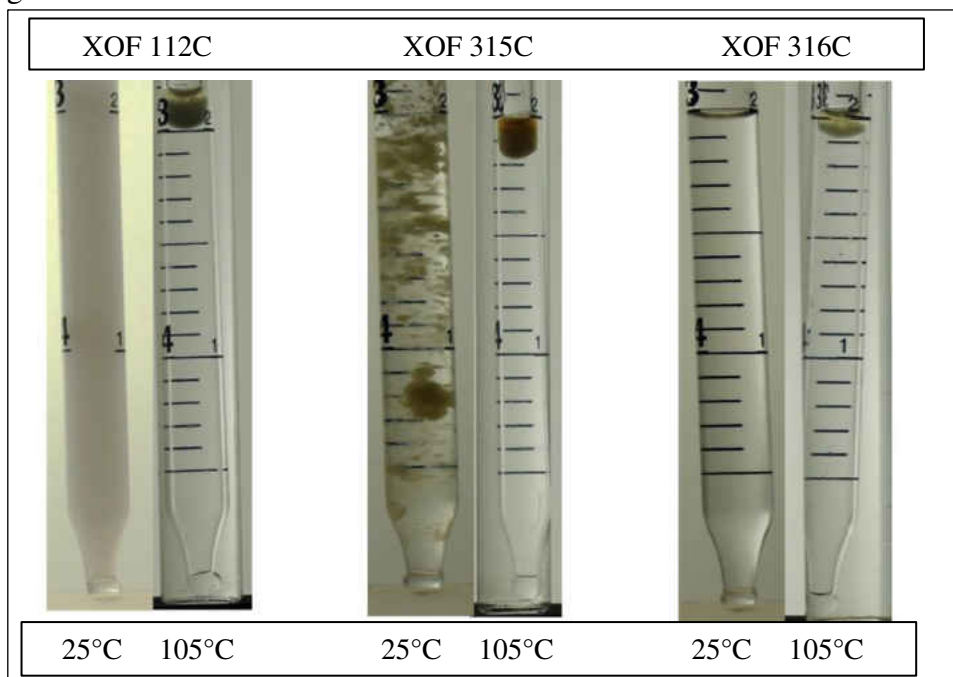


Figure 46- Aqueous Solution 4% in Formation Brine at 25°C and after Equilibration at 105°C

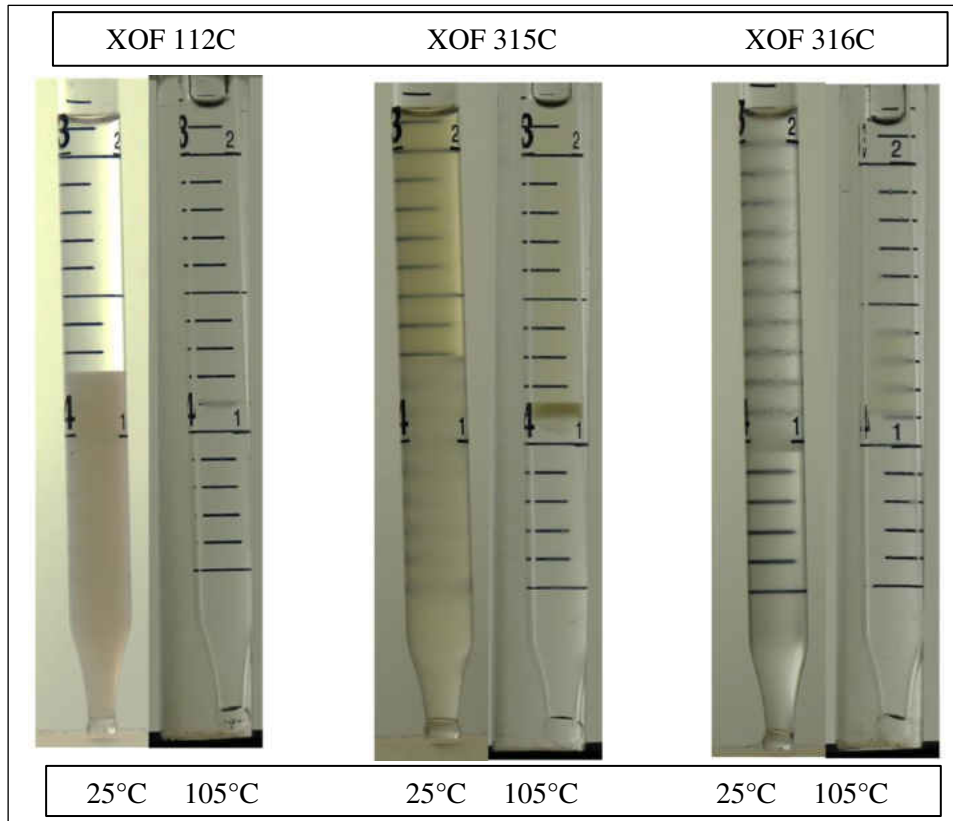


Figure 47- Phase Behavior Test at 25°C (after mixing) and after Equilibration at 105°C

Phase behavior screening was conducted by mixing 24 surfactant blends to find formulation suitable for spontaneous imbibition test. All the phase behavior blend scans were conducted using octane as a model oil and Bakken formation brine as water phase. Due to the large number of the conducted surfactant blends and the similarity in most of the results, examples of the blends results will be discussed.

Figure 48 shows the blend scan of 2% overall of XOF 315C and Dowfax 2A1 with water/oil ratio (WOR)~1 after equilibration at 105°C. For the 100% XOF 315C the surfactant is present in the oleic phase but starting from (9/1) XOF 315C/Dowfax 2A1, the surfactant starts to be present in the water phase with insignificant amount present in the oleic phase till (1/9) XOF 315C/Dowfax 2A1 and in the 100% Dowfax 2A1 the surfactant is completely in the water phase.

Figure 49 shows the blend scan of 2% overall of XOF 316C and Dowfax 2A1 with water/oil ratio (WOR)~1 after equilibration at 105°C. The samples (8/2) & (4/6) XOF 316C/Dowfax 2A1 were lost because of leakage. Starting from the

100% XOF 316C the surfactant is present in the middle phase and the oleic phase while the middle phase thickness decreases by increasing Dowfax 2A1 and the surfactant presence in the water phase increases gradually till (1/9) XOF 316C/Dowfax 2A1 while in the 100% Dowfax 2A1 the surfactant is completely in the water phase. The middle phase has small amount of water.

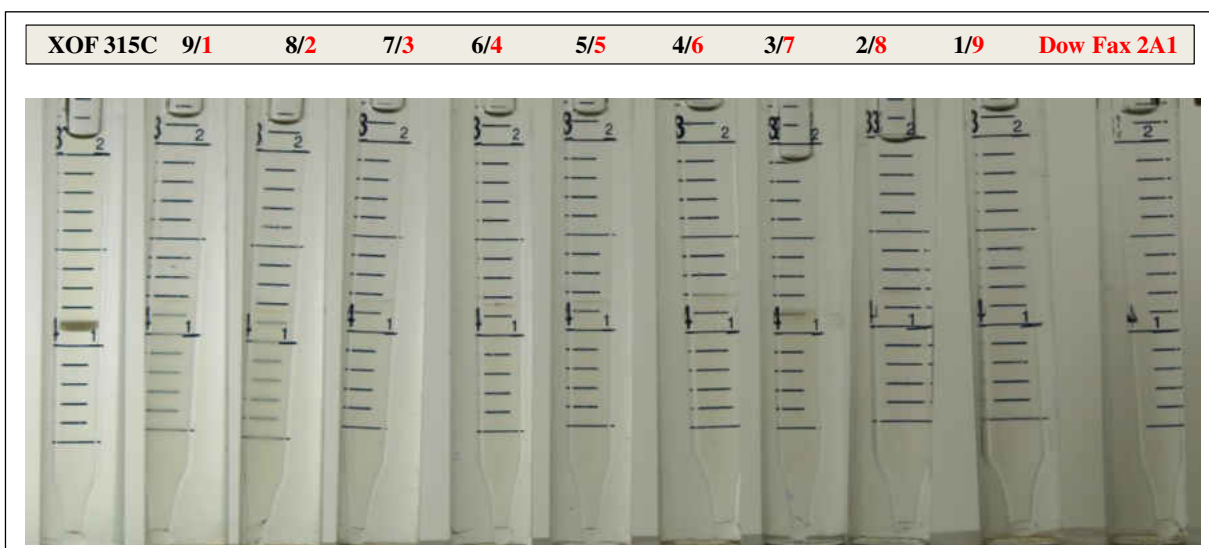


Figure 48- Blend Scan: 2% over all [XOF 315C&Dow Fax 2A1] WOR ~1 n-Octane/Bakken Brine (309K ppm) ~105°C

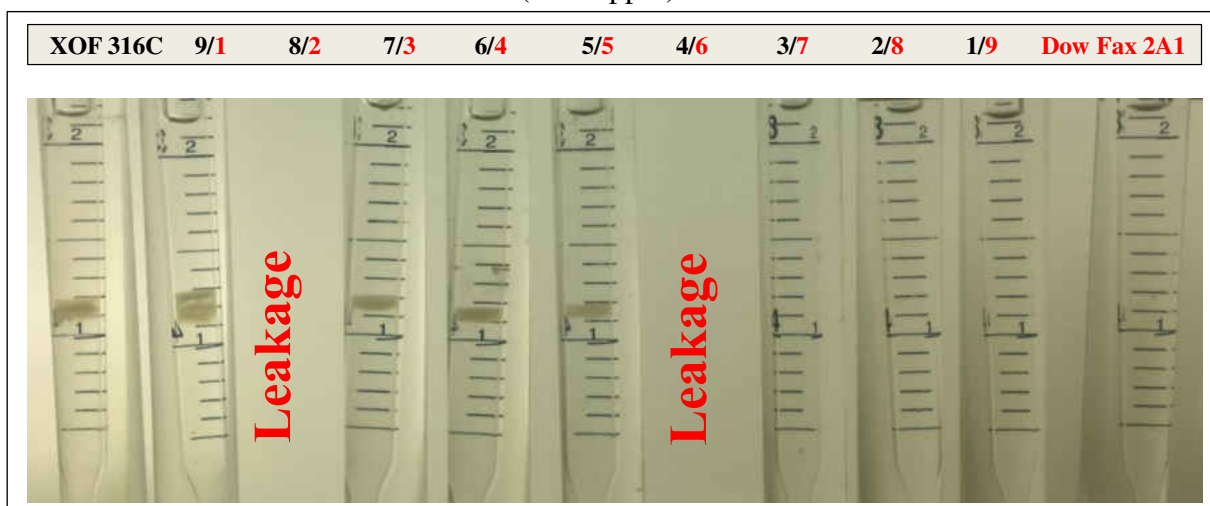


Figure 49- Blend Scan: 2% over all [XOF 316C&Dow Fax 2A1] WOR ~1 n-Octane/Bakken Brine (309K ppm) ~105°C

Figure 50 shows the blend scan of 2% overall of XOF 112C and XOF 316C with water/oil ratio (WOR)~1 after equilibration at 105°C. Starting from the 100% XOF 112C the surfactant is present in the oleic phase with small amount in the

water phase till (2/8) XOF 112C/XOF 316C while in (1/9) XOF 112C/XOF 316C the surfactant is present in the middle phase and in the 100% XOF 316C the surfactant is in the middle phase and the oleic phase. The middle phase has small amount of octane.

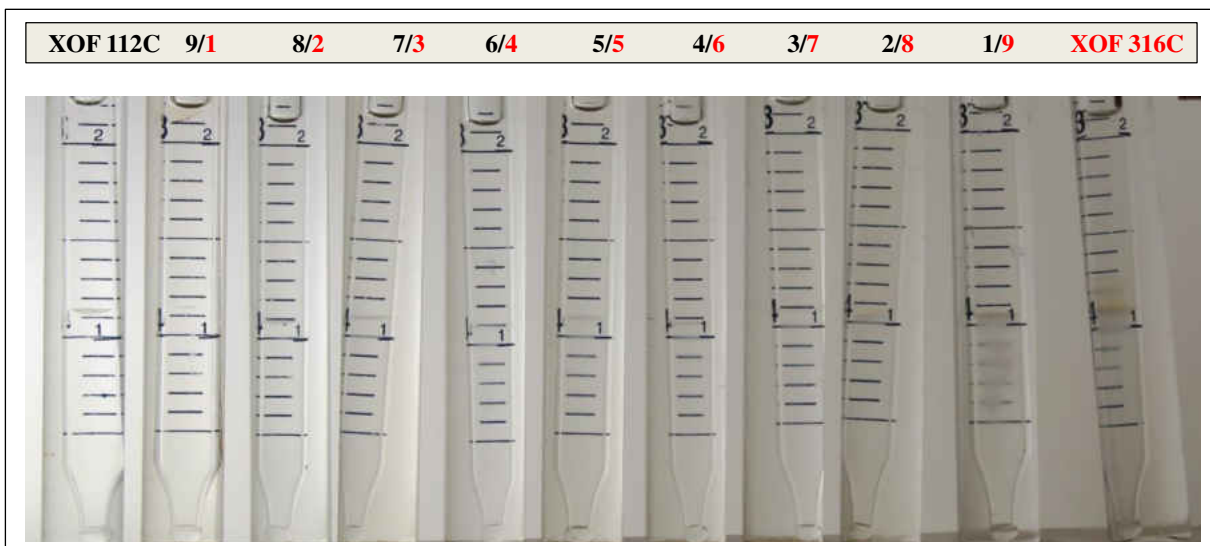


Figure 50- Blend Scan: 2% over all [XOF 112C&XOF 316C] WOR ~1 n-Octane/Bakken Brine (309K ppm) ~105°C

Figure 51 shows the blend scan of 2% overall of Avanel S150 CGN and XOF 315C with water/oil ratio (WOR)~1 after equilibration at 105°C. In the 100% Avanel S150 CGN the surfactant is present in the middle phase. Starting from (9/1) Avanel S150 CGN/XOF 315C the surfactant is in the oleic phase with insignificant amount in the lower phase with gel precipitation when the sample start to cool down just before taking the picture till (1/9) Avanel S150 CGN/XOF 315C and in the 100% XOF 315C the surfactant is in the oleic phase. The middle phase has small amount of water.

Figure 52 shows the blend scan of 2% overall of L38 (after neutralization with NaOH) and Dowfax 2A1 with water/oil ratio (WOR)~1 after equilibration at 105°C. For the 100% L38 and (9/1) L38/Dowfax 2A1, the surfactant is present in the middle phase and oleic phase. For (8/2) and (7/3) L38/Dowfax 2A1, the surfactant is in the oleic phase. For (6/4), (5/5) and (4/6) L38/Dowfax 2A1, the surfactant is in the middle phase and starting from (3/7) L38/Dowfax 2A1 till 100% Dowfax 2A1, the surfactant is in the water phase. The middle phase has no water.

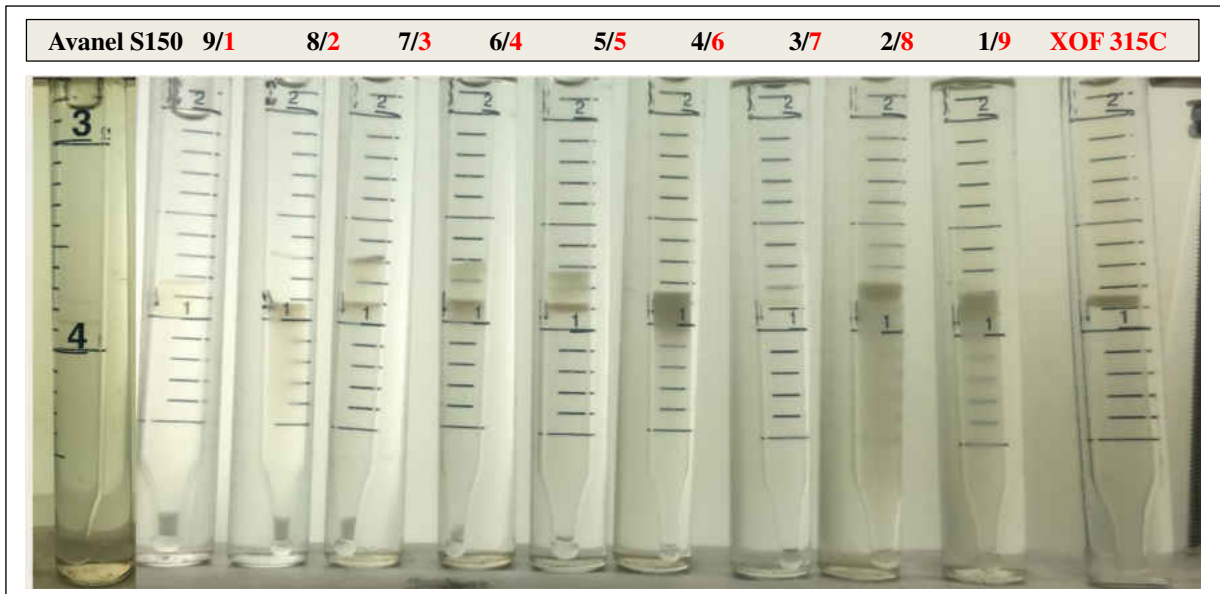


Figure 51- Blend Scan: 2% over all [Avanel S150&XOF 315C] WOR ~1 n-Octane/Bakken Brine (309K ppm) ~105°C



Figure 52- Blend Scan: 2% over all [L 38&Dowfax 2A1] WOR ~1 n-Octane/Bakken Brine (309K ppm) ~105°C

Figure 53 shows the blend scan of 2% overall of L38 (after neutralization with NaOH) and Dowfax 8390 with water/oil ratio (WOR)~1 after equilibration at 105°C. For the 100% L38 and (9/1) L38/Dowfax 8390, the surfactant is present

in the middle phase and oleic phase. For (8/2) and (7/3) L38/Dowfax 8390, the surfactant is in the oleic phase. For (6/4), (5/5) and (4/6) L38/Dowfax 8390, the surfactant is in the middle phase and starting from (3/7) L38/Dowfax 8390 till 100% Dowfax 8390, the surfactant is in the water phase. The middle phase has no water.



Figure 53- Blend Scan: 2% over all [L 38&Dowfax 8390] WOR ~1 n-Octane/Bakken Brine (309K ppm) ~105°C

Figure 54 shows the blend scan of 2% overall of Dowfax 8390 and ENORDET 0332 with water/oil ratio (WOR)~1 after equilibration at 105°C. starting with the 100% Dowfax 8390 to (6/4) Dowfax 8390/ENORDET 0332, the surfactant is present in the water phase. For (5/5) and (4/6) Dowfax 8390/ENORDET 0332, the surfactant is in the middle phase. From (3/7) to 100% ENORDET 0332, the surfactant is in the oleic phase. The (V_o/V_s) for the middle phase of blend ratio (5/5) and (4/6) Dowfax 8390/ENORDET 0332 are 1.25 and 3.5 respectively and the (V_w/V_s) are 3.25 and 1.25 which indicates that the middle phase does not have equal water to oil ratio.



Figure 54- Blend Scan: 2% over all [Dowfax 8390&EN 0332] WOR ~1 n-Octane/Bakken Brine (309K ppm) ~105°C

Figure 55 shows the blend scan of 2% overall of Dowfax 2A1 and ENORDET 0332 with water/oil ratio (WOR)~1 after equilibration at 105°C. starting with the 100% Dowfax 2A1 to (5/5) Dowfax 2A1/ENORDET 0332, the surfactant is present in the water phase. For the (4/6) Dowfax 2A1/ENORDET 0332, the surfactant is in the middle phase. From (3/7) to 100% ENORDET 0332, the surfactant is in the oleic phase. The (V_o/V_s) for the middle phase of blend ratio (4/6) Dowfax 2A1/ENORDET 0332 is 4.75 and the (V_w/V_s) is 1.25 which indicates that the middle phase does not have equal water to oil ratio.

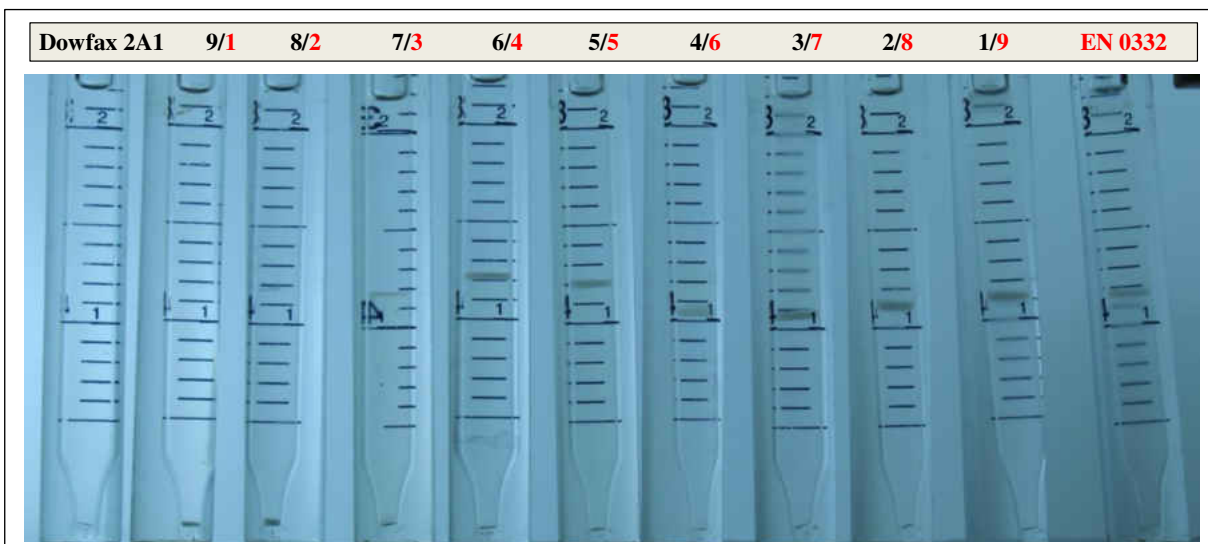


Figure 55- Blend Scan: 2% over all [Dowfax 2A1&EN 0332] WOR ~1 n-Octane Bakken Brine (309K ppm) ~105°C:

Figure 55 shows the blend scan of 2% overall of ENORDET 0332 and Avel S150 CGN with water/oil ratio (WOR)~1 after equilibration at 105°C. starting

with the 100% ENORDET 0332 to (4/6) ENORDET 0332 /Avel S150 CGN, the surfactant is present in the oleic phase. From the (3/7) ENORDET 0332 /Avel S150 CGN to the 100% Avel S150 CGN, the surfactant is in the water phase. This blend has an interesting sample, blend ratio (3/7) ENORDET 0332 /Avel S150 CGN, Winsor I with (V_o/V_s) equals to 6 and (V_w/V_s) equals 25 but the sample has precipitate that is why this blend ratio was excluded. Figure 56 shows the solubilization parameters for this blend scan.



Figure 56- Blend Scan: 2% over all [EN 0332& Avel S150] WOR ~1 n-Octane/Bakken Brine (309K ppm) ~105°C

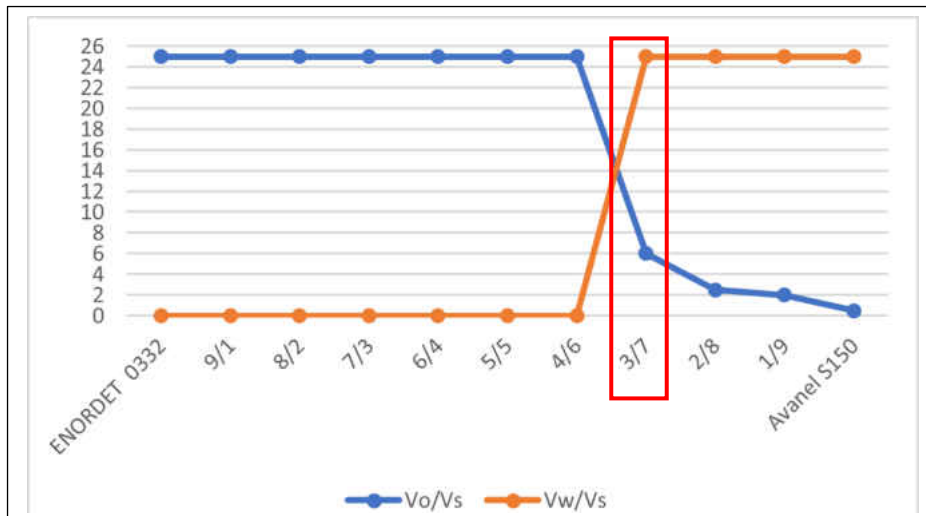


Figure 57- Solubilization Parameters for ENORDET 0332/Avel S150 CGN Blend Scan The most interesting blend scan which has the blend ratio that was chosen for the IFT and spontaneous imbibition test is shown in Figure 58. Figure 58 shows the

blend scan of 2% overall of LB and ENORDET 0332 with water/oil ratio (WOR)~1 after equilibration at 105°C. starting with the 100% LB to (8/2) LB/ENORDET 0332, the surfactant is present in the water phase. From the (7/3) LB/ENORDET 0332 to the 100% ENORDET 0332, the surfactant is in the oleic phase. The sample (2/8) LB/ENORDET 0332 was lost due to leakage. The interesting blend ratio is (8/2) LB/ENORDET 0332, Winsor I with (V_o/V_s) equals to 6.25 and (V_w/V_s) equals 25 and the sample has no precipitation. Figure 59 shows the solubilization parameters for this blend scan.

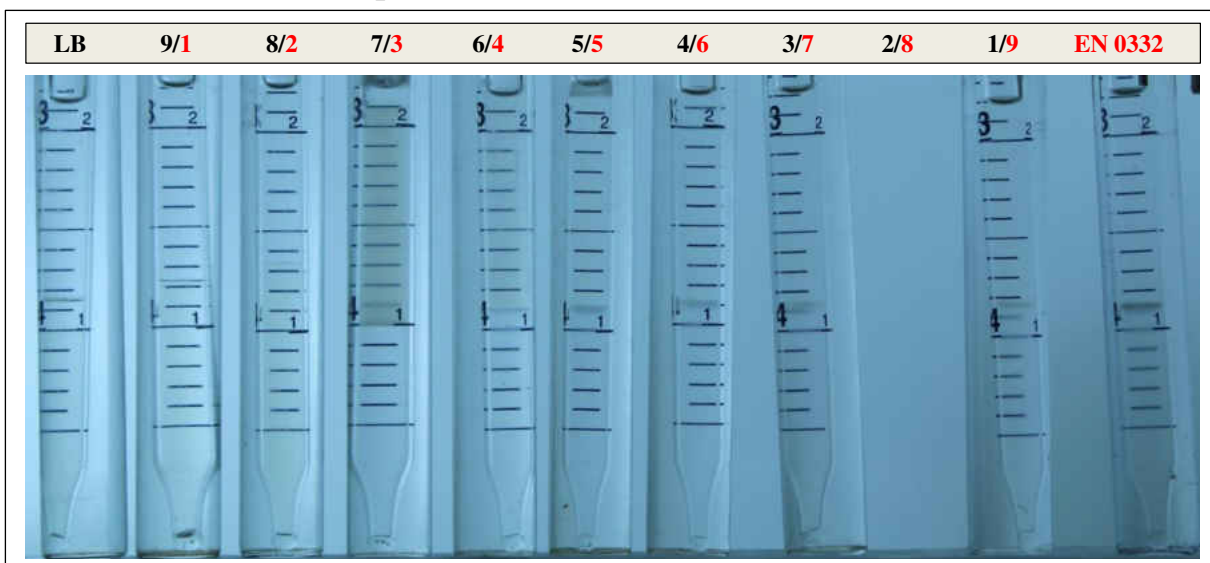


Figure 58- Blend Scan: 2% over all [Lauryl Betaine&EN 0332] WOR ~1 n-Octane/Bakken Brine (309K ppm) ~105°C

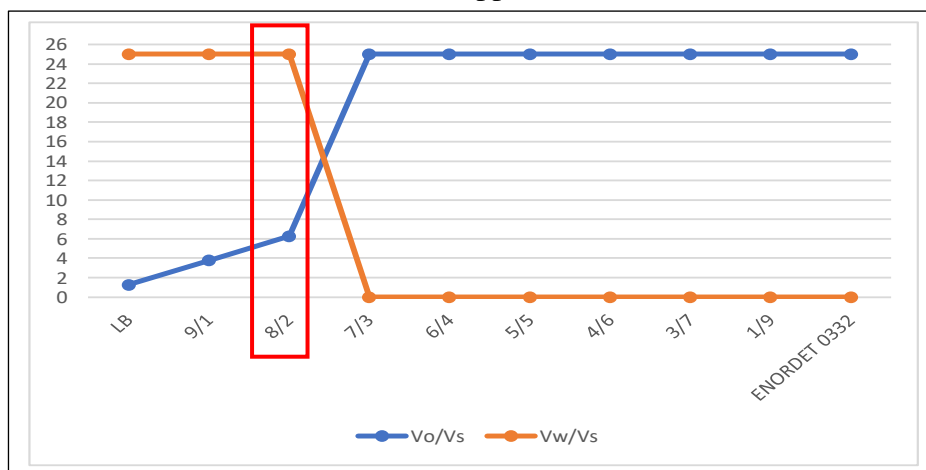


Figure 59- Solubilization Parameters for LB/ENORDET 0332 Blend Scan

3.5 IFT Measurements:

The chosen surfactant blend (8/2) LB/ENORDET 0332 was used to measure the IFT using both octane and the light crude that has similar properties to the Bakken crude oil. The highest temperature that the spinning drop equipment used to measure IFT can reach is 100°C and it was not applicable to measure the IFT of octane and surfactant above 80°C. So IFT of octane and surfactant solution was measured at 25°, 50° and 80°C while IFT for crude oil and the surfactant solution was measured at 25°, 50°, 80° and 100°C. All the measurements were plotted on linear scale and extrapolated to get the IFT value at 105°C for both octane and crude oil with the surfactant blend.

Using the spinning drop equipment, the diameter of spinning oil droplet immersed in the surfactant solution will be measured as well as recording the RPM at which the sample is rotating. The RPM will be used to calculate the angular velocity by using Equation 3, then the angular velocity (AV), the diameter of the oil droplet (r), density of filler (ρ_f) and density of droplet (ρ_d) are used to calculate the IFT using Equation 4 and the results in Table 7. Figures 60 and 61 show the IFT extrapolation. The IFT between octane and the surfactant blend is 0.16 mN/m and the IFT between crude oil and the surfactant blend is 0.22 mN/m.

$$\text{Angular Velocity (AV)} = 2\pi * (\text{RPM}/60)$$

Equation 3- Angular Velocity Calculation Equation

$$\text{IFT} = \frac{(\rho_f - \rho_d) * 1000 * (\text{AV}^2) * (r/1000)^3}{4}$$

Equation 4- Calculation Equation

Density : g/cc		Angular Velocity	¹ Refractive Index	² Drop diameter as seen in Monitor	Drop diameter r corrected for RI	Drop Radius actual	IFT		
Drop	Filler	rad/sec		mm	mm	mm	N/m	mN/m	
0.825	1.185	754.3	1.333	0.5947	0.45	0.2231	0.000568	0.57	Crude Oil
0.825	1.185	755.9	1.333	0.592	0.44	0.2221	0.000563	0.56	Crude Oil
0.825	1.175	336.3	1.333	0.9018	0.68	0.3383	0.000383	0.38	Crude Oil
0.812	1.175	593.1	1.333	0.5942	0.45	0.2229	0.000353	0.35	Crude Oil
0.812	1.175	819.0	1.333	0.4863	0.36	0.1824	0.000369	0.37	Crude Oil
0.792	1.16	541.7	1.333	0.5876	0.44	0.2204	0.000289	0.29	Crude Oil
0.792	1.16	542.1	1.333	0.6065	0.45	0.2275	0.000318	0.32	Crude Oil
0.792	1.16	654.7	1.333	0.5456	0.41	0.2047	0.000338	0.34	Crude Oil
0.792	1.16	784.7	1.333	0.4846	0.36	0.1818	0.000340	0.34	Crude Oil
0.772	1.145	451.7	1.333	0.6184	0.46	0.2320	0.000237	0.24	Crude Oil
0.772	1.145	571.7	1.333	0.5454	0.41	0.2046	0.000261	0.26	Crude Oil
0.772	1.145	571.8	1.333	0.5309	0.40	0.1991	0.000241	0.24	Crude Oil
0.772	1.145	715.6	1.333	0.4361	0.33	0.1636	0.000209	0.21	Crude Oil
0.703	1.185	404.0	1.333	0.9596	0.72	0.3599	0.000917	0.92	Octane
0.703	1.185	524.0	1.333	0.7878	0.59	0.2955	0.000854	0.85	Octane
0.703	1.185	758.7	1.333	0.643	0.48	0.2412	0.000973	0.97	Octane
0.703	1.185	636.0	1.333	0.6402	0.48	0.2401	0.000675	0.67	Octane
0.69	1.175	469.7	1.333	0.7067	0.53	0.2651	0.000498	0.50	Octane
0.69	1.175	526.2	1.333	0.6558	0.49	0.2460	0.000500	0.50	Octane
0.69	1.175	528.0	1.333	0.6558	0.49	0.2460	0.000503	0.50	Octane
0.69	1.175	687.1	1.333	0.5424	0.41	0.2035	0.000482	0.48	Octane
0.69	1.175	756.2	1.333	0.4924	0.37	0.1847	0.000437	0.44	Octane
0.67	1.16	379.7	1.333	0.6168	0.46	0.2314	0.000219	0.22	Octane
0.67	1.16	553.0	1.333	0.5819	0.44	0.2183	0.000390	0.39	Octane
0.67	1.16	587.9	1.333	0.5254	0.39	0.1971	0.000324	0.32	Octane
0.67	1.16	738.4	1.333	0.4518	0.34	0.1695	0.000325	0.33	Octane

Table 7- IFT Calculation results with using Octane and Crude Oil

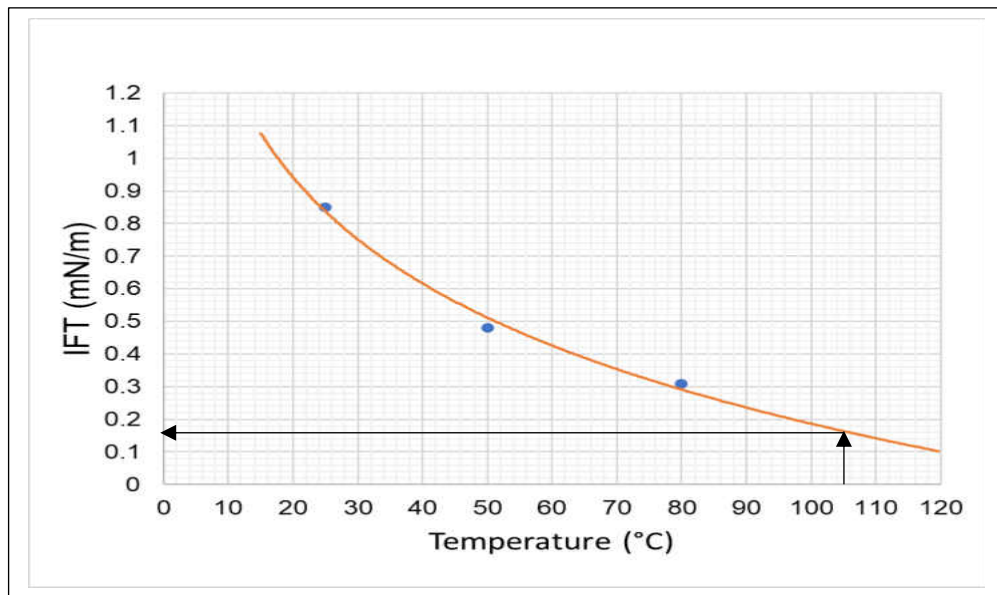


Figure 60- IFT Extrapolation for Octane and the Surfactant Blend

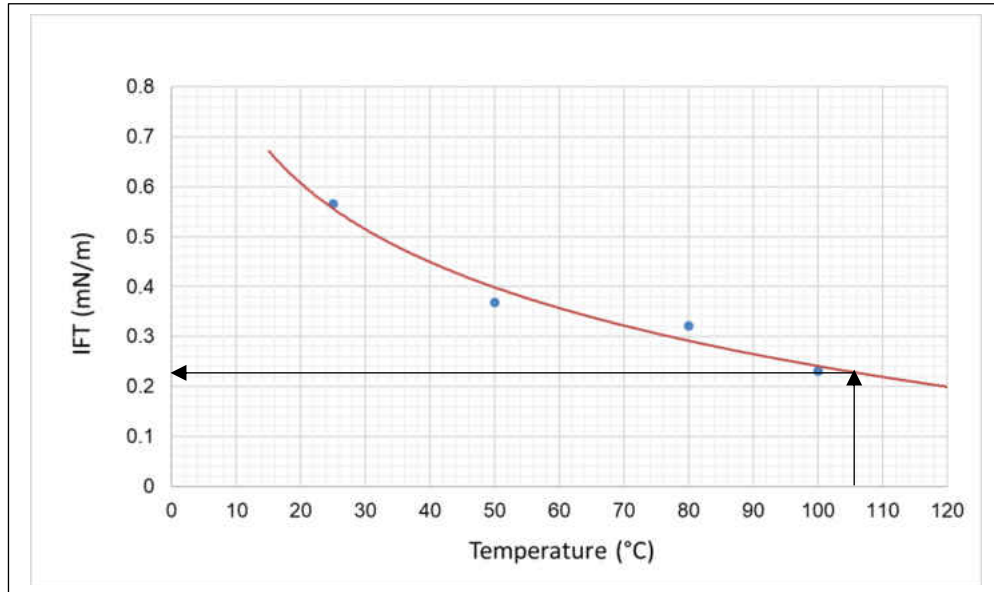


Figure 61- IFT Extrapolation for Crude Oil and the Surfactant Blend

3.6 Spontaneous Imbibition:

To have clear injectable solution at room temperature, many additives have been tried but the best option was adding 0.02% white oil and injecting the solution as micro-emulsion Figure 62. Back pressure up to 15 psi was applied to the spontaneous imbibition cells using pressure relief valve to decrease and/or eliminate the solution gas drive Figure 63. After the crude oil saturation, the saturated core samples were aged for 20 days at 105°C.

The recovery time in case of the brine blank samples was 6 hours in case of octane saturated sample and 35 hours while in case of the crude oil saturated sample. The recovery time in case of the surfactant blend was 6 hours while in case of the octane saturated sample and 5 hours in case of the crude oil saturated sample.

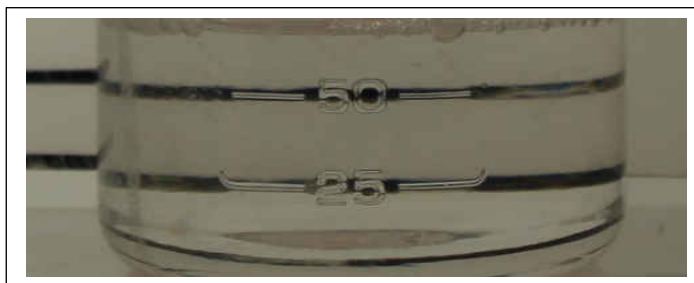


Figure 62- The Injection Composition (0.8% LB+0.2% ENORDET 0332 + 0.02% White Oil)

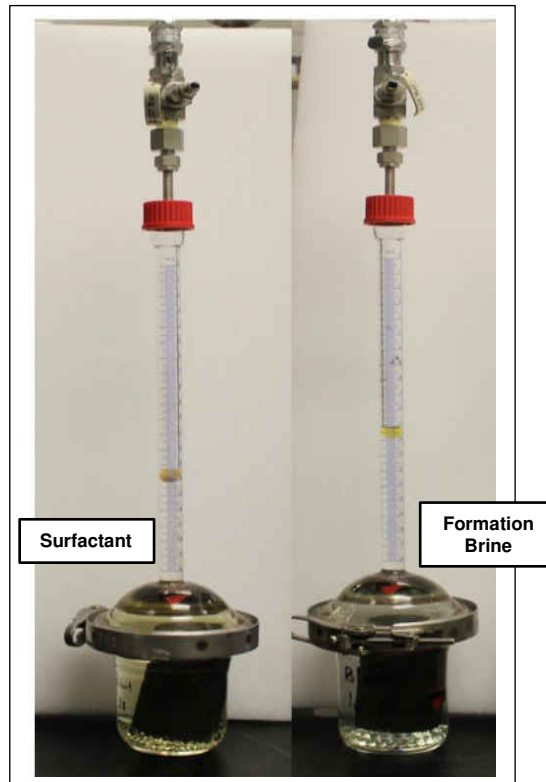


Figure 63- Spontaneous Imbibition Cells used in the Test

The surfactant blend was able to solubilize crude oil as shown in Figure 64. The surfactant blend was able to recover 18.5% OOIP in case of octane saturated cores comparing to 7.8% OOIP recovery with brine. In case of the crude oil saturated core samples, the surfactant blend recovered 20% OOIP compared to 6.1% OOIP recovery with brine. The brine took longer time to start recovering oil in case of crude oil saturated samples than the octane saturated cores which indicates that the crude oil saturated cores are more oil wet than the octane saturated cores as result of 20 days of aging at reservoir temperature.

After the end of the spontaneous imbibition test and getting the cells out of the oven there is two important observations. The first observation is once the cell starts to cool down there is enormous amount of bubbles in all the cells, the surfactant and brine solution octane and crude oil saturated core samples, and additional 8-10% oil recovery observed but not included in the reported oil recovery which give indication that the 15 psi back pressure was able to prevent the solution gas drive. The second observation is the presence of extracted impurities from the cores in case of the surfactant samples only, mainly in case of the octane saturated core samples comparing to small amount in case amount in

the crude oil saturated core samples. Figure 65 shows the oil recovery at 105°C before the impurities start to accumulate. Figure 66 Shows the impurities after accumulation and pictures of the impurities under microscope. These impurities might be caused by incomplete cleaning of the core samples.

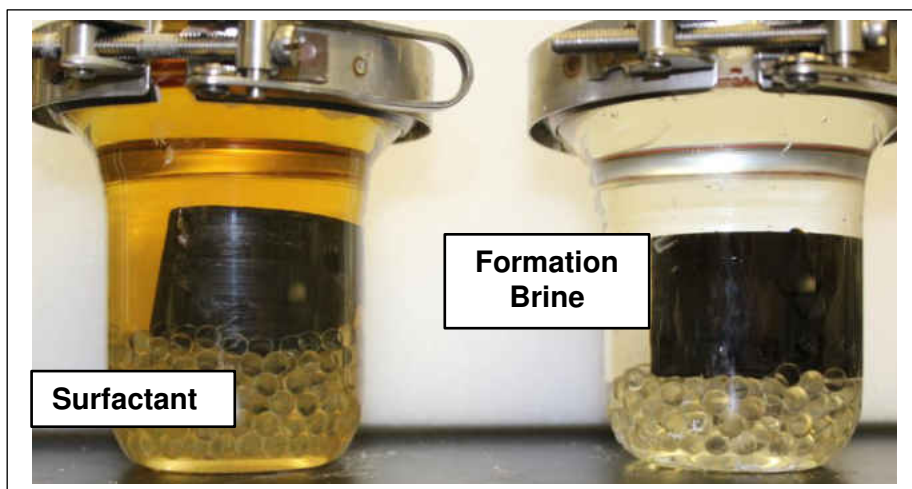


Figure 64- Crude Oil Solubilization with the surfactant Blend



Figure 65- Oil Recovery at 105°C

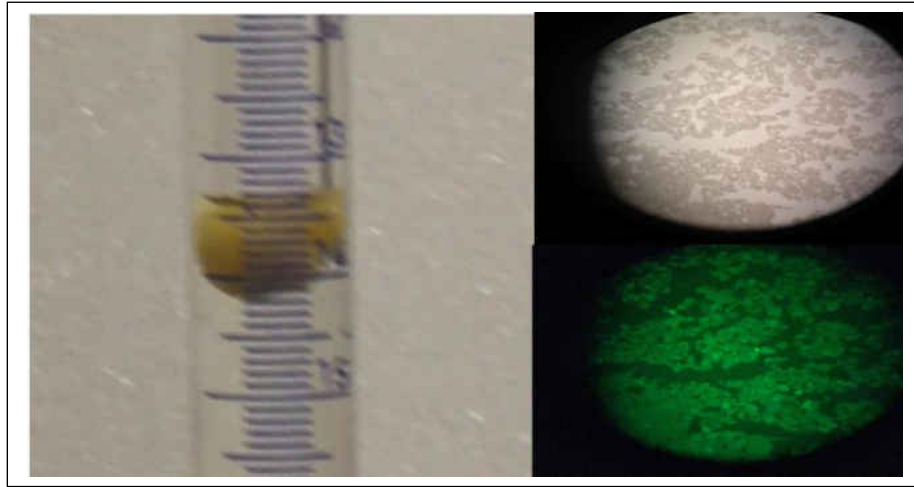


Figure 66- Picture of the Impurities after the End of the Test at Room Temperature and Under the Microscope

Figures 67 and 68 show the recovery efficiency for the octane and crude oil saturated cores with the surfactant blend and brine only.

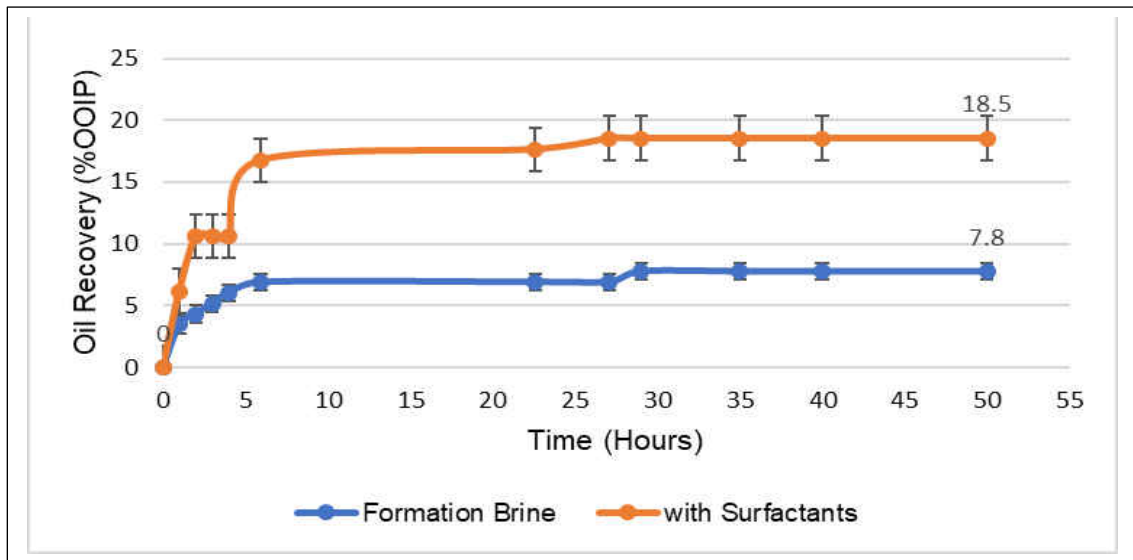


Figure 67- Recovery Efficiency – Octane Saturated Core Samples

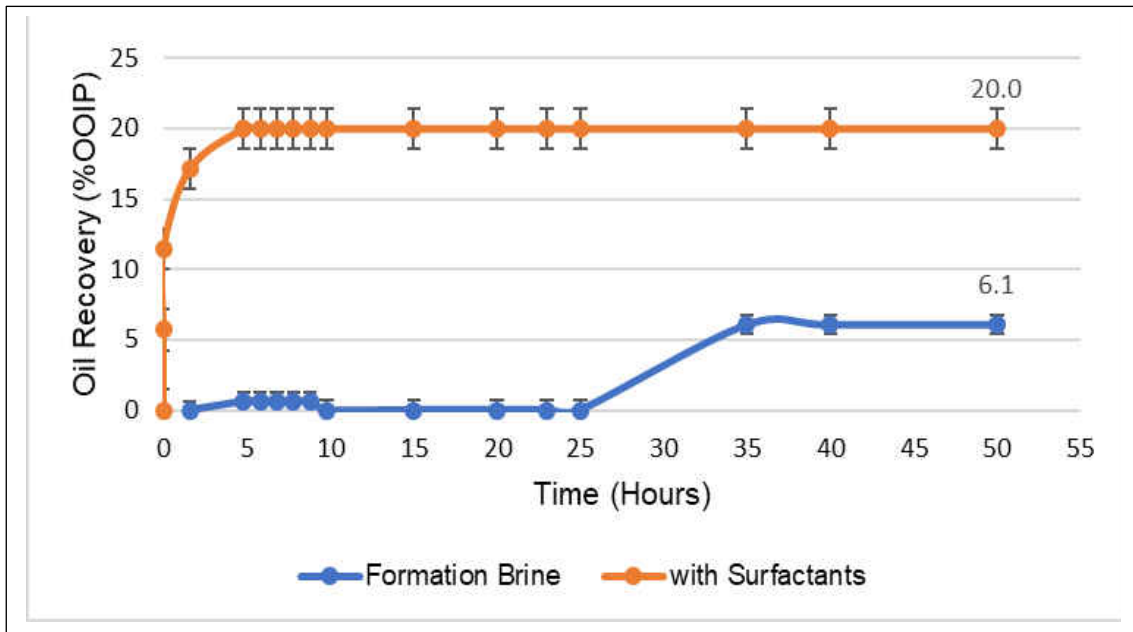


Figure 68- Recovery Efficiency – Crude Oil Saturated Core Samples

CHAPTER 4 : CONCLUSIONS

Core samples from the Upper Bakken, Middle Bakken and Three Forks were characterized by measuring NMR response using 2.3 MHz at ambient temperature and at 100°C as well as the NMR response using 22 MHz. Surfactants screening was performed and surfactant blend that is tolerant to the Bakken formation brine salinity and stable at the reservoir temperature (105°C) was chosen to the IFT and spontaneous imbibition test.

From all the previous measurements, results and discussion we have found that:

- 1- Based on NMR measurements using 2.3 MHz Larmor frequency Upper Bakken is preferentially oil wet and the Middle Bakken and Three Forks is preferentially water wet or intermediate wet.
- 2- NMR with 22 MHz Larmor frequency can detect the presence of bitumen in the Upper Bakken core samples.
- 3- No internal gradient observed in the Upper Bakken with using high frequency (22 MHz).
- 4- Strong internal gradient in the Middle Bakken and Three Forks core samples octane saturated while mild internal gradient in the Middle Bakken and Three Forks core samples Brine saturated.
- 5- T_1 shows little frequency dependence in case of Middle Bakken and Three Forks.
- 6- Upper Bakken core samples show temperature dependence with both octane or brine saturation which indicated H-H dipole-dipole relaxation mechanism.
- 7- Middle Bakken core samples show temperature dependence with octane saturation while no temperature dependence with brine saturation.
- 8- Three Forks core samples show no temperature dependence with both octane or brine saturation which indicated paramagnetic relaxation mechanism.
- 9- (8/2) Lauryl Betaine and ENORDET 0332 surfactant blend can lower IFT at high salinity and high temperature.
- 10- Octane is a good model oil for light crude oil and can be used as replacement for light crude oil in the surfactant screening tests because the

phase behavior as well as oil recovery values from spontaneous imbibition test are similar for octane and light crude oil.

- 11- Applying back pressure up to in spontaneous imbibition tests for light oils can prevent the effect of solution gas drive.
- 12- (8/2) LB/ENORDET 0332 surfactant blend was able to recover:
 - Octane: 18.5% OOIP comparing to 7.8% OOIP brine only.
 - Crude oil: 20% OOIP comparing to 6.1% OOIP brine only.
- 13- The surfactant blend was able to clean non-indigenous material from the cores because of in appropriate cleaning or other unknown causes.

REFERENCES

- [1] Press, “Son of Bakken formation namesake remains reserved,” 2012. [Online]. Available: https://missoulian.com/news/state-and-regional/son-of-bakken-formation-namesake-remains-reserved/article_2c99aea2-3d7c-11e2-8049-001a4bcf887a.html.
- [2] J. W. Nordquist, “MISSISSIPPIAN STRATIGRAPHY OF NORTHERN MONTANA*,” 1953.
- [3] North Dakota Geological Survey, “Overview of the Petroleum Geology of the North Dakota Williston Basin.” [Online]. Available: <https://www.dmr.nd.gov/ndgs/Resources/>.
- [4] J. P. Bluemle, S. B. Anderson, J. A. Andrew, D. W. Fischer, and J. A. LeFever, “North Dakota Stratigraphic Column,” *North Dakota Geologic Survey: Miscellaneous Series 66*. pp. 1–5, 1986.
- [5] P. G. Jessop and M. F. Cunningham, “Switchable Surfactants Sustainable biorefining techniques and process engineering View project Bio-oil Recovery & CO2 Recycling by Waste Stream Enhanced Microalgal Growth & Low Energy CO2-Induced Extraction View project,” 2006.
- [6] J. J. Wylde, J. L. Slayer, and V. Barbu, “Polymeric and Alkali-Surfactant Polymer Enhanced Oil Recovery Chemical Treatment: Chemistry and Strategies Required After Breakthrough Into the Process,” in *SPE International Symposium on Oilfield Chemistry*, 2013.
- [7] M. Dawson, D. Nguyen, N. Champion, and H. Li, “Designing an Optimized Surfactant Flood in the Bakken,” in *SPE/CSUR Unconventional Resources Conference*, 2015, pp. 20–22.
- [8] F. F. Craig, *The Reservoir Engineering Aspects Of Waterflooding*, Second Edi. Richardson, TX (1971): SPE Monograph Series Vol. 3, 1993.
- [9] Adamson, *Physical Chemistry of Surfaces*, 4th ed., vol. 44, no. 11. New York: John Wiley and Sons, 1985.
- [10] D. F. Boneau and R. L. Clampitt, “A Surfactant System for the Oil-Wet Sandstone Of the North Burbank Unit,” *J. Pet. Technol.*, vol. 29, no. 05, pp. 501–506, May 1977.

- [11] W. Paul Glover, "Formation Evaluation MSc Course Notes Chapter 7: Wettability."
- [12] G. J. Hirasaki, "Training Material."
- [13] W. G. Anderson, "Wettability Literature Survey- Part 1: Rock/Oil/Brine Interactions and the Effects of Core Handling on Wettability," *J. Pet. Technol.*, vol. 38, no. 10, pp. 1125–1144, Oct. 1986.
- [14] P. G. Nutting, "Some Physical and Chemical Properties of Reservoir Rocks Bearing on the Accumulation and Discharge of Oil," *Probl. Pet. Geol. Wrather F.H. Lahee (eds.), AAPG*, pp. 825–832, 1934.
- [15] G. V. Chilingar and T. F. Yen, "Some Notes on Wettability and Relative Permeabilities of Carbonate Reservoir Rocks, II," *Energy Sources*, vol. 7, no. 1, pp. 67–75, Jan. 1983.
- [16] F. C. Benner, W. W. Riches, and F. E. Bartell, "Nature and Importance of Surface Forces in Production of Petroleum," Jan. 1938.
- [17] F. C. Benner and F. E. Bartel, "The Effect Of Polar Impurities Upon Capillary And Surface Phenomena In Petroleum Production," Jan. 1941.
- [18] F. C. Benner, C. G. Dodd, and F. E. Bartell, "Evaluation Of Effective Displacement Pressures For Petroleum Oil-Water Silica Systems," Jan. 1942.
- [19] F. C. Benner, C. G. Dodd, and F. E. Bartell, "Evaluation Of Effective Displacement Pressures For Petroleum Oil-Water Silica Systems," Jan. 1942.
- [20] P. C.-A. O. P. O. THE and undefined 1973, "WETTABILITY STUDIES WITH NON-HYDROCARBON CONSTITUENTS OF CRUDE-OIL," *Chem. SOC 1155 16TH ST, NW*
- [21] M. O. Denekas, C. C. Mattax, and G. T. Davis, "Effects of Crude Oil Components on Rock Wettability," Jan. 1959.
- [22] A. C. Lowe, M. C. Phillips, and A. C. Riddiford, "On the Wetting of Carbonate Surfaces By Oil And Water," *J. Can. Pet. Technol.*, vol. 12, no. 02, Apr. 1973.
- [23] D. . Schechter, D. Zhou, and F. . Orr, "Low IFT drainage and imbibition," *J. Pet. Sci. Eng.*, vol. 11, no. 4, pp. 283–300, Sep. 1994.

- [24] G. Sharma and K. K. Mohanty, “Wettability Alteration in High Temperature and High Salinity Carbonate Reservoirs,” in *SPE Annual Technical Conference and Exhibition*, 2011, no. 2010.
- [25] D. Wang, R. S. Seright, and J. Zhang, “Wettability Survey in Bakken Shale Using Surfactant Formulation Imbibition,” in *SPE Improved Oil Recovery Symposium*, 2012, pp. 695–705.
- [26] J. O. Alvarez and D. S. Schechter, “Altering Wettability in Bakken Shale by Surfactant Additives and Potential of Improving Oil Recovery During Injection of Completion Fluids,” in *SPE Improved Oil Recovery Conference*, 2016, pp. 11–13.
- [27] D. Wang, R. Butler, H. Liu, and S. Ahmed, “Surfactant Formulation Study For Bakken Shale Imbibition,” in *SPE Annual Technical Conference and Exhibition*, 2011, no. November.
- [28] H. L. M. Dawson, D. Nguyen, “Designing an Optimized Surfactant Flood in the Bakken,” *J. Pet. Technol.*, vol. 68, no. 01, pp. 58–92, Jan. 2016.
- [29] S. Karimi and H. Kazemi, “Capillary Pressure Measurement using Reservoir Fluids in a Middle Bakken Core,” in *SPE Western Regional Meeting*, 2015, pp. 27–30.
- [30] G. Hirasaki, C. A. Miller, and M. Puerto, “Recent Advances in Surfactant EOR,” *SPE J.*, vol. 16, no. 04, pp. 889–907, Dec. 2011.
- [31] H. B. Todd and J. G. Evans, “Improved Oil Recovery IOR Pilot Projects in the Bakken Formation,” in *SPE Low Perm Symposium*, 2016.
- [32] K. Ling and J. He, “A New Correlation to Calculate Oil-Water Interfacial Tension,” in *SPE Kuwait International Petroleum Conference and Exhibition*, 2012.
- [33] K. Ling and Z. Shen, “Including the Effect of Capillary Pressure to Estimate Critical Rate in Water Coning Well,” in *North Africa Technical Conference and Exhibition*, 2012.
- [34] F. Bloch, W. W. Hansen, and M. Packard, “Nuclear Induction,” *Phys. Rev.*, vol. 69, no. 3–4, pp. 127–127, Feb. 1946.
- [35] F. Bloch, “Nuclear Induction,” *Phys. Rev.*, vol. 70, no. 7–8, pp. 460–474, Oct. 1946.

- [36] E. M. Purcell, H. C. Torrey, and R. V. Pound, "Resonance Absorption by Nuclear Magnetic Moments in a Solid," *Phys. Rev.*, vol. 69, no. 1–2, pp. 37–38, Jan. 1946.
- [37] D. E. Woessner, "The early days of NMR in the Southwest," *Concepts Magn. Reson.*, vol. 13, no. 2, pp. 77–102, Jan. 2001.
- [38] K.-J. (Keh-J. Dunn, D. J. (David J. . Bergman, and G. A. (Gerald A. . Latorraca, *Nuclear magnetic resonance: petrophysical and logging applications*. Pergamon, 2002.
- [39] D. O. Seevers, "A Method of Determining Permeability by Means of a Pulsed NMR and an Application of the Method to the Study of a Gulf Coast Supernormally Pressured Well," in *Abnormal Subsurface Pressure Symposium*, 1972.
- [40] A. Timur, "Effective Porosity and Permeability Of Sandstones Investigated Through Nuclear Magnetic Resonance Principles," Jan. 1968.
- [41] R. J. S. Brown and I. Fatt, "Measurements Of Fractional Wettability Of Oil Fields' Rocks By The Nuclear Magnetic Relaxation Method," in *Fall Meeting of the Petroleum Branch of AIME*, 1956.
- [42] H. C. Torrey, J. Korringa, D. O. Seevers, and J. Uebersfeld, "Magnetic Spin Pumping in Fluids Contained in Porous Media," *Phys. Rev. Lett.*, vol. 3, no. 9, pp. 418–419, Nov. 1959.
- [43] KLEINBERG and R. L., "Well logging," *Encycl. Nucl. Magn. Reson.*, pp. 4960–4969, 1996.
- [44] R. J. S. Brown and B. W. Gamson, "Nuclear Magnetism Logging," Jan. 1960.
- [45] J. E. Coolidge, I. Ritchie, B. W. Gamson, and L. Shane, "NML Resolves Difficult Logging Problems," Jan. 1962.
- [46] R. C. Herrick, S. H. Couturie, and D. L. Best, "An Improved Nuclear Magnetism Logging System And Its Application To Formation Evaluation," in *SPE Annual Technical Conference and Exhibition*, 1979.
- [47] M. Saidian and M. Prasad, "Effect of mineralogy on nuclear magnetic resonance surface relaxivity: A case study of Middle Bakken and Three Forks formations," *Fuel*, vol. 161, pp. 197–206, Dec. 2015.

- [48] S. Karimi, M. Saidian, and H. Kazemi, “Experimental Study of the Effect of Core Aging on Fluid Distribution in Middle Bakken Cores,” in *SPE Low Perm Symposium*, 2016, pp. 5–6.
- [49] Z. H. Xie and Z. Gan, “Value of 20Mhz NMR Core Analysis for Unconventional Mudstones,” Jun. 2018.
- [50] R. Kausik, K. Fellah, L. Feng, D. Freed, and G. Simpson, “High- and Low-Field NMR Relaxometry and Diffusometry of the Bakken Petroleum System,” Jun. 2016.
- [51] E. O. Odusina, C. H. Sondergeld, and C. S. Rai, “NMR Study of Shale Wettability,” in *Canadian Unconventional Resources Conference*, 2011.
- [52] R. Kausik, K. Fellah, L. Feng, D. Freed, and G. Simpson, “Temperature Dependence of 2D NMR T_1 - T_2 Maps of Shale,” Jun. 2018.
- [53] G. A. Simpson, N. S. Fishman, and S. Hari-Roy, “New Nuclear Magnetic Resonance Log T_2 Cut-Off Interpret Parameters for the Unconventional Tight Oil of the Bakken Petroleum System Using 2-D NMR Core Laboratory Measurements on Native State and Post-Cleaned Core Samples,” Jun. 2018.
- [54] H. Pu and Y. Li, “CO₂ EOR Mechanisms in Bakken Shale Oil Reservoirs,” in *Carbon Management Technology Conference*, 2015, no. November, pp. 17–19.
- [55] Halliburton, *Shale Developments III*. 2012.
- [56] Steven Ward, “The Bakken Trend: Lost Dutchmen Mine of the Oil Patch?” [Online]. Available: <https://seekingalpha.com/article/60933-the-bakken-trend-lost-dutchmen-mine-of-the-oil-patch>. [Accessed: 17-Apr-2019].
- [57] R. M. Pollastro, L. N. R. Roberts, T. A. Cook, and M. D. Lewan, “Assessment of Undiscovered Technically Recoverable Oil and Gas Resources of the Bakken Formation, Williston Basin, Montana and North Dakota, 2008,” 2008.
- [58] R. L. Webster, “PETROLEUM SOURCE ROCKS AND STRATIGRAPHY OF THE BAKKEN FORMATION IN NORTH DAKOTA,” 1984.
- [59] T. Tran, P. D. Sinurat, and B. A. Wattenbarger, “Production Characteristics of the Bakken Shale Oil,” in *SPE Annual Technical Conference and*

Exhibition, 2011.

- [60] L. C. Price, “Origins and Characteristics of the Basin-Centered Continuous-Reservoir Unconventional Oil-Resource Base of the Bakken Source System, Williston Basin: The Energy & Environmental Research Center (EERC),” 1999. [Online]. Available: <http://www.undeerc.org/News-Publications/Leigh-Price-Paper/Default.aspx>. [Accessed: 22-Oct-2015].
- [61] E. F. R. Lefever, Julie A, Martiniuk, C.D., Dancsock, “Petroleum Potential of Middle Bakken_6th WBS.pdf,” *Saskatchewan Geological Society Special Publication No. 11*. pp. 76–94, 1991.
- [62] EERC, “Lithology | Bakken - Beyond the Boom: The Energy & Environmental Research Center (EERC).” [Online]. Available: <https://www.undeerc.org/bakken/lithology.aspx>. [Accessed: 02-Apr-2019].
- [63] J. K. Pitman, L. C. Price, and J. A. Lefever, “Diagenesis and Fracture Development in the Bakken Formation, Williston Basin: Implications for Reservoir Quality in the Middle Member,” 2001.
- [64] J. A. Lefever, “North Dakota Geological Survey,” 2007.
- [65] J. George H. Murray, *Quantitative Fracture Study--Sanish Pool, Mckenzie County, North Dakota*, vol. 52, no. 1. American Association of Petroleum Geologists, 1968.
- [66] W. Yu, H. Lashgari, and K. Sepehrnoori, “Simulation Study of CO₂ Huff-n-Puff Process in Bakken Tight Oil Reservoirs,” in *SPE Western North American and Rocky Mountain Joint Meeting*, 2014.
- [67] B. Nojabaei, R. T. Johns, and L. Chu, “Effect of Capillary Pressure on Phase Behavior in Tight Rocks and Shales,” *SPE Reserv. Eval. Eng.*, vol. 16, no. 03, pp. 281–289, Aug. 2013.
- [68] F. F. Meissner, “Petroleum Geology of the Bakken Formation Williston Basin, North Dakota and Montana,” *Willist. Basin Symp. , Mont. Geol. Soc. 24th Annu. Conf. Billings, Mont.*, pp. 159–179, 1978.
- [69] H. T. Iampen and B. J. Rostron, “Hydrogeochemistry of pre-Mississippian brines, Williston Basin, Canada–USA,” *J. Geochemical Explor.*, vol. 69–70, pp. 29–35, Jun. 2000.
- [70] NDIC, “Well File B.”

- [71] M. C. Puerto and R. L. Reed, “Surfactant Selection With the Three-Parameter Diagram,” 1990.
- [72] NDIC, “Well File A.”
- [73] “Recommended Practices for Core Analysis.”
- [74] F. Soxhlet, “The weight-analytical determination of milk fat,” *Polytech. J.*, vol. 232, 1879.
- [75] O. Torsaeter and M. Abtahi, “EXPERIMENTAL RESERVOIR ENGINEERING LABORATORY WORK BOOK,” 2000.
- [76] M. Puerto, G. J. Hirasaki, C. A. Miller, and J. R. Barnes, “Surfactant Systems for EOR in High-Temperature, High-Salinity Environments,” *SPE J.*, vol. 17, no. 01, pp. 11–19, Mar. 2012.